

# **Transgenic approaches to improve photosynthesis and nitrogen use in wheat**

**Saqer Sultan Alotaibi**

A thesis submitted for the degree of Doctor of Philosophy

Department of Biological Sciences

University of Essex

**Date of submission**

October 2016

## **Acknowledgements**

I would like to express my sincere gratitude to my supervisor Professor Christine Raines for all of the support and encouragement. Also thank you to Dr Julie Lloyd for the comments and suggestions given at all board meetings during my PhD studies.

Additionally, I would like to thank all lab members and Dr Tracy Lawson and her lab member. Also, thank you for people in Rothamsted, West Common, Harpenden, UK for producing transgenic wheat plants throughout this study.

An extremely big thanks you and sincere gratitude to my wife for supporting me spiritually during my PhD studies and my life in general.

## Summary

To meet the rapid growth of the global population and the expected demand for food, significant enhancements in yields are needed, together with optimised N fertilisation and environmental issues, particularly in the production of major grain crops, such as wheat and rice. Improving photosynthesis, together with NUE, has been considered an unexploited opportunity in the research on improving crop yields. Therefore, transgenic wheat plants with increased SBPase activity showed an improved photosynthetic leaf rate and total biomass production. The Rubisco protein is a major N investment in crops, but it has also been exhibited that under some environmental conditions, there may be an excess of Rubisco greater than that needed to maintain photosynthesis. This raises the question of whether a small reduction in the amount of the Rubisco enzyme can be used to improve NUE without any negative effects on plant yield. To address the question, wheat plants with decreased Rubisco were produced. Physiological studies were performed on five independent transgenic lines with different levels of Rubisco, and the photosynthetic rates, biomass and grain yields were determined. Rubisco RNAi lines with reductions in the Rubisco protein of more than 40% showed a significant decrease in photosynthesis, growth and grain yield. Interestingly, the plants with the lowest level of Rubisco activity had significantly higher levels of leaf and seed N when compared to WT plants. In contrast, small reductions in the Rubisco protein of between about 10% and 25% did not have an adverse effect on photosynthesis, growth or grain yield in two independent transgenic wheat lines. Furthermore, to search for new promoters to drive good transgene expressions specialised to wheat leaves, two *Brachypodium* promoters, SBPase and FBPA, were cloned upstream of the GUS fusion gene and transformed into wheat leaves. Consequently, both promoters resulted in detectable GUS expression in wheat leaves at different growth stages and did not show expressions in the roots.

## Abbreviations

<b>ATP</b>	Adenosine triphosphate
<b>bp</b>	Base pairs
<b>BLAST</b>	Basic Local Alignment Search Tool
<b>°C</b>	Temperature
<b>CO<sub>2</sub></b>	Carbon dioxide
<b>DNA</b>	Deoxyribonucleic acid
<b>dNTP</b>	Deoxynucleoside- 5'- phosphate
<b>EDTA</b>	Ethylenediaminetetra-acetic acid (disodium salt)
<b>DTT</b>	1-deoxy-d-xylulose 5-phosphate dithiothreitol
<b>FWD</b>	Forward primer
<b>FBPA</b>	Fructose 1,6-bisphosphate aldolase
<b>G3P</b>	Glyceraldehyde 3-phosphate
<b>GUS</b>	β-glucuronidase
<b>h</b>	Hour
<b>HEPES</b>	4-(2-hydroxyethyl) piperazine-1-ethanesulfonic acid
<b>kb</b>	Kilobase
<b>m</b>	Minute
<b>μl</b>	Microliter
<b>ml</b>	Millilitre
<b>NADP</b>	Nicotinamide adenine dinucleotide phosphate

<b>NADPH</b>	Reduced nicotinamide adenine dinucleotide phosphate
<b>NADH</b>	Nicotinamide adenine dinucleotide (reduced form)
<b>NAD<sup>+</sup></b>	Nicotinamide adenine dinucleotide (oxidized form)
<b>PCR</b>	Polymerase Chain Reaction
<b>PRK</b>	Phosphoribulokinase
<b>REV</b>	Reverse primer
<b>rpm</b>	Revolution per minut
<b>RT</b>	Room Temperature
<b>RuBisCO</b>	Ribulose-1,5-bisphosphate carboxylase oxygenase
<b>RuBP</b>	Ribulose 1,5-bisphosphate
<b>s</b>	Second
<b>SBPase</b>	Sedoheptulose 1,7-bisphosphatase
<b>SDS</b>	Sodium dodecyl sulfate
<b>TAE</b>	TRIS-base, acetic acid and edta
<b>TBA</b>	Tris-base, Borate and EDTA
<b>Temed</b>	Tetramethylethylenediamine
<b>TK</b>	Transketolase

<b>Tris</b>	2-amino-2-(hydroxymethyl) propane 1,3-diol
<b>Tween-20</b>	Polysorbate 20
<b>UTR</b>	Untranslated region
<b>V</b>	Volt

## Table of Contents

Acknowledgements .....	2
Summary.....	3
Abbreviations .....	4
Table of Figures .....	10
<b>Chapter 1: Literature review .....</b>	<b>13</b>
<b>1.1 General background .....</b>	<b>14</b>
<b>1.2 The Calvin–Benson cycle .....</b>	<b>16</b>
1.2.1 Reactions of the Calvin–Benson cycle.....	19
1.2.2 Regulation of the Calvin-Benson cycle .....	19
1.2.3 The Rubisco enzyme.....	22
1.2.3.1 Structure and genetics.....	22
1.2.3.2 Regulation of Rubisco.....	23
<b>1.3 The Calvin–Benson cycle as a target to improve photosynthesis and NUE.....</b>	<b>24</b>
<b>1.4 Contributions and transgenic studies of the individual enzymes of the Calvin–     Benson cycle in the photosynthesis process .....</b>	<b>26</b>
1.4.1 The Rubisco enzyme as a target for antisense studies .....	26
1.4.2 Sedoheptulose-1, 7-bisphosphatase (SBPase).....	27
1.4.3 Fructose-1, 6-bisphosphate (FBP) aldolase .....	30
<b>1.5 Regulation of gene constructs in transgenic plants .....</b>	<b>32</b>
<b>1.6 Identification of promoters of the Calvin–Benson cycle gene encoded enzymes...34</b>	<b>34</b>
<b>1.7 Aims of this study.....</b>	<b>36</b>
<b>Chapter 2: Materials and Methods .....</b>	<b>38</b>
<b>2.1 Materials .....</b>	<b>39</b>
2.1.1 Chemicals, antibiotics and molecular biology reagents .....	39
2.1.2 Enzyme.....	39
2.1.3 Bacterial strains.....	39
2.1.4 Plasmid vectors and primers.....	42
2.1.5 Plant material.....	42
2.1.6 Gas exchange apparatus.....	42
<b>2.2 Methods .....</b>	<b>46</b>
2.2.1 Bioinformatics analysis.....	46
<b>2.2.2 Molecular biology approaches .....</b>	<b>46</b>
2.2.2.1 DNA Extraction from wheat leaves .....	46
2.2.2.2 Primers design.....	47
2.2.2.3 Polymerase chain reaction (PCR).....	47
2.2.2.3.1 Amplification of specific gene fragment for cloning using PCR .....	47
2.2.2.3.2 Amplification of specific gene fragment for screening using PCR.....	47
2.2.2.3.3 Colony screening using polymerase chain reaction (PCR) .....	48
2.2.2.4 Agarose gel electrophoresis analysis of DNA and RNA.....	49
2.2.2.5 Preparation of E.coli competent cells using CaCl <sub>2</sub> method.....	49
2.2.2.6 Transformation of E.coli competent cells (TOP10) using heat shock.....	49
2.2.2.7 Preparation of <i>Agrobacterium</i> competent cells .....	50
2.2.2.8 Transformation of <i>Agrobacterium</i> competent cells by electroporation.....	50
2.2.2.9 Cloning of SBPase and FBPadolase promoters for expression analysis.....	51
2.2.2.9.1 Cloning of SBPase and FBPadolase promoters using Gateway technology for the transient expression analysis in <i>N. benthamiana</i> leaves .....	51
2.2.2.9.2 Traditional cloning of SBPase and FBPadolase promoters for the transient expression analysis in wheat leaves .....	52

2.2.2.10 Plasmids DNA preparation from bacterial cells using Mini prep kit.....	52
2.2.2.11 Plasmids DNA isolation from bacterial cells using Quiagen Midi prep kit.....	53
2.2.2.12 Restriction Digest of plasmid DNAs.....	54
2.2.2.13 RNA extraction from wheat leaves.....	55
2.2.2.14 First strand cDNA synthesis using superscript II RT.....	55
2.2.2.15 Gene expression analysis using q-PCR.....	56
<b>2.3 Biochemistry approaches .....</b>	<b>57</b>
2.3.1 Protein extraction .....	57
2.3.2 Protein quantification.....	57
2.3.3 Preparation of Sodium Dodecyl Sulphate polyacrylamide gel electrophoresis (SDS_PAGE).....	58
2.3.4 Proteins separation into SDS-PAGE polyacrylamide gel.....	58
2.3.5 Coomassie Brilliant Blue staining .....	59
2.3.6 Western blotting of proteins to cellulose nitrate membrane.....	59
2.3.7 Immunoblotting and Detection.....	60
2.3.8 Red Ponceau staining of cellulose nitrate membrane .....	60
2.3.9 Rubisco Activity assay.....	61
<b>2.4 Growth and Physiological analyses.....</b>	<b>62</b>
2.4.1 Growth of plants and conditions.....	62
2.4.2 Developmental measurement.....	62
2.4.3 Transient expression assay in <i>N. benthamiana</i> leaves.....	62
2.4.4 Microscopy observation .....	63
2.4.5 Histochemical GUS assays.....	63
2.4.6 Gas exchange measurement.....	64
2.4.7 The measurement of SBPase activity .....	64
2.4.7.1 Protein extraction for SBPase activity measurement.....	65
2.4.7.2 SBPase activity determination by phosphate release.....	65
2.4.8 Determination of total Biomass .....	66
<b>Chapter 3: Increased SBPase activity improves photosynthesis and grain yield in wheat grown in greenhouse conditions .....</b>	<b>67</b>
<b>3.1 Introduction .....</b>	<b>68</b>
<b>3.2 Results.....</b>	<b>71</b>
3.2.1 Gene expression analysis of the <i>SBPase</i> construct in transgenic wheat plants using qPCR.....	71
3.2.2 SBPase activity in transgenic T3 wheat plants.....	74
3.2.3 The effects of increased levels of <i>SBPase</i> activity on photosynthesis and growth in transgenic wheat T3 plants grown in greenhouse conditions .....	76
3.2.3.1 The effects of increased levels of <i>SBPase</i> activity on CO <sub>2</sub> assimilation ( <i>A/Ci</i> analysis) .....	76
3.2.3.2 The effect of increased SBPase activity on transgenic wheat plants' growth and visual phenotypes.....	81
3.2.3.3 The effect of higher levels of <i>SBPase</i> activity on plant biomass and seed production.....	83
<b>3.3 Discussion .....</b>	<b>85</b>
<b>Chapter 4: Effect of decreased Rubisco by <i>RbcS</i> RNAi on wheat photosynthesis, growth and grain quality under natural sunlight in the UK spring/ summer seasons .....</b>	<b>88</b>
<b>4.1 Introduction .....</b>	<b>89</b>
<b>4.2 Results.....</b>	<b>93</b>
4.2.1 Construction and transformation of <i>RbcS</i> RNAi into wheat leaf.....	93
4.2.2 Selection of primary transformants wheat plants (T0): Expression of Rubisco small subunit ( <i>RbcS</i> ) cDNA using a quantitative polymerase chain reaction (q-PCR) .....	95

4.2.3 Preliminary screening of T1 progeny .....	97
4.2.3.1 Confirming the presence of transgenic <i>RbcS</i> in transgenic wheat T1 plants using PCR .....	97
4.2.3.2 Gene expression analysis of coding sequence <i>RbcS</i> in transgenic wheat plants T1 using q-PCR.....	99
4.2.3.3 Protein expression analysis of <i>RbcS</i> in transgenic T1 wheat plants using Western blot.....	102
4.2.3.4 <i>A/C<sub>j</sub></i> photosynthetic gas exchange measurement .....	105
4.2.3.5 The effect of decreased level of Rubisco protein on T1 plant biomass.....	109
4.2.3.6 The effect of decreased content of Rubisco protein on individual plant photosynthesis.....	111
4.2.4 Molecular analyses of T2 progeny: DNA screening, <i>RbcS</i> gene expression and <i>RbcS</i> protein content.....	114
4.2.4. 1 Confirming the presence of transgenic <i>RbcS</i> RNAi in wheat T2 plants using PCR .....	114
4.2.4.2 Gene expression analysis of the coding sequence of the <i>RbcS</i> gene in transgenic wheat plants (T2) using q-PCR.....	116
4.2.4.3 Protein expression analysis of <i>RbcS</i> in transgenic wheat plants (T2) using the Western blot approach.....	118
5.2.1.4 Rubisco activity in <i>RbcS</i> RNAi wheat plants.....	120
4.2.5 The effect of different decreased levels of Rubisco activity on photosynthesis and growth in wheat <i>RbcS</i> RNAi transgenic plants grown under natural sunlight in the UK spring/ summer seasons. ....	122
4.2.5.1 CO <sub>2</sub> assimilation in leaves at different developmental growth stages of Zadoks scale .....	122
4.2.5.2 The effect of decreased Rubisco activity on plants growth and visual phenotypes .....	127
4.2.5.3 The effect of different levels of decreased Rubisco activity on plant biomass and seed production.....	129
4.2.5.4 The effect of different levels of decreased Rubisco activity on carbon and nitrogen distributions in leaves and seeds .....	132
<b>4.3 Discussion .....</b>	<b>134</b>
<b>Chapter 5: Genetic Engineering Tools to Improve Photosynthetic Efficiency in Wheat Leaf .....</b>	<b>139</b>
<b>5.1 Introduction .....</b>	<b>140</b>
<b>5.2 Results.....</b>	<b>143</b>
5.2.1 Identification of <i>Brachypodium distachyon</i> SBPase and FBPaldolase .....	143
5.2.2 Building transcriptional fusion constructs of <i>Brachypodium</i> SBPase and FBPaldolase promoters for transient expression analysis into <i>N. benthamiana</i> leaves .....	151
5.2.3 Transient expression analysis in <i>Nicotiana benthamiana</i> leaves .....	158
5.2.4 Building transcriptional fusion constructs of <i>Brachypodium</i> SBPase and FBPaldolase promoters for transient and stable expression analysis into wheat leaves.....	161
6.2.5 Stable expression analysis into wheat leaves.....	168
6.2.5.1 GUS expression into T0 tissues .....	168
6.2.5.2 GUS expression into T1 tissues at different Zadoks scale growth stages.....	173
<b>5.3 Discussion .....</b>	<b>176</b>
<b>Chapter 6: General Discussion.....</b>	<b>181</b>
<b>References .....</b>	<b>191</b>

## Table of Figures

**Figure 1.1:** The Calvin–Benson cycle map.

**Figure 3.1:** Determination the level of *Brachypodium SBPase* gene expression in transgenic T3 wheat plants.

**Figure 3.2:** Determination the level of native *SBPase* gene expression in transgenic T3 wheat plants.

**Figure 3.3:** increase in total extractable *SBPase* activity in transgenic *SBPase* wheat plant T3 progeny.

**Figure 3.4:** Photosynthetic CO<sub>2</sub> assimilation (*A*) response to different internal concentrations of CO<sub>2</sub> (*C<sub>i</sub>*) (*A/C<sub>i</sub>* curve) of two independent overexpressed *SBPase* T3 lines compared to the WT line.

**Figure 3.5:** The CO<sub>2</sub> assimilation rates at ambient (*A<sub>sat</sub>*) and saturating CO<sub>2</sub> (*A<sub>max</sub>*) of transgenic overexpressed *SBPase* T3 wheat plants.

**Figure 3.6:** Visual phenotypes of *SBPase* transgenic T3 lines and WT plants.

**Figure 3.7:** Biomass analysis of transgenic *SBPase* lines and WT lines.

**Figure 4.1:** Rubisco small subunit RNAi construct used for particle bombardment transformation into wheat.

**Figure 4.2:** Relative gene expression analysis of the wheat *RbcS* gene in transformant T0 wheat plants using q-PCR.

**Figure 4.3:** PCR analysis of genomic DNA to confirm the presence of the *RbcS* RNAi construct in T1 wheat leaves.

**Figure 4.4:** Determination of the transcript levels of the *RbcS* transcript in T1 transgenic wheat plants.

**Figure 4.5:** Optimizing the protein dilution to detect *RbcS* in T1 wheat plants.

**Figure 4.6:** Immunoblot analysis of transgenic *RbcS* RNAi T1 wheat plants.

**Figure 4.7:** Photosynthetic CO<sub>2</sub> assimilation (*A*) response to increasing internal concentration of CO<sub>2</sub> (*C<sub>i</sub>*) (*A/C<sub>i</sub>* curve) for five independent *RbcS* RNAi T1 lines compared to the WT plants.

**Figure 4.8:** Maximum rate of carboxylation allowed by the Rubisco enzyme (*V<sub>c, max</sub>*) and the maximum electron transport required for RuBP regeneration (*J<sub>max</sub>*).

**Figure 4.9:** Total biomass analysis of *RbcS* RNAi wheat T1 plants grown in a controlled-environment greenhouse.

**Figure 4.10:** Photosynthetic CO<sub>2</sub> assimilation (*A*) response to different internal concentrations of CO<sub>2</sub> (*C<sub>i</sub>*) (*A/C<sub>i</sub>* curve) for five individual *RbcS* RNAi T1 plants compared to the WT plant.

**Figure 4.11:** Maximum rate of carboxylation allowed by the Rubisco enzyme (*V<sub>c, max</sub>*) and the maximum electron transport required for RuBP regeneration (*J<sub>max</sub>*).

**Figure 4.12:** PCR analysis of genomic DNA to confirm the presence of the *RbcS* RNAi construct in T2 wheat leaves.

**Figure 4.13:** Determination the level of *RbcS* gene expression in transgenic T2 wheat plants.

**Figure 4.14:** Immunoblot analysis of transgenic *RbcS* RNAi T2 wheat plants.

**Figure 4.15:** Decrease in total extractable Rubisco activity in *RbcS* RNAi wheat plant T2 progeny.

**Figure 4.16:** Photosynthetic CO<sub>2</sub> assimilation (*A*) response to different internal concentrations of CO<sub>2</sub> (*C<sub>i</sub>*) (*A/C<sub>i</sub>* curve) of five independent *RbcS* RNAi T2 lines compared to the WT line.

**Figure 4.17:** The CO<sub>2</sub> assimilation rates at ambient (*A<sub>sat</sub>*) and saturating CO<sub>2</sub> (*A<sub>max</sub>*) of transgenic *RbcS* RNAi T2 wheat plants.

**Figure 4.18:** Growth analysis and visual phenotypes of *RbcS* RNAi transgenic T2 lines and WT plants.

**Figure 4.19:** Biomass analysis of *RbcS* RNAi lines and WT lines.

**Figure 4.20:** Seed analysis of *RbcS* RNAi T2 transgenic lines and WT lines.

**Figure 4.21:** Nitrogen and carbon analysis into leaves and seeds of *RbcS* RNAi T2 lines and WT lines.

**Figure 5.1:** The structure of the gene showing the 2-kb region that taken from *Brachypodium* SBPase and FBPa (FBPaldolase) genes to make the constructs.

**Figure 5.2:** *Brachypodium* FBPa (FBPaldolase) promoter motif sequences.

**Figure 5.3:** *Brachypodium* SBPase promoter motif sequences.

**Figure 5.4:** Building transcriptional fusions of *Brachypodium* SBPase construct to the β-glucuronidase (GUS) for expression analysis into *N. benthamiana* leaves.

**Figure 5.5:** Building transcriptional fusions of *Brachypodium* SBPase construct to the enhanced yellow fluorescence protein (eYFP) for expression analysis into *N. benthamiana* leaves.

**Figure 5.6:** Colony PCRs of the construction of SBPase with the chimeric expression cassettes (GUS and eYFP) into *E. coli*.

**Figure 5.7:** Building transcriptional fusions of *Brachypodium* FBPa (FBPaldolase) construct to the β-glucuronidase (GUS) for expression analysis into *N. benthamiana* leaves.

**Figure 5.8:** Building transcriptional fusions of *Brachypodium* FBPA construct to the enhanced yellow fluorescence protein (eYFP) for expression analysis into *N. benthamiana* leaves.

**Figure 5.9:** Colony PCR of the construction of FBPA with the chimeric expression cassettes (GUS and eYFP) into *E. coli*.

**Figure 5.10:** Histochemical GUS assay of agro-infiltrated *N. benthamiana* leaves.

**Figure 5.11:** Confocal Fluorescent images of eYFP-agro-infiltrated leaves *N. benthamiana* plants.

**Figure 5.12:** Building transcriptional fusions of *Brachypodium* SBPase construct to the  $\beta$ -glucuronidase (GUS) for expression analysis into *wheat* leaves.

**Figure 5.13:** Building transcriptional fusions of *Brachypodium* FBPA construct to the  $\beta$ -glucuronidase (GUS) for expression analysis into *wheat* leaves.

**Figure 5.14.** Colony PCR of the construction of SBPase and FBPA promoters with the chimeric expression cassettes (GUS) into *E coli*.

**Figure 5.15:** Digestion analyses of SBPase::GUS and FBPA::GUS plasmids.

**Figure 5.16:** Histochemical GUS assay for transient testing of *Brachypodium* SBPase and FBPA into wheat leaves.

**Figure 5.17:** Histochemical analysis of GUS activity in stable transformed wheat T0 plants with *Brachypodium* SBPase promoter.

**Figure 5.18:** Histochemical analysis of GUS activity in stable transformed wheat T0 plants with *Brachypodium* FBPA promoter.

**Figure 5.19:** Microscopy observation of GUS expression localisation in wheat T0 leaves driven by *Brachypodium* SBPase promoter.

**Figure 5.20:** Microscopy observation of GUS expression localisation in wheat T0 leaves driven by *Brachypodium* FBPA.

**Figure 5.21:** Histochemical analysis of GUS activity in stable transformed wheat T1 plants with *Brachypodium* SBPase promoter.

**Figure 5.22:** Histochemical analysis of GUS activity in stable transformed wheat T1 plants with *Brachypodium* FBPA promoter.

## **Chapter 1: Literature review**

## 1.1 General background

The rapid and continuing growth of the global population has significantly increased the demand for food and biofuel, thereby threatening food availability; this especially in the case for major grain crops, such as wheat and rice. There are approximately 850 million undernourished people in the world, mostly living in developing countries, and by the year 2050, the global demand for cereal production is expected to increase by 60% as the global population rises to about 9.6 billion (Food and Agriculture Organization [FAO], 2012). An approximately 50% increase in cereal yields is necessary to meet the demand and to ensure universal food availability (Horton, 2000; Fischer and Edmeads, 2010; Uematsu *et al*, 2012).

The increase in cereal production has significantly increasing the use of N fertilization to achieve the maximum high yield together with the required grain protein quality. For example, although approximately 250 to 300 kg N ha<sup>-1</sup> are currently being applied to wheat crop in order to attain about 13% protein content that required for breedmaking in the UK, a 10 tonnes ha<sup>-1</sup> of crop including 13% protein content exploits only 230 kg N ha<sup>-1</sup> of total applied N. Consequently, about 70 kg N ha<sup>-1</sup> could significantly be lost in the soil and impact on environment as well as economic issue (Shewry, 2009). A high input of energy and natural gases and oil are required for the production of N fertilisers through the process of Haber-Bosch. Subsequently, this involves in releasing considerable amounts of greenhouse gases such as CO<sub>2</sub> into the air, which lead to atmospheric pollution. When the N applied, oxygen depletion in the soils could be caused as a result of high amount of non-absorbed N which therefore, preventing the functional role of microorganisms in the soils to metabolize the non-absorbed N (known

as eutrophication) and reduce the soils fertility. As a consequence of soils eutrophication, there could be some toxic gaseous and ammonia ( $\text{NH}_3$ ) emissions of oxides N causing atmospheric pollutions from producing N. The loss of N fertiliser affects also economic cost to the farmers due to the increase price of N fertilisers compared with the grain yield price (Ramos, 1996). Therefore, increasing NUE has been a significant target for sustainable agriculture and environment together with improving yield.

In striving to achieve these goals, the process of photosynthesis should be considered, as this is known to be significant in determining the productivity of crops. Therefore, photosynthesis represents an unexploited opportunity in research aiming to increase crop yields. For example, it may be possible to increase crop yields using genetic manipulation to improve photosynthetic carbon fixation (Horton, 2000; Sharma-Natu and Ghildiyal, 2005; Raines, 2006; Feng *et al*, 2007; Rosenthal *et al*, 2011).

Photosynthesis is a process by which the sun's energy is absorbed and converted this to ATP and NADPH for the synthesis of a wide array of organic molecules. This process provides carbon skeletons that can be used for biosynthesis and metabolic energy in all cellular processes. This process also provides oxygen molecules, which are necessary for all aerobic organisms. This photochemical process consists of two distinct and associated phases and pathways. First, a light reaction occurs in the thylakoid membranes of chloroplast, where the light is converted into chemical energy (ATP) and reducing power (NADPH) and  $\text{O}_2$  is released (under light conditions). Second, there are reductive photosynthetic carbon reactions, also called the Calvin-Benson or  $\text{C}_3$  cycle (under dark reactions), in the chloroplast stroma. In the second

phase, the ATP and NADPH produced from light reactions are used to reduce and fix inorganic CO<sub>2</sub> to organic components (carbon skeletons), which are used for the biosynthesis of carbohydrate and are necessary for plant's growth; this process is called carbon fixation or assimilation (Bassham *et al*, 1950; Bassham, 2003; Raines and Paul, 2006; Stitt *et al*, 2010; Kramer and Evans, 2011; Jones *et al*, 2012).

Photosynthetic carbon metabolism in plants consists of two associated pathways – the Calvin–Benson cycle and the photorespiratory or C<sub>2</sub> cycle. Both pathways are initiated by the catalytic reaction of ribulose-1, 5-bisphosphate carboxylase/oxygenase (Rubisco) enzyme on the CO<sub>2</sub> acceptor molecule ribulose-1, 5-bisphosphate (RuBP). Carboxylation of RuBP produces 3-phosphoglycerate (3-PGA), whereas RuBP oxygenation yields one molecule of 3-PGA and one molecule of 2-phosphoglycolate (2PG; Figure 1). The CO<sub>2</sub>/O<sub>2</sub> ratio in leaves determines the balance between the carboxylation and oxygenation reactions (Kebeish *et al*, 2007; Maurino and Peterhansel, 2010).

## **1.2 The Calvin–Benson cycle**

Photosynthetic CO<sub>2</sub> assimilation occurs in the chloroplasts of plants, and inorganic carbon is usually assimilated by a specific cycle known as the Calvin–Benson cycle. This cycle of photosynthetic carbon reduction (PCR) is the major pathway of carbon fixation occurring in the chloroplast's stroma. In addition, this cycle plays a key role in the metabolism of plants, as well as in carbon flux (Geiger and Servaites, 1994). The sequence of this cycle of reactions was elucidated in the 1950s by Melvin Calvin and his colleagues, and this was followed by the identification of the enzymes that act to catalyse the reactions of this cycle. Finally, their kinetic properties were studied *in vitro*.

The net products of CO<sub>2</sub> assimilation are the triose phosphates, which are the key intermediates of the Calvin–Benson cycle and the main supply of starch and/or sucrose for the other biosynthetic pathways within the cycle (Bassham *et al*, 1950; Spreitzer, 1993; Raines, 2003; Lefebvre *et al*, 2005).

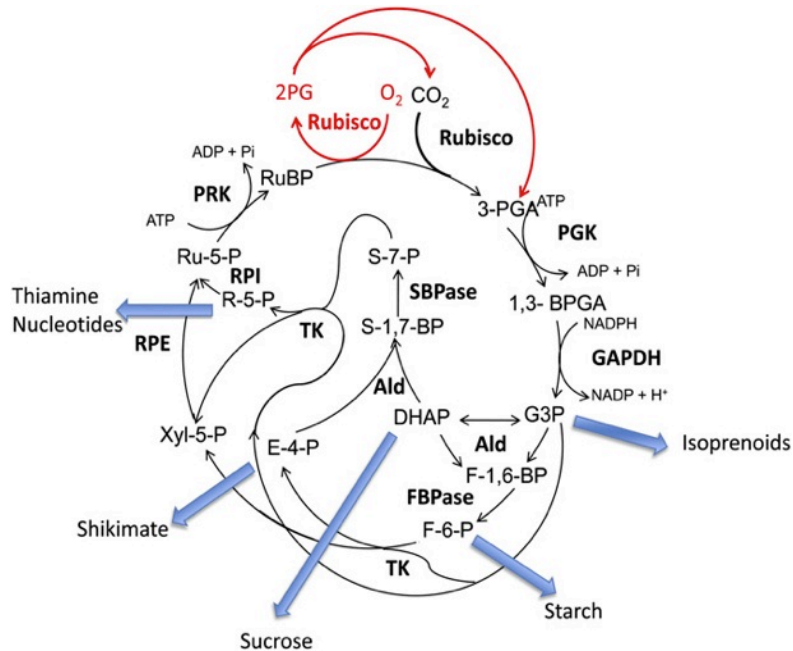


**Figure 1.1: The Calvin-Benson cycle map.** It starts with the Rubisco carboxylation reaction of the  $\text{CO}_2$  acceptor molecule RuBP, and results in 2 molecules of the stable three-carbon product phosphoglycerate (3-PGA). This is followed by the reductive phase of the cycle, which includes two reactions catalysed by 3-PGA kinase (PGK) and GAPDH, generating G-3-P. The G-3-P then enters the regenerative phase, catalysed by aldolase (ALD) and either FBPase or SBPase, generating Fru-6-P (F-6-P) and sedoheptulose-7-P (S-7-P). The F-6-P and S-7-P are usually exploited in reactions catalysed by TK, R-5-P isomerase (RPI) and ribulose-5-P (Ru-5-P) epimerase (RPE), generating Ru-5-P. This is followed, finally, by the conversion of Ru-5-P to RuBP, catalysed by PRK. The reaction of Rubisco oxygenation fixes  $\text{O}_2$  into the acceptor molecule RuBP, resulting in 3-PGA and 2-phosphoglycolate (2-PG), and  $\text{CO}_2$  and PGA are released through the photorespiration process (red arrows). As a consequence of this cycle, five significant products are created (blue arrows) (adapted from Raines, 2011).

### **1.2.1 Reactions of the Calvin–Benson cycle**

This cycle consists of 11 enzymes that act to catalyse 13 different reactions (Figure 1). Moreover, it comprises three distinct stages, namely carboxylation, reduction and a final regenerative stage. The first stage includes the carboxylation of the CO<sub>2</sub> acceptor molecule RuBP by Rubisco; subsequently, two molecules of a stable three-carbon product known as 3-PGA are formed. For this reason, this pathway is known as the C3 cycle. Then, the ATP and NADPH products of the photosynthetic light reactions are consumed in the reductive stage through two reactions utilising 3-PGA for atmospheric CO<sub>2</sub> fixation into carbon skeletons, triose phosphate, glyceraldehyde 3-phosphate (G3P) and dihydroxyacetone phosphate (DHAP); at this stage, they are directly exploited as key fuel for the rest of the metabolic process of higher plants. Finally, the CO<sub>2</sub> acceptor molecule (RuBP) is produced by the use of the triose phosphates in the regenerative phase. The carbon compounds generated within the cycle are exploited for plant growth (Woodrow and Berry, 1988; Geiger and Servaites, 1994; Lichtenthaler, 1999; Raines *et al*, 1999; Raines, 2003; 2011).

### **1.2.2 Regulation of the Calvin-Benson cycle**

A crucial balance between the export and regeneration of carbon needs to be maintained to prevent the consumption or loss of the main intermediates and to support continued cycle functions. This balance can be achieved by the high regulation of catalytic activities of several enzymes in the cycle. Particularly, the activities of several enzymes, including sedoheptulose-1, 7-bisphosphatase (SBPase) and fructose-1, 6-bisphosphate (FBP) aldolase, are usually controlled by the redox regulation properties through the ferredoxin/thioredoxin system, which modulates the activity of specific enzymes in response to the conditions of light and/or dark (Scheibe, 1990; Buchanan,

1991; Raines *et al*, 1999). In addition, it is quite possible that other conditions or limitations, such as stromal  $Mg^{+2}$  and pH, have a potential role in regulating and modulating the activities of Calvin–Benson cycle enzymes, such as SBPase, FBPase and Rubisco; these factors usually change in the chloroplast during the transition from dark to light. The majority of the Calvin–Benson cycle enzymes work at approximately pH=8, and the stromal pH is most likely to increase from 7 to 8 during the transition from dark to light (Nishizawa and Buchanan, 1981; Heldt *et al*, 1973; Werdan *et al*, 1975). This significant plant regulation plays a significant role in ensuring the flexibility of the plant (plastid) metabolism, which shifts from the reductive pentose phosphate pathway responsible for  $CO_2$  fixation during illumination to the oxidative pentose phosphate (OPP) pathway to generate NADPH at night (Schnarrenberger *et al*, 1995; Michels *et al*, 2005).

Thioredoxins are identified as small ubiquitous proteins of a molecular mass of approximately 12–14 kDa that include the conserved active site motif CGPC and can be found in both eukaryotes and prokaryotes. They play essential functions as protein disulphide oxidoreductases via their ability to control and reduce a redox disulphide bridge of target enzymes or proteins *in vitro* through the exchange reactions of cysteine thiol-disulphide (Meyer *et al*, 1999; Jacquot *et al*, 2002). It has been found that these proteins act as essential regulatory elements in the assimilation of carbon in oxygenic photosynthetic cells. Furthermore, two thioredoxin types have been recognised in bacteria and animal cells, whereas various forms are found in plants tissues; in plants, two types are found in chloroplasts, and the cytoplasm contains only one type and also one in mitochondria. The structural complementarity of these thioredoxin forms leads to the specificity and differentiation in their functions that makes specific interaction

between the different thioredoxin types and their target proteins possible, although they all share some similarities in size and redox properties. Based on their location in cells, a different electron donor system reduces thioredoxins. Therefore, thioredoxins found in either non-photosynthetic cells or the cytosolic photosynthetic tissues can be reduced by electrons from NADPH through the NADP/thioredoxin system. However, the chloroplastic thioredoxins of both plants and algae and oxygenic photosynthetic prokaryotes can usually be reduced through the ferredoxin/thioredoxin system; this is accomplished using electrons delivered by photosynthetic electron transport (Faske *et al*, 1995; Schürmann and Jacquot, 2000).

A light regulation pathway through the ferredoxin/thioredoxin system has a significant role in constituting the interface between the light reactions at the thylakoid membranes and exploiting the produced metabolites for further biosynthetic pathway purposes. For example, hexose phosphates are converted by the OPP pathway in the plastids of land plant into pentose phosphates generating NADPH. These reactions are contrary to that of the Calvin–Benson cycle, which is also known as the reductive pentose phosphate pathway; obtaining both pathways active simultaneously in the same compartment would result in a futile cycle with an utilisation of three ATPs per fixed CO<sub>2</sub>. As a result, a number of Calvin–Benson cycle enzymes can be activated in the light, as previously described, while the Glc-6-P dehydrogenase (G6PDH), which catalyses the first oxidative reaction of the OPP, is controlled and blocked after thioredoxin reduction (Wenderoth *et al*, 1997; Michels *et al*, 2005). Moreover, the activities of the Calvin–Benson cycle enzymes SBPase, FBPase, PRK and GAPDH are controlled by the ferredoxin/thioredoxin system during the day conditions (light and dark periods). There are some factors, such as CP12 protein, that that found to act regulating some

enzymes in the Calvin–Benson cycle such as PRK and GAPDH, where it forms a complex with these enzymes. It has been identified that CP12 protein can be found in all photosynthetic chloroplastic organisms at 12 kDa molecular mass. Moreover, it has been suggested that the Calvin–Benson cycle enzymes could be regulated via a NADPH-mediated reversible reaction of the complex form of PRK/CP12/GAPDH (Wedel *et al*, 1997; Wedel and Soll, 1998; Graciet *et al*, 2003).

### **1.2.3 The Rubisco enzyme**

#### **1.2.3.1 Structure and genetics**

Rubisco is classified as a complex, abundant enzyme that can be found in the stroma of photosynthetic eukaryotic organisms. It has a hexadecameric structure, and consists of two different subunit polypeptides with eight dimeric large (55 kDa) and eight tetrameric small (15 kDa) subunits. The large subunit is encoded as the *rbcL* gene in the chloroplast and includes the catalytic site and binding sites of the enzyme. Each large subunit contains two major domains, namely an N-terminal and C-terminal structural domain, which are organised in barrel alpha/beta. The majority of the residues of the active site are donated by some loop areas at the barrelled alpha/beta mouth, whereas some of the residues are contributed by two other loops that can be found in the N-terminal structural domain in the other large subunit (Parry *et al*, 1987; Parry *et al*, 2008). The small subunit is encoded by the nuclear genome *rbcS* gene and does not carry the enzyme catalytic site, but there is evidence that it can modulate Rubisco catalysis activity. As previously mentioned, Rubisco is responsible for catalysing the carboxylation reaction on RuBP to form two molecules of 3-PGA within the Calvin–Benson cycle. In addition, it acts to catalyse the oxygenation reaction on

RuBP, as well as to form one molecule of 2-PGA and one molecule of 3-PG during photorespiration (Ellis, 1979; Jones *et al*, 2012).

### 1.2.3.2 Regulation of Rubisco

Rubisco has been identified as a highly regulated enzyme that acts as a flux-controlling factor through the Calvin–Benson cycle in response to different environmental conditions (Geiger and Servaites, 1994). The mechanisms of Rubisco regulation are usually initiated when its *in vivo* activity is modulated by carbamylation and/or tight binding of inhibitors (I). Carbamylation involves the binding of an activator molecule of CO<sub>2</sub> (distancing from CO<sub>2</sub> reacting with the acceptor molecule, RuBP, throughout catalysis process) to a vital lysine residue in the catalytic site of the Rubisco enzyme (E), which results in stabilisation of the carbamate group via the consequent binding of Mg<sup>2+</sup>; as a result, a catalytically active complex form (E.CO<sub>2</sub>. Mg<sup>2+</sup>) is established. Sugar phosphates can block the enzyme's active site and work to prevent carbamylation by binding to the non-carbamylated or carbamylated enzyme form. Therefore, to remove the tightly bound inhibitor from the active sites of the enzyme, Rubisco activase enzyme is necessary to ensure that catalytic sites are unblocked and carbamylation is facilitated (Parry *et al*, 2008; Carmo-Silva *et al*, 2014) with the requirement of ATP (Wang and Portis, 1992).

Rubisco activase enzyme is found in all species of plants (Spreitzer and Salvucci, 2002). The functionality importance of this enzyme was explored in analytical studies on an Arabidopsis (*rca*) mutant from which plants could not grow and that died under the condition of ambient CO<sub>2</sub> (Somerville *et al.*, 1982); this was found to occur because of the lack of the Rubisco activase enzyme (Salvucci *et al.*, 1985). Subsequently, this

enzyme has been shown to be essentially required for activating and maintaining the Rubisco activity through its promotion function to remove and unblock the catalytic Rubisco site from any inhibitory factors, such as 2-carboxyarabinitol-1-phosphate (CA1P) (Robinson and Portis, 1988, 1989; Portis, 1992; Parry *et al*, 2008).

### **1.3 The Calvin–Benson cycle as a target to improve photosynthesis and NUE**

A goal of plant engineering research is to understand and manipulate several responses and enzymes within the Calvin–Benson cycle to create plant crops with enhanced yields through identification of the limitations of the enzymes in this process (Raines, 2003). Many research efforts have concentrated on gene manipulation techniques for improving the capacity of plant photosynthesis and increasing plant productivity as well as identifying and overcoming the restrictions imposed through the rate-limiting steps of the C3 cycle.

The limitations of C3 carbon fixation in restricted CO<sub>2</sub> conditions, such as high temperatures or drought, can be controlled by controlling the activity of the Rubisco enzyme; therefore, this enzyme has been considered a main target of research as it is the most significant limiting enzyme under ambient stress. These studies have focused on manipulating catalytic properties for improving the performance of plant photosynthesis by improving the carboxylase reaction efficiency in order to reduce photorespiration and significantly enhance carbon assimilation, as well as to improve yields. RuBP is catalysed by the Rubisco enzyme, despite the fact that this latter enzyme has both a low affinity for CO<sub>2</sub> and a low turnover rate of Rubisco. Moreover, one of the disadvantages of Rubisco in carbon fixation is that the 2-phosphoglycolate

product produced by RuBP oxygenation is recycled through the pathway of photorespiration with the release of CO<sub>2</sub> and NH<sub>3</sub>. Therefore, a variety of approaches, such as engineering the Rubisco protein, introducing genes encoding C4 cycle enzymes and genetically engineering the pathways of photorespiration, are being utilised to overcome these drawbacks (Uematsu *et al*, 2012; Raines, 2006). Three approaches have been implemented to reduce photorespiration, with an increase in the efficiency of Rubisco carboxylation being the centre of attention of two approaches. Both of these concentrate on the direct reduction of the reaction of oxygenase or Rubisco manipulation via increasing CO<sub>2</sub> concentrations around the Rubisco region. Alternatively, manipulating several enzymes in the Rubisco area is a main target of the third method of decreasing photorespiration (Raines, 2006). Nevertheless, these approaches not have been fully successful because there are other limitations imposed by the capacity of RuBP regeneration, which is determined by the electron transport chain capacity of ATP and NADPH to supplement the reaction of the regenerative phase of the C3 cycle. Moreover, C3 photosynthesis is stimulated by elevated CO<sub>2</sub>, increasing the substrate for the carboxylation reaction, and through the reduction of photorespiration. The methods for controlling photosynthesis are shifting from the limitations of the Rubisco enzymes to the limitations of RuBP regeneration (Rosenthal *et al*, 2011).

Furthermore, Rubisco represents approximately 50% of the total proteins in leaves and about 30% of leaf nitrogen (Mae *et al.*, 1993); therefore, it is considered as a key investment of nitrogen storage in crops (Parry *et al*, 2003). Nitrogen is known to be a main limitation and simultaneously an expensive nutrition source in agricultural systems (Parry *et al*, 2011). Data obtained from transgenic and dynamic modelling studies concerning growth of plants in conditions of elevated CO<sub>2</sub> provide robust evidence that

there is an over-investment in Rubisco. Therefore, a reduction in the Rubisco enzyme content in crops is an important requirement for reducing total leaf nitrogen in order to increase nitrogen use efficiency (NUE) (Ainsworth & Long, 2005).

## **1.4 Contributions and transgenic studies of the individual enzymes of the Calvin–Benson cycle in the photosynthesis process**

### **1.4.1 The Rubisco enzyme as a target for antisense studies**

Previous studies have identified Rubisco as an important target for genetic engineering using RNAi technology in the small subunit to investigate the limitations it imposes on photosynthetic capacity and growth performance by attempting to improve NUE (Rodermeil *et al*, 1988; Hudson *et al*, 1992). It has been found that the rates of both photosynthesis and growth are not significantly affected under low light conditions ( $340 \mu\text{mol m}^{-2} \text{s}^{-1}$ ) when the activity of Rubisco is reduced to about half of what is found in the WT (Quick *et al*, 1991). In contrast, under high light ( $1,050 \mu\text{mol m}^{-2} \text{s}^{-1}$ ), the photosynthetic capacity and growth of tobacco antisense plants were significantly affected (Stitt *et al*, 1991; Hudson *et al*, 1992). Hence, the results for transgenic plants with reduced levels of Rubisco grown in high  $\text{CO}_2$  illustrate that a reduction of 15–20% in the Rubisco protein levels could cause an approximately 10% reduction in the demand for nitrogen without having any negative effect on the photosynthetic efficiency of plants (Parry *et al*, 2013). Consequently, one aim of this project is to provide novel varieties of plants with less Rubisco for immediate and projected environmental conditions. This approach would be of particular benefit for future crops growing in the presence of elevated atmospheric  $\text{CO}_2$  concentrations (Stitt and Schulze, 1994).

Furthermore, an antisense approach was used with tobacco plants with reduced

Rubisco enzymes to investigate the photosynthetic N economy and growth rate under the condition of ambient CO<sub>2</sub>. Consequently, tobacco plants with 50–87% less Rubisco activity compared to the wild type were produced; the growth of tobacco plants with a large reduction in Rubisco activity was different from that of WT plants under 330 µbar of CO<sub>2</sub>, as they were found to grow much more slowly and showed an increased level of nitrate pool. In addition, the N investment per unit of organic matter was shown to be significantly reduced at the total plant level. However, at elevated CO<sub>2</sub> (930 µbar), plants with reduced Rubisco level were growing as the wild type (Masle *et al*, 1993). The antisense technology was also applied to rice, targeting the *RbcS* subunit under the control of the rice *RbcS* promoter to produce plants with less Rubisco, and this resulted in a 35% reduction in Rubisco activity in rice; the plants were then grown with different supplements of N concentrations, and subsequently, an improvement in the photosynthetic NUE under saturated CO<sub>2</sub> conditions was shown (Makino *et al.*, 1997). Therefore, this could be applicable to wheat plant.

#### **1.4.2 Sedoheptulose-1, 7-bisphosphatase (SBPase)**

The SBPase enzyme acts to catalyse the SBP dephosphorylation to sedoheptulose-7-phosphate (S7P). Its activity is found to be increased in the light by more than 10-fold as a consequence of the thioredoxin system through light-modulated activation. The levels of Mg<sup>+2</sup> and pH in the stroma can also regulate SBPase (Ölçer *et al*, 2001). Moreover, it has been highlighted as a controlled carbon flux enzyme in the Calvin–Benson cycle because of its regulatory features, as well as its localisation between two stages of the cycle – namely the assimilatory (the biosynthesis of starch and sucrose) and regenerative stages of RuBP (Raines *et al*, 1999; Rosenthal *et al*, 2011). Therefore, several metabolic approaches with transgenic and manipulatory tools will

have to be exploited to understand the regulatory mechanisms of this enzyme and the influence of these approaches on photosynthesis, as well as plant yields (Raines, 2003; Rosenthal *et al*, 2011).

Harrison *et al* (1997) used genetic manipulation methods to produce transgenic antisense tobacco plants (*Nicotiana tabacum*) by manipulating in SBPase activity through a reduction in SBPase levels. An antisense construct was used to produce these transgenic plants, where the expression of cDNA clone of SBPase antisense tobacco plants was driven by the use of the cauliflower mosaic virus (CaMV) promoter. As a result, it has been significantly observed that there were some clear changes in phenotype including reductions in the growth rate and chlorosis in the transgenic plants with reduced SBPase level 20% less than wild type. In addition, photosynthetic measurements showed considerable reductions in the rates of both the content of carbohydrate and starch levels in leaves and light saturated photosynthesis and CO<sub>2</sub> assimilation as well that have led to a reduction in the capacity of photosynthesis. Therefore, it is possible that the carbon assimilation rate may be limited by the activity of SBPase (Harrison *et al.*, 1997).

Transgenic antisense tobacco plants with variety-decreased levels of SBPase were utilised to investigate the suggestion that the activity of Rubisco enzyme is not affected by a possible decrease in RuBP regeneration. The results from this study indicated that the capacity of maximum RuBP regeneration dropped and the antisense plants did not display any important clear change in *in vivo* Rubisco activity. Hence, it was demonstrated that CO<sub>2</sub> assimilation could be limited by a small decrease in the activity

of SBPase through the capacity reduction for RuBP regeneration (Harrison *et al*, 2001). In another study, Consequently, it was shown that there were significant increases in both the photosynthesis rates and in the leaves area of transgenic plants with improved levels of SBPase. The greatest photosynthetic rate was in young leaves 12% relative to fully leaves expand (6%) in transgenic plants compared to wild type, under the condition of light saturation. In addition, more accumulated biomass (approximately 30%) was also observed compared to wild type plants. Therefore, it is strongly possible that the overexpression of the Calvin–Benson cycle enzyme SBPase can enhance both the plant growth and the capacity of photosynthesis in an early stage of plant development, as well as improving yielding plants (Lefebvre *et al.*, 2005). Moreover, Rosenthal *et al.*, (2011) performed another experiment using metabolic engineering approach to produce transgenic tobacco plants by overexpressing cDNA of SBPase *Arabidopsis thaliana* in order to examine the hypothesis that more photosynthesis stimulation and yield would be exhibited by transformants plants than wild type plants under growth conditions of completely open air at elevated CO<sub>2</sub>. Consequently, compared to WT tobacco plants, greater enhanced yield has obtained as a result of the greater rates of both CO<sub>2</sub> assimilation and electron transport for transformants tobacco plants at CO<sub>2</sub> elevated condition.

Furthermore, Feng and his co-workers have exploited this technique by producing transgenic rice plant through the overexpression of SBPase cDNA from rice cultivar 9311 (*Oryza sativa* ssp. *indica*) into rice cultivar zhonghua11 (*Oryza sativa* L. ssp. *Japonica*) under salt condition. As a result, plants with accumulated chloroplastic SBPase were generated with highly tolerant to salts conditions at the stages of young seedlings, and significantly, resulted in plants with improved CO<sub>2</sub> assimilation and more enhanced tolerance to the stress of salt relative to wild type. Hence, it has shown that

the SBPase over-expression has led to an enhancement the tolerance plants against salt condition during their growth and also photosynthesis (Feng *et al.*, 2007a). Furthermore, The SBPase cDNA of Rice plants (*Oryza sativa* L.) was over-expressed in rice plants zhonghua11 (*Oryza sativa* L.) to produce plants with enhanced activity of SBPase enzyme under high temperature condition during the young seedling growth. This study has significantly resulted in producing transgenic rice plants with enhanced photosynthesis and improved tolerance to heat condition compared to wild type plants as a result of increased SBPase content and activity. The activation of Rubisco enzyme was maintained by SBPase activity throughout acting to prevent the confiscation of Rubisco activase to the membranes of thylakoid from the soluble part of stroma and therefore, enhancing the tolerance of carbon assimilation to the condition of high temperature (Feng *et al.*, 2007b).

#### **1.4.3 Fructose-1, 6-bisphosphate (FBP) aldolase**

FBPaldolase enzyme is classified as non-regulated enzyme in the Calvin–Benson cycle that its activity can be regulated through either expression regulation or the degradation of protein. This enzyme acts to catalyse the reversible reaction to convert glyceraldehydes-3-phosphate (G-3-P) and dihydroxyacetone phosphate to fructose 1,6-bisphosphate and also function to convert erythrose 4-phosphate and dihydroxyacetone phosphate to sedoheptulose 1,7-bisphosphate (Haake *et al.*, 1999; Graciet *et al.*, 2004). Modelling and transgenic studies shows that the non-regulated Calvin–Benson cycle enzymes such TK and FBPaldolase, could potentially be significant controlling enzymes of photosynthesis in which they need to be considered for overexpression studies to explore the effect of this on crops photosynthesis and biomass production (Uematsu *et al.*, 2012).

Genetic manipulation tools are used and transgenic tobacco plants (*Nicotiana tabacum*) were produced with increased levels of plastid *FBPaldolase* cDNA from *Arabidopsis* plants by the introduction in the CaMV 35S promoter. As a result of the overexpression of plastid aldolase, ribulose 1,5-bisphosphate (RuBP) and its precursors have increased and accelerated; whereas, 3-phosphoglycerate levels was decreased. Consequently, greater photosynthesis rate was conducted in these transgenic plants due to the high activity of aldolase (1.4-1.9 fold), compared to wild type, that lead to the enhanced growth and biomass accumulation, especially under the condition of high CO<sub>2</sub> concentration (700 ppm) with the association with photosynthetic CO<sub>2</sub> elevation (Uematsu *et al.*, 2012).

As results of previous experimental studies, regeneration can be limited by several enzymes of the Calvin–Benson cycle that participated in the regeneration phase of RuBP such as *FBAaldolase* and *SBPase* enzymes (Haake *et al.*, 1999). In addition, the limitation to CO<sub>2</sub> assimilation that caused by RuBP regeneration when stomata are completely open, and also the rate of photosynthesis and also accumulated biomass can essentially be amended and improve by the increase of the RuBP supply to the pathway of Rubisco through the *SBPase* over-expression (Harrison *et al.*, 1998; Lefebvre *et al.*, 2005; Tamoi *et al.*, 2005). In addition, it was suggested that increasing the *SBPase* activity in rice under drought and high temperature conditions were resulted in plants with improved both photosynthesis and yields through the protection of both Rubisco chaperone and activase (Feng *et al.*, 2007). Therefore, over-expressing both *FBPaldolase* and *SBPase* enzymes has increased the photosynthetic rate in plants in previous studies in rice and this could be applied to wheat plant.

## 1.5 Regulation of gene constructs in transgenic plants

The structure of plant genes, like that of other eukaryotic genes, generally consists of the following components: chromosomal DNA, a primary transcript (pre-mRNA) and messenger RNA (mRNA). The chromosomal DNA comprises a promoter and a 5' region upstream of the beginning of the mRNA; the coding region, including a protein-coding region (exons) and a non-coding section (introns); the stop codon region (terminator); and finally, a 3' untranslated region (Hughes, 1996; Heslop-Harrison and Schwarzbacher, 2011).

Plants, like other multicellular organisms, conserve their inherited genetic information in the majority of their cells through different processes and also through a collection of various molecular mechanisms comprising coordinated gene expression that controls metabolism during different growth and developmental stages. Regulation of specific gene expression in various tissues during different developmental and growth stages is commonly mediated at three different levels: the transcriptional, post-transcriptional, and post-translational levels. Moreover, the activation and suppression of gene expression are mainly controlled at the transcriptional regulation level, which is significantly controlled and driven by promoters' elements (Peremarti *et al*, 2010; Hernandez-Garcia and Finer, 2014).

The promoter is known to be 1-2 kb upstream of the gene and consists of various *cis*-acting elements, which are specific binding sites for proteins involved in controlling transcription regulation (Peremarti *et al*, 2010). Two elements can be found at promoter regions: core and promoter regulatory components. The core element of the promoter is responsible for the specific pattern expression of a gene and is located ~40 bp

upstream from the transcriptional start site of the gene. It includes the TATA box (the binding site for the transcriptional initiation protein), which participates in orientating RNA polymerase II in the process of mRNA synthesis. The promoter regulatory component plays a role in activating, repressing or modulating gene expression located upstream of the core components. It consists of a variety of regulatory elements such as *cis*-acting enhancers and silencers elements, including two types of motifs: the box of either CAAT or AGGA (acts to regulate the transcriptional level). The promoter also contains the transcription factor elements that are an essential requirement for enhancing gene transcription by binding to the regulatory elements of the promoter. Both the availability of active transcription factors around the promoter and the type and number of regulatory elements in the promoter are essential for efficient transcriptional regulation (Hughes, 1996; Hernandez-Garcia & Finer, 2014; Jones *et al*, 2012).

In the genetic engineering of plants, three categories of promoters can be identified: constitutive, spatiotemporal and inducible. The constitutive promoter is identified as an active promoter in most or all species tissues during all periods of growth and development. The activation of the spatiotemporal promoter can be observed in specific tissues, such as photosynthetic plant tissues, and at specific developmental times. The inducible promoter is inactive until induced by a chemical application (biotic factors) or in response to abiotic factors, such as light and heat; therefore, the timing of expression can be controlled. All promoter types share the same core sequences, including the elements of an initiator, the box of TATA and the *cis*-acting motifs in which they bind to the transcription factors in order to control the expression of genes. These transcription factors play a significant role in controlling the activity of promoters as regulatory proteins (Peremarti *et al*, 2010; Jones *et al*, 2012).

## **1.6 Identification of promoters of the Calvin–Benson cycle gene encoded enzymes**

The Calvin–Benson cycle enzymes, including SBPase and FBPaldolase, are mainly located and expressed in the leaves chloroplast. Their regulation activity is driven by light and other environmental changes, and they were demonstrated to have significant participations in photosynthesis process (Raines *et al*, 1999; Lefebvre *et al.*, 2005). The transcriptional nuclear gene-encoding protein of the Calvin–Benson cycle is directly activated by light. This can be mediated by the presence of *cis*-acting elements, which are sensitive to light. For example, the promoters of all different enzymes encoded by different genes of the Calvin–Benson cycle contain the G-box (Hughes *et al*, 2000), that necessary for the expression activity at the level of transcription (Gilmartin *et al.*, 1990). In case of SBPase enzyme, it is known to be highly regulated by the control of light, and expressed completely in the leaves chloroplast. In addition, it is found as a single gene in the majority of higher plants (Willingham *et al.*, 1994). Therefore, the chance is going to be high of its promoter to drive strong expression in the mesophyll cells of wheat.

Producing a certain chimeric gene product with the required level of expression in the targeted tissues is the most important requirement for efficient genetic engineering that can easily be accomplished by controlling and driving the modified gene with particular and strong promoter elements. A variety of characterised promoters have been made widely available to date. For example, the CaMV 35S constitutive promoter is commonly used to drive high expression levels of transgenic dicotyledonous plants. However, low activities have also been observed in monocotyledonous crops. Moreover, the promoters that are derived from monocot plants have higher activities in

transgenic monocots than in transgenic dicots. Consequently, various promoters need to be developed and made widely available for both monocots and dicots. It has been found that different promoters drive high levels of constitutive gene expression in transgenic monocots, such as *Ubi1* from maize (*Zea mays*), and some rice-derived promoters, including *Act1*, *OsTubA1*, *OsCc1*, *RUBQ1* and *RbcS* promoters. The most common promoter used in monocot crops is *Ubi1* and rice *Act1* promoters because it can efficiently drive strong, constitutive expression in almost all plant tissues whereas its activity is shown only in young tissues and tends to decrease during the growth and development of organs (Jang *et al.*, 2002; Park *et al.*, 2010).

Recently, five constitutive gene promoters, APX, SCP1, PGD1, R1G1B and EIF5, were analysed from the data of rice microarray and assessed in transgenic rice (Park *et al.*, 2010). Subsequently, the APX, R1G1B and PGD1 gene promoters exhibited high, distinct and strong activities in all plant tissues and at all growth development stages. In addition, some studies have investigated derived promoters from viruses to be used for monocot transformation, e.g. common oat (*Avena sativa*) (Tzafrir *et al.*, 1998). Moreover, previous studies on the mesophyll-specific expression of gene were mainly concentrated on several genes which have a role in photosynthesis process such as Rubisco small subunit (*rbcS*), chlorophyll a/b binding protein (*cab*) family and, as a result, many *cis*-elements have been reported and with leaf-specific and light-response expression. However, chloroplast enzymes are found to be encoded in all these genes that confer mesophyll-specific expression. Less information regarding the elements of promoters involved in the synthesis of sucrose has been accumulated in monocots (Ha and An, 1988).

Although many efforts have been made to isolate and characterise efficient constitutive mesophyll-specific promoters from dicot plants and other sources, there is still a shortage of available strong and capable mesophyll promoters for driving strong expression levels in wheat (*Triticum aestivum*) under different growth and developmental conditions. Therefore, it is important to continue the search for and design new promoters and transcriptional regulatory elements with the desired features and characteristics to being used for driving strong desired expression level in wheat mesophyll (Tao *et al.*, 2002; Abdul *et al.*, 2010; Park *et al.*, 2010). Moreover, a wide variety of useful native promoters can be derived from genomic plants (monocots or dicots) that can be used to discover some *cis*-acting elements, and subsequently, the regulation of gene expression can be better understood (Hernandez-Garcia *et al.*, 2010).

### **1.7 Aims of this study**

As previously discussed, several studies have shown that increased levels of regeneration-phase enzymes of the Calvin–Benson cycle, such as SBPase, could stimulate the rate of photosynthesis and improve plant growth and total biomass (Lefebvre *et al.*, 2005; Feng *et al.*, 2007a; Feng *et al.*, 2007b; Rosenthal *et al.*, 2011; Parry *et al.*, 2011). Moreover, data obtained from transgenic and dynamic modelling studies concerning growth of plants in conditions of elevated CO<sub>2</sub> provide robust evidence that there is an over-investment in Rubisco. Therefore, a reduction in the Rubisco enzyme content in crops is an important requirement for increasing NUE (Ainsworth and Long, 2005). Furthermore, the searching for new promoters to be used for driving a strong expression level in wheat mesophyll is a significant target as a new tool to improve wheat leaf photosynthesis, as there is still a shortage of mesophyll

promoters with the appropriate expression levels in wheat (*Triticum aestivum*) under different growth and developmental stages and conditions (Tao *et al*, 2002; Abdul *et al*, 2010; Park *et al*, 2010).

The first aim of this project was to screen and analyse transgenic wheat plants with increased SBPase activity to test the hypothesis that increasing SBPase activity level could lead to improvements in wheat photosynthesis, growth and plant biomass. The second aim was to test the hypothesis that a slight reduction in Rubisco activity in wheat does not affect photosynthesis and to determine the extent to which Rubisco activity can be decreased without any negative effect on photosynthesis in an attempt to improve NUE by producing transgenic wheat plants where the Rubisco small subunit enzyme has been down regulated. The final aim was to identify and analyse *Brachypodium* SBPase and FBPaldolase promoters to drive strong expression of photosynthetic transgenes in wheat leaf to improve photosynthesis using genetic manipulation approaches.

## **Chapter 2: Materials and Methods**

## **2.1 Materials**

### **2.1.1 Chemicals, antibiotics and molecular biology reagents**

All chemicals and antibiotics used in this study were purchased from Sigma except acrylamide, ECL reagent that were purchased from Amresco and Pierce, respectively, and Biomol Green reagent was purchased from Biomol (Biomol, AK-111).

PCR DNA purification kit was purchased from GE- Health care. Furthermore, the optimal concentrations of antibiotics were determined to select for transformed plants or bacteria. The antibiotics were added to bacteria growing media at the concentrations given in table 2.1.

### **2.1.2 Enzyme**

Restriction enzymes were purchased either from Invitrogen or Fermentas and used with the appropriate buffers recommended by the manufacturer. All other enzymes were purchased from Invitrogen, Roche, Sigma, Biolabs and Echelon Biosciences Inc and stored as recommended by the company (Table 2.2).

### **2.1.3 Bacterial strains**

The *Escherichia coli* (*E.coli*) strain that used throughout this study was TOP10. *Agrobacterium tumefaciens* strain was GV 3101, which is routinely used in the laboratory for the Tobacco transient transformation.

**Table 2.1. Antibiotics used during this study.**

<b>Antibiotic</b>	<b>Stock concentration</b>	<b>Storage</b>	<b>Working concentration (in bacteria)</b>
Ampicillin	100 mg mL <sup>-1</sup> in H <sub>2</sub> O	-20 °C	100µg mL <sup>-1</sup>
Carbenicillin	100 mg mL <sup>-1</sup> in H <sub>2</sub> O	-20 °C	100µg mL <sup>-1</sup>
Kanamycin	100 mg mL <sup>-1</sup> in H <sub>2</sub> O	-20 °C	100µg mL <sup>-1</sup>
Hygromycin	100 mg mL <sup>-1</sup> in H <sub>2</sub> O	-20 °C	100µg mL <sup>-1</sup>
Genamycin	100 mg mL <sup>-1</sup> in H <sub>2</sub> O	-20 °C	100µg mL <sup>-1</sup>
Rifampicin	100 mg mL <sup>-1</sup> in H <sub>2</sub> O	-20 °C	100µg mL <sup>-1</sup>

**Table 2.2. Enzymes and intermediates purchased plus their details**

<b>Enzymes</b>	<b>Company</b>	<b>Catalogue Numbers</b>
<b><u>DNA Polymerases</u></b>		
Phusion High-Fidelity DNA Polymerase	BioLabs	F-530
T4 DNA ligase	Invitrogen	15224-017
Dream <i>Taq</i> DNA Polymerase	Fermentas	EP0401
Super script <sup>TM</sup> II Reverse Transcriptase	Invitrogen	18064-022

#### **2.1.4 Plasmid vectors and primers**

All plasmid expression vectors were used throughout this research is detailed in Table 2.3 with corresponding antibiotic resistance.

All synthetic primers used in this project were synthesized by Invitrogen and detailed in Table 2.4. Primers stock concentration was 100 pmole  $\mu\text{l}^{-1}$  and the working concentration of primers for PCR was 10 pmole  $\mu\text{l}^{-1}$ , hence, to make a appropriate working concentration, the stock primers were diluted ten times.

#### **2.1.5 Plant material**

Wild type *Brachypodium distachyon* was used for the cloning of both SBPase, and FBPAldolase 2-kb promoters. All the other analyses were performed on *Nicotiana benthamiana* and wheat plants.

#### **2.1.6 Gas exchange apparatus**

An open infra-red gas analysis (IRGA) of photosynthesis rate was done using the gas exchange system with an integral blue-red LED light source (LI-COR 6400; LI-COR, Lincoln, Nebraska).

**Table 2.3. Plasmid vectors, bacteria cell strain and appropriate resistance antibiotic**

<b>Plasmids</b>	<b>Antibiotic resistance</b>	<b>Working concentration</b>	<b>Vectors Supplier</b>
pRRes14.14 vector	Carbencyllin	100 $\mu\text{g mL}^{-1}$	Rothamsted Research Centre
pENTR <sup>™</sup> Directional TOPO®	Kanamycin	100 $\mu\text{g mL}^{-1}$	Invitrogen
PGWB3 vector	Kanamycin and Hygromycin	100 $\mu\text{g mL}^{-1}$	Nakagawa <i>et al.</i> , (2007)
PGWB40 vector	Kanamycin and Hygromycin	100 $\mu\text{g mL}^{-1}$	Nakagawa <i>et al.</i> , (2007)
P19	Kanamycin	100 $\mu\text{g mL}^{-1}$	Prepared in the lab
GV1301	Rifmycin, Kanamycin, Hygromycin and Genamycin	100 $\mu\text{g mL}^{-1}$	Prepared in the lab

**Table 2.4: Primers used in this study**

<b>Primer names</b>	<b>Sequences</b>	<b>Genes amplified</b>	<b>Features</b>
Gateway-clo_SBPase F	<u>CACCTCGACGTCCATATGGCCCA</u>	<i>Brachypodium</i> SBPase promoter	Additional CACC
Gateway-clo_SBPaseR	TGCTGCGATGCGAGCTGC	<i>Brachypodium</i> SBPase promoter	-
Gateway.clo_FBPA.F	<u>CACCTCATTGGACGTGTTGATGTGC</u>	<i>Brachypodium</i> FBPaldolase promoter	Additional CACC
Gateway-clon_FBPA. R	TGTTTCTGGCTCCAAAGG	<i>Brachypodium</i> FBPaldolase promoter	-
Cloning_SBPase F	5'- <u>ttggcgcgcc</u> -TCGACGTCCATATGGCCCA	Wheat SBPase promoter	MluI restriction site
Cloning_SBPase R	5'- <u>ttacgcgt</u> -TGCTGCGATGCGAGCTGC	Wheat SBPase promoter	AscI restriction site
Cloning_FBPA. F	5'- <u>accggg</u> -TCATTGGACGTGTTGATGTGC	Wheat FBPaldolase promoter	XmaI restriction site
Cloning_FBPA. R	<u>5'-ttgaattc</u> -TGTTTCTGGCTCCAAAGG	Wheat FBPaldolase	EcoRI restriction site
Screening_RbcS F	AAGAAGTTCGAGACCCTGTCTTA	Wheat RbcS	-
Screening_RbcS R	GTAAATTGCACTCTAGATTTTGCTT	Wheat RbcS	-
qPCR_RbcS F	agttcagcaaggttgcttc	Wheat RbcS	-
qPCR_RbcS R	cctcgttgagcacctgtgta	Wheat RbcS	-
qPCR_SBPase F	CATGTCAAGGACACCACGAC	Wheat SBPase cDNA	-

qPCR_SBPase R	GTCAAATGTGGCCCTCAGAT	Wheat SBPase cDNA	-
qPCR_2291- F	GCTCTCCAACAACATTGCCAAC		Reference gene, Paolacci <i>et al.</i> , (2009).
qPCR_2291- R	GCTTCTGCCTGTCACATACGC		Reference gene, Paolacci <i>et al.</i> , (2009).
Actin-F	5'-GAATCCATGAGACCACCTAC-3'		Reference gene
Actin-R	5'-AATCCAGACACTGTACTTCC-3'		Reference gene

## 2.2 Methods

### 2.2.1 Bioinformatics analysis

The *Brachypodium* sequences of 2-kb upstream promoter region SBPase (Bradi2g55150), FBPAldolase (Bradi4g24367), were obtained from the Universal Protein Resource (UniProt) (<http://www.uniprot.org/>) and Phytozome database (<http://www.phytozome.net>). Each gene sequence was aligned, at the protein level, using ClustalW (Larkin *et al.*, 2007) to obtain the most conserved sequence of each gene in dicot and monocot plants in order to identify the similarities between the genes in *Brachypodium*, wheat.

### 2.2.2 Molecular biology approaches

#### 2.2.2.1 DNA Extraction from wheat leaves

DNA was extracted from one-week old *Brachypodium distachyon* and wheat leaves as follows: tissues were placed into 2 ml micro-tubes (in a 96 tube rack), frozen in dry ice and freeze-dried overnight. After that, the freeze-dried tissues were ground using the Qiagen grinder (Retsch mill, Type MM 300) for 5 minutes at a frequency of 25/second. Then, 600 µl of pre-heated extraction buffer was added to the tubes and incubated at 65°C for 30 min. Next, the samples were cooled down in the fridge for 15 min before adding 300 µl of 6 M ammonium acetate and then left to stand for 15 min in the fridge. Samples were then centrifuged at 13000 g and 4°C to collect the precipitated proteins and plant tissues. 600 µl of the supernatant was recovered into a new collection tube containing 360 µl of isopropanol. In order to pellet the DNA, samples were centrifuged for 15 min at 13000 g at 4°C. Then the DNA pellets were washed using 70% ethanol

and centrifuged for 15 minutes at 13000 g and 4°C. Finally, the pellets were re-suspended in 50 µl of purified water, and stored at -20°C for further screening analysis.

### **2.2.2.2 Primers design**

The primers used for gateway, traditional cloning, and expression analysis were designed and formatted using the primer extension analyses (Primer3 plus) software (Table 2.4) (Untergrasser *et al.*, 2012).

### **2.2.2.3 Polymerase chain reaction (PCR)**

#### **2.2.2.3.1 Amplification of specific gene fragment for cloning using PCR**

To amplify 2-kb promoter of SBPase, FBPaldolase from *Brachypodium distachyon* extracted DNA for cloning purpose, high fidelity PCRs were performed using a high fidelity system in a 50 µl total volume. The reactions were prepared as follows: 1.5 µL of forward primer (10 pmol), 1.5 µL of reverse primer (10 pmol), 5 µL of phusion high fidelity buffer (containing 0.1 M Tris-HCl; pH 8.3, 0.1 mg/ml gelatine, 500 mM KCl, and 25 mM MgCl<sub>2</sub>), 1 µl of phusion high fidelity polymerase enzyme and 1 µL of dNTPs were mixed in 2 µL of extracted DNA and 38 µL sterile double purified water.

The PCR conditions were: 30 seconds at 98°C, followed by 35 cycles of 15 seconds at 98°C, 30 seconds at 60-68°C (based on primers T<sub>m</sub>), 2 min/kbp elongation stage at 72°C and finally 10 minutes at 72°C, before the incubation at 4°C.

#### **2.2.2.3.2 Amplification of specific gene fragment for screening using PCR**

To confirm the presence of transgenic genes into transgenic wheat plants, PCR was

used. The reactions were prepared as follows: 1  $\mu\text{L}$  of forward primer (10 pmol), 1  $\mu\text{L}$  of 10 pmol reverse primer, 2  $\mu\text{L}$  of 10x buffer (containing 0.1 M Tris-HCl; pH 8.3, 0.1 mg/ml gelatine, 500 mM KCl, and 25 mM  $\text{MgCl}_2$ ), 0.2  $\mu\text{L}$  of Dream *Taq* polymerase enzyme and 0.2  $\mu\text{L}$  of dNTPs were mixed with 1.5  $\mu\text{L}$  of extracted DNA samples and 14.1  $\mu\text{L}$  sterile double purified water.

The PCR specifications were as follows: 3 minutes at 98°C, followed by 35 cycles of 30 seconds each at 98°C, 30 seconds at 60-68°C (based on primers  $T_m$  of each gene), 1 min at 72°C, and finally, 10 min at 72°C and was kept at 4°C.

#### **2.2.2.3.3 Colony screening using polymerase chain reaction (PCR)**

To confirm the success of the constructs, a colony PCR was used to detect the presence of the inserts into the expression vector clone. The gene of interest could easily be detected in the transformed *E. coli* or *Agrobacterium* cells using their specific primers without any need for plasmid DNA purification. The reactions were prepared as follows: 10 colonies from each plate were picked and re-suspended separately in 14.1  $\mu\text{L}$  of sterile double distilled water. One  $\mu\text{L}$  of forward primer (10 pmol), 1  $\mu\text{L}$  of 10 pmol reverse primer, 2  $\mu\text{L}$  of 10x buffer (containing 0.1 M Tris-HCl; pH 8.3, 0.1 mg/ml gelatine, 500 mM KCl, and 25 mM  $\text{MgCl}_2$ ), 0.2  $\mu\text{L}$  of Dream *Taq* polymerase enzyme and 0.2  $\mu\text{L}$  of dNTPs were mixed into the tubes containing re-suspension cells.

The PCR specifications were as follows: 3 minutes at 98°C, followed by 35 cycles of 30 seconds each at 98°C, 30 seconds at 60-68°C (based on primers  $T_m$ ), 1-2 minutes at 72°C (based on product size), and finally, 10 minutes at 72°C.

#### **2.2.2.4 Agarose gel electrophoresis analysis of DNA and RNA**

Agarose gel electrophoresis was used as a common technique in biochemistry and molecular biology to separate DNA or RNA molecules by size. Samples were mixed with 10X loading dye buffer (0.25% bromophenol blue, 50% glycerol, 450 mM Tris-borate (pH.8), 12 mM EDTA) and then loaded individually on 1% or 0.5% agarose (Fisher Scientific) in TBE (Tris-borate (TBE) buffer (90 mM Tris-borate, 2 mM EDTA pH.8) containing 0.5 µg sybre save. The gels were run at 110V for 30 mins using power supply (Kikusui electronic corp., Taiwan). 5 µl of DNA 1kb Ladder (Invitrogen) used as a DNA marker along with 0.5X TBE buffer.

#### **2.2.2.5 Preparation of E.coli competent cells using CaCl<sub>2</sub> method**

A single colony of *E.coli* was selected, and inoculated into 10 ml of Luria Broth (LB) and was left to grow by shaking overnight at 37°C. then 1 ml of the culture was transferred into 150 ml of LB and the cells were grown shaking at 37°C for about 2 h, until the cells were reached to the optical density at 600 nm. The culture was centrifuge for 15 min at 3,000g and 4°C, to harvest the cells. The supernatant was discarded and the pellet cells were re-suspended in 20 ml of ice cold 0.1 M CaCl<sub>2</sub>. Then the cells were placed on ice for 20 min and centrifuged for 15 min at 3,000 g and 4°C, to harvest the cells. The pellet was re-suspended again in 2 ml of 0.1 M CaCl<sub>2</sub>. Consequently, the competent cells were ready for transformation and stored at -80°C.

#### **2.2.2.6 Transformation of E.coli competent cells (TOP10) using heat shock**

A total 2.5-5 µl of plasmid (about 10 ng) was incubated in 50 µl of *E.coli* competent cells (TOP10) and placed on ice for 30 min. The cells were then heat shocked in a water bath for 60-90 S at 42°C. The samples were chilled on ice for 2 min and 1ml of

LB was added. The cells were incubated in shaker for an hour at 37°C to recover and start expressing antibiotic resistance. The cells were harvested by centrifugation for 5 mins at 3000 g. Then 150 µl to 200 µl of cells were re-suspended and spread on LB agar plates containing the appropriate antibiotic. Then plates were incubated upside down at 37°C for overnight.

#### **2.2.2.7 Preparation of *Agrobacterium* competent cells**

A single colony of *Agrobacterium* (GV3101) was inoculated into 10 ml LB liquid media containing 100 mg L<sup>-1</sup> of rifampicin and grown shaking at 28°C for overnight. The next day, 2 ml of the culture were transferred into 50 ml LB liquid media containing 100 mg L<sup>-1</sup> of rifampicin and allowed to grow at a shaker at 180 rpm and 28°C until reach to the optimal density (OD600 of 0.5-0.1). Then, the culture was rapidly chilled on ice and centrifuged for 15 min, at 3000 g at 4°C. The supernatant was discarded and the pellets were re-suspended in 4 ml ice-cold 10% glycerol as well as centrifugation at 3000 g for 15 min at 4°C. The washing step was repeated for two further times with ice-cold 10% glycerol. The *Agrobacterium* pelleted cells were re-suspended in 1 ml ice-cold 10% glycerol. Finally, 50 µl aliquots of competent cells were transferred into 1.5 ml tubes, and snapped freeze in N<sub>2</sub> and stored at -80°C and ready for transformation.

#### **2.2.2.8 Transformation of *Agrobacterium* competent cells by electroporation**

An aliquot of *Agrobacterium* competent cells (50 µL) was placed in a chilled purified cuvette (ThermoHybaid, EP-ECU-102) on ice, with 2 µL of purified plasmid DNA from mini-prep, and was left on ice for 20 min. The *Agrobacterium* transformation was carried out using electroporation (Easyject plus, EquiBio LTD, Angleur, Belgium) at

2500 V, 192  $\Omega$  and 40  $\mu$ F. They were then incubated in 300 $\mu$ l of LB liquid media shaking at 150 rpm at 28°C for 3 hours, followed by a centrifugation step at 3000 g for 5 min. They were re-suspended in 100  $\mu$ L LB, and spread on LB agar media containing rifampicin (50 mg L<sup>-1</sup>), gentamicin (25 mg L<sup>-1</sup>), Kanamycin (50 mg L<sup>-1</sup>), and hygromycin (33 mg L<sup>-1</sup>) antibiotics and incubated upside-down at 28°C for 3 days.

### **2.2.2.9 Cloning of SBPase and FBPadolase promoters for expression analysis**

#### **2.2.2.9.1 Cloning of SBPase and FBPadolase promoters using Gateway technology for the transient expression analysis in *N. benthamiana* leaves**

For the transient expression analysis in *N. benthamiana* leaves, the 2-kb promoter fragment of *Brachypodium* SBPase (Bradi2g55150) and FBPaldolase (Bradi4g24367) genes were separately PCR-amplified from genomic DNA (as described in the method 2.2.4.1) and cloned separately into the Gateway entry vector pENTR™ Directional TOPO® (supplied by Invitrogen) through BP reaction (entry clone). After that, LR reactions were performed with the destination vectors pGWB3 to produce binary vectors carrying the fusion constructs with GUS (SBPase::GUS and FBPaldolase::GUS) (expression clone).

In order to study the sub-cellular localization of the 2kb promoter of both SBPase and FBPaldolase, the destination vector pGWB40 was used to generate two binary vectors carrying the fusion constructs with eYFP (enhanced yellow fluorescence protein) (SBPase::eYFP and FBPaldolase::eYFP).

#### **2.2.2.9.2 Traditional cloning of SBPase and FBPaldolase promoters for the transient expression analysis in wheat leaves**

For the transient expression analysis in wheat, the 2-kb promoter fragment of *Brachypodium* SBPase and FBPaldolase genes were also PCR-amplified and purified using NT1 binding buffer and NT3 washing buffer. Then, 2-kb of SBPase was cloned into the *Ascl* and *Mlul* sites of the pRRes14.041 vector (with GUS, supplied by Rothamsted Laboratories) to generate an expression vector for the wheat transient transformation. Similarly, the 2-kb of FBPaldolase was cloned into the *Xmal* and *EcoRI* sites of the pRRes14.041 vector to generate another expression vector for the wheat transient transformation using the T4 DNA ligase enzyme as described in Invitrogen's manual protocol. Primers used for the construction of plasmids are listed in Table 2.1.

#### **2.2.2.10 Plasmids DNA preparation from bacterial cells using Mini prep kit**

The plasmid DNAs were purified using Thermo Scientific GeneJET Midi prep kit (K0502, K0503).

A single colony from a fresh streaked plate was picked and inoculated in 5-10 ml LB liquid media with appropriate antibiotics, and incubated for overnight shaking at 240 rpm at 37°C. then the bacterial culture was harvested by centrifugation at 14000 g for 15 min at 4°C. After discarding the supernatant, the pelleted cells were re-suspended in 250 µl of the re-suspension solution, and the cell suspension was transferred to a microcentrifuge tube and pipet up and down to re-suspend the bacterial cells completely. 250 µl of the Lysis solution was added and gently mixed thoroughly by inverting the tube 4-6 times until the solution becomes slightly clear and viscous. Then 350 µl of the Neutralization solution was added and gently mixed immediately by inversion 4-6 times to avoid localized bacterial debris precipitation. Then it was

centrifuged at 13000 g for 5 min to pellet cells. The supernatant was transferred to the supplied GeneJET spin column and centrifuged for 1 min at 13000 g. then the supernatant was discarded and 500 µl the washing solution was added to the column and centrifuged at 13000g. The washing step was repeated again. The pelleted DNA was air-dried for 2 min. Finally, 50 µl sterile double distilled water was added to the centre of the column membrane, and plasmid DNA was collected in a new micro-centrifuge tube by centrifugation at 13000 g for 2 min, and stored at -20°C.

To prepare a high concentration of plasmids for wheat bombardment transformation (50 µg at 1 mg/ml), plasmids were isolated using the Quiagen Midi prep kit as described below.

#### **2.2.2.11 Plasmids DNA isolation from bacterial cells using Quiagen Midi prep kit**

To obtain a pure plasmid DNA with high concentration that required for sequencing, digestion as well as transformation, the plasmid DNAs were purified using Quiagen Midi prep kit (Quiagen 12143) protocol.

A single positive colony containing the plasmid was picked and inoculated in 5 ml LB liquid culture with appropriate antibiotics as a starter culture, and incubated for 7 h shaking at 240 rpm at 37°C. Then the starter culture of 5 ml was diluted in 200 ml LB media with appropriate antibiotics and was allowed to grow at 37°C shaking overnight at 240 rpm. The culture was spun down at 12000 g (SS-34 fixed angle roter Sorvall RC5C) for 15 min at 4°C to harvest bacterial cells. After discarding the supernatant, the pelleted cells were re-suspended in 8 ml of buffer P1 (50 mM Glucose, 25 mM Tris-HCl pH 8, 10 mM EDTA, 100 mg L<sup>-1</sup> RNase A) by pipetting up and down. Then, 8 ml of lysis

buffer P2 (200 mM NaOH, 1% SDS) was added and gently mixed thoroughly by inverting the tube 4-6 times and incubated for 5 min at room temperature. 8 ml of neutralization buffer P3 (3 M potassium acetate, 11.5% glacial acetic acid) was added and immediately mixed by inversion the tube 4-6 times, and then incubated on ice for 20 min. the tube were centrifuged for 30 min at 4°C at 20.000 g (14000 rpm) to precipitate the cell debris. The supernatant was carefully applied into a Quiagen column that was pre-equilibrated with 10 ml QBT (750 mM NaCl, 50 mM MOPS [PH 7], 15% (v/v) isopropanol, 0.15% triton X-100 (v/v)). The supernatant was allowed to enter the column matrix by gravity flow and was washed two times with 20 ml QC buffer (1.0 M NaCl, 50 mM MOPS PH 7.0, 15% Isopropanol (v/v)). The elution of DNA was done with 5 ml buffer QF (1.25 M NaCl, 50 mM Tris-HCl PH 8.5, 15% Isopropanol (v/v) and collected in a new tube. The DNA was then precipitated by the addition of 3.5 ml of isopropanol, and immediately mixed and centrifuged for 30 min at 14000 g at 4°C to pellet the DNA. The pelleted DNA was washed with 70% ethanol and centrifuged again at 14000 g for 15 min. The ethanol supernatant was discarded and the pelleted DNA was air-dried and then re-suspended in 50 µl sterile double distilled water, and stored at -20°C.

#### **2.2.2.12 Restriction Digest of plasmid DNAs**

The SBPase and FBPAldolase GUS Quiagen midi prep plasmids (1 µg to 1.5 µg) were digested separately to confirm the presence of the insert in the GUS vector. The total volume was 30 µL using 1 µL PvuII (10 units) restriction enzymes with 4 µL of the corresponding buffer, 0.5 µL of BSA, 4 µL of the plasmid and 20.5 µL sterile double distilled water. The solution was then incubated at 37°C for 3 h. To confirm the success of the construct, the purified plasmids were sent to the Bioscience Company for

sequencing using special primers listed in Table 2.4.

#### **2.2.2.13 RNA extraction from wheat leaves**

Total RNA was extracted by grinding 3 cm<sup>2</sup> of mature leaf in N<sub>2</sub> using Trizol reagent (Sigma T9429). 1 ml of Tri reagent was added to a powder grinded materials and vortexed for 1 min and incubated for less than 5 min at RT. Then it was centrifuged for 10 min at 13000 g at 4°C. the supernatant was then mixed with 200 µl chloroform, incubated for 15 min at RT and centrifuged at 13000g for 15 min at 4°C. 450 µl of aqueous phase was transferred and mixed with 500 µl of isopropanol, allowed at RT for 10 min and centrifuged for 15 min at 13000 g and 4°C to pellet the RNA. This RNA pellet was then washed with 1 ml 75% ethanol, allowed to air dry before re-dissolving the pellet in 400 µl of water. Then 400 µl of chloroform was mixed with it, shake for about 15 sec and centrifuged for 5 min at 13000 g at 4°C. 300 µl of upper phase was mixed with both of 30 µl 3 M sodium acetate and 750 µl ice-cold 100% ethanol, incubated on dry ice for 30 min and centrifuged for 30 min at 13000 g and 4°C. The pelleted RNA was washed with 75% ethanol, allowed to air dry as well as re-suspension in 50 µl ultra pure sterile water. The extracted RNA concentration and purity was estimated by the measurement of the absorbance at 260 nm using the NanoDrop spectrophotometer, and stored at -80°C for further analyses.

#### **2.2.2.14 First strand cDNA synthesis using superscript II RT**

First strand cDNA was synthesized from total extracted RNA using superscript™ First-strand synthesis System for qRT-PCR as described below. Before starting the cDNA synthesis reaction, the DNase treatment was performed on a mixture containing 1 µg of

total RNA, 1  $\mu$ l of 10 mM dNTP mix, 1  $\mu$ l of 10X DNase I reaction buffer (10 mM Tris-HCL, 2.5 mM MgCl<sub>2</sub>, 0.5 mM CaCl<sub>2</sub> [pH 7.6]), 1  $\mu$ l of DNase I enzyme (2000 unit/ml) and 4  $\mu$ l sterile distilled water, incubated for 25 min at 37°C. Followed by an inactivation of DNase enzyme by the addition of 1  $\mu$ l of 25 mM EDTA solution, heated at 65°C for 10 min. Then the cDNA synthesis reaction was carried out by adding 1  $\mu$ l of 0.5  $\mu$ g  $\mu$ l<sup>-1</sup> Oligo (dT)<sub>12-18</sub> primer. It was heated at 65°C for 5 min in a water bath, and chilled for 2 min on ice. Then 4  $\mu$ l of 5X first strand buffer (250 mM Tris-HCL [pH 8.3], 375 mM KCL, 15 mM MgCl<sub>2</sub>), 2  $\mu$ l of 10 mM dNTP mix, 1  $\mu$ l of 200 unit  $\mu$ l<sup>-1</sup> superscript II reverse transcriptase was added and finally 1  $\mu$ l of sterile distilled water were added to the reaction. Then the reaction proceeded for 60 min at 42°C followed by 10 min at 70°C to inactivate the reverse transcriptase enzyme. The cDNA was stored at -20°C until qPCR analysis.

#### **2.2.2.15 Gene expression analysis using q-PCR**

To study genes expression, the synthesized cDNAs were amplified using quantitative PCR (qPCR) to identify whether or not the transformed genes were expressed. A mix containing 7.5  $\mu$ l of Sybre, 1  $\mu$ L of forward primer (10 pmol) and 1  $\mu$ L of 10 pmol reverse primer were prepared. Total 9  $\mu$ L of the master mix were added in triplicate into 96 wells plates including 6  $\mu$ L of cDNAs and mixed together by quick centrifugation. Then the q-PCR cycling conditions were applied as following: 95°C for 3 min, (95°C for 10 sec, 62°C for 30 sec) (45 cycles). qPCR reactions were performed using SensiFast SYBR No-ROX mix (Bioline Reagents Ltd, London, UK) as specified by the manufacturer.

## **2.3 Biochemistry approaches**

### **2.3.1 Protein extraction**

The proteins of wheat leaves were extracted by grinding approximately 3 cm<sup>2</sup> of frozen leaf tissues in N<sub>2</sub>. Samples were kept frozen and transferred to a pre-chilled 1.5ml micro-tube. After all the samples were ground, 1 ml of protein extraction buffer (50 mM HEPES (pH 8.2), 5 mM MgCl<sub>2</sub>, 1 mM EDTA, 10% Glycerol, 0.1% Triton X-100, 2 mM Benzamidine, 2 mM Aminocaproic acid, 10 mM dithiothreitol (DTT) and 0.5 mM phenylmethylsulphonyl fluoride (PMSF)) was added and shaken vigorously. Samples were spun down for 1 min at 14,000g at 4 °C. Then the supernatant was separated and aliquoted into two new tubes of 200 µl each, snapped freeze in N<sub>2</sub> and stored in -80 °C in order to be used for protein quantification (Bradford assay) and western blotting analysis.

### **2.3.2 Protein quantification**

The quantification of wheat proteins samples, which extracted from previous step 2.3.1, was determined as described by Bradford (1976). 2.5 µl of extracted proteins were loaded on 96 wells plates with 5 µl of protein standard (from 0 to 1.4 µg µl<sup>-1</sup>) bovine serum albumin (BSA) in triplicate. Then 250 µl of Bradford reagent was loaded and mixed with the samples and standard. They were incubated for 10 min at RT, and then the absorbance was measured at 595 nm using micro-plate reader (SpectroStar Omega, BMC Labtech, Aylesbury, UK).

### **2.3.3 Preparation of Sodium Dodecyl Sulphate polyacrylamide gel electrophoresis (SDS\_PAGE)**

Sodium Dodecyl Sulphate (SDS) polyacrylamide gel electrophoresis (PAGE) were employed to separate the proteins for analysis.

Two clean glass plates (160 mm long, 160 mm in width) were assembled and clipped together with a seal of 1 mm thickness in between. For two gels, total volume of 10 mL of 12% resolving solution (3.8 mL of 1.5 M Tris- HCl [pH 8.8], 6 mL of Acrylamide–bisacrylamid [30% w/v acrylamid 0.8% w/v bisacrylamration 37.5:1], 1.5 mL of 10% SDS, 4.9 ml of water) was prepared. The polymerization was started by the addition of 150 µl of freshly 10% ammonium per sulfate (APS) to the mix followed by the addition of 6 µl of N, N, N', N'-tetramethylethylenediamine (TEMED). After that, the resolving solution was poured between the glasses into the cassettes, and 100% ethanol was added to ensure a straight gel top surface as well as preventing the oxidation. It was left for 20 to 30 min until the resolving gel was completely polymerized, then the ethanol was removed. Then 10 ml of 4% stacking solution (2.5 mL of 1 M Tris- HCl [pH 6.8], 1.33 mL of acrylamide-bisacrylamide mix, 6.1 mL of water, 100 µL 10% SDS, 50 µL of freshly 10% APS and 10 µl of TEMED) was poured on the top of resolving gel. Then a clean comb was placed into stacking gel before the polymerization, and left for 30 min to polymerize.

### **2.3.4 Proteins separation into SDS-PAGE polyacrylamide gel**

The gel plate sandwich was placed into a tank, attached to the electrode assembly and placed in the gel running chamber. The tank and between gel plates were filled with the running buffer (25 mM Tris-HCl 192 mM glycine and 0.1% (w/v) SDS), after the loading of quantified protein samples into the gels. Molecular weight markers were used to

estimate protein molecular weight. Finally, the gel was run using adjusted power supply at 80 V, 150 mA and 150 W for 30 min until the marker separated, then the voltage was increased to 100 V, 150 mA and 150 W for another 30 min to complete the protein migration throughout the gel.

### **2.3.5 Coomassie Brilliant Blue staining**

To evaluate the transfer efficiency of proteins, gels were incubated in 0.1% Coomassie Blue (250R) solution prepared in 50% (w/v) methanol and 10% (v:v) acetic acid for about 20 min. then the gels were de-stained in a destaining solution (10% acetic acid and 50% methanol) for approximately 40 min until the background was clear, with changing the solution regularly.

### **2.3.6 Western blotting of proteins to cellulose nitrate membrane**

The transfer of Proteins, from SDS gel, was performed to 0.45  $\mu\text{m}$  pore size cellulose nitrate membrane (Millipore Immobilon-P Transfer Membrane) by the use of the Bio-Rad mini Protean II blotting apparatus. The proteins transfer was completed in blotting buffer (25 mM Tris-HCL, 192 mM glycine and 20% methanol). A sandwich of sponge, filter paper, the gel, membrane, filter paper and sponge was prepared in a cassette with the removal of any bubbles. The cassette was then inserted into the tank with the nitro-cellulose membrane between the gel and the positive electrode. The tank was filled with transfer buffer (25mM TRIS-HCl, 192 mM glycine and 20% (v/v) methanol) and the transfer process was started using adjustable power supply at 110 V, 150 mA and 1 W for 1 h.

### **2.3.7 Immunoblotting and Detection**

The blotted membrane containing the proteins was passed through different processes: blocking, washing, primary antibody, washing, secondary antibody, washing. It was blocked at a shaker at RT for 1 h, using a solution of 6% dehydrated skimmed milk (Marvel, Tesco) in phosphate buffered saline (137 mM NaCl, 2.7 mM KCl, 10 mM  $\text{Na}_2\text{HPO}_4$ , and 2 mM  $\text{KH}_2\text{PO}_4$ ). Then the blot was washed shaking at RT in PBS with 0.05% Tween-20 three times of 10 min. It was incubated shaking at RT for 1 h in a primary antibody solution (3% dehydrated skimmed milk with 1:1000 primary antibody raised against specific protein such as Rubisco). After that, it was washed shaking at RT in PBS with 0.05% Tween-20 three times of 10, 15, and 20 min respectively with changing the buffer regularly. The secondary antibody with 3% dehydrated skimmed milk solution (dilution of 1:2000) was then added to the blot, incubated overnight at a shaker at 4°C. the final wash was finally applied with shaking at RT in PBS with 0.05% Tween-20 three times of 10 min each (30 min). Then the membrane was incubated in Pierce ECL chemiluminescence detection reagent (Thermo Scientific, Rockford IL, USA) mix (1:1, v:v to a volume of 3 ml for two gels) for 1 min, drained and placed a clean petri dish or plastic wraps and exposed and imaged using a FUSION FX chemiluminescence detection system (Fusion FX, Peqlab, Sarisbury Green, UK).

### **2.3.8 Red Ponceau staining of cellulose nitrate membrane**

To evaluate the efficiency of proteins transfer and the equal amount of loaded proteins, the cellulose nitrate membrane was stained for around 3-5 min in 0.5% Red Ponceau solution. After that, the membrane was washed with water, drained and imaged using a conversion detection system (Fusion FX, Peqlab, Sarisbury Green, UK).

### 2.3.9 Rubisco Activity assay

The activity of the photosynthetic enzyme Rubisco was measured as previously described by Pengelly et al., (2010), with some modifications. The proteins of wheat leaves were extracted by grinding 3 cm<sup>2</sup> of frozen leaf tissues in N<sub>2</sub>. Samples were then kept frozen and transferred to a pre-chilled 1.5ml micro-tube. After that, 800 µl of protein extraction buffer (50 mM HEPES (pH 8.2), 5 mM MgCl<sub>2</sub>, 1 mM EDTA, 10% Glycerol, 0.1% Triton X-100, 2 mM Benzamidine, 2 mM Aminocaproic acid, 10 mM dithiothreitol (DTT) and 0.5 mM phenylmethylsulphonyl fluoride (PMSF)) and 10 µl of protease inhibitor cocktail (Sigma) were added and shaken vigorously. Samples were spun down for 2 min at 14,000g at 4°C. Then the supernatant was separated and aliquoted into two new tubes of 200 µl each and the supernatant was used for assays. For Rubisco, 5 µl of leaf extract was combined with 970 µl of assay buffer (50 mM EPPS-NaOH pH=8, 10 mM MgCl<sub>2</sub>, 0.5 mM EDTA, 1 mM ATP, 5 mM phosphocreatine, 20 mM NaHCO<sub>3</sub>, 0.2 mM NADH, 50 U ml<sup>-1</sup> creatine phosphokinase, 0.2 mg carbonic anhydrase, 50 U ml<sup>-1</sup> 3- phosphoglycerate kinase, 40 U ml<sup>-1</sup> glyceraldehyde-3-phosphate dehydrogenase, 113 U m<sup>-1</sup> Triose-phosphate isomerase, 39 U ml<sup>-1</sup> glycerol-3-phosphate dehydrogenase). And then the activity of Rubisco enzyme was calculated by observing the reduction of NADH absorbance at the wavelength of 340 nm after the reaction initiation by 5 µl of 21.9 mM of RuBP substrate spectrophotometric micro-plate reader (SpectroStar Omega, BMC Labtech, Aylesbury, UK).

## **2.4 Growth and Physiological analyses**

### **2.4.1 Growth of plants and conditions**

All transgenic wheat seeds were planted and germinated in compost (Levington F2S, Fisons, Ipswich, UK) in a climate controlled growth room for 3 weeks (22°C, 16 h light periods, and at 20°C for 8h with 16% humidity for the dark period). Selected seedlings plants were then transferred into large pots to a controlled environment greenhouse (25-32 °C day/ 18 °C night, 16h photoperiod of natural irradiance supplemented with high pressure sodium lamps). Plants were watered and moved regularly.

### **2.4.2 Developmental measurement**

The main stages of wheat growth and development were measured using Zadoks scale (Zadoks et al., 1974). Leaves, tillers are counted regularly every week with the observation of nodes and ears maturity levels.

### **2.4.3 Transient expression assay in *N. benthamiana* leaves**

The transient expression procedure was carried out in 3-week-old *N. benthamiana* leaves as described in Sparkes *et al.*, (2006) with an additional alteration. A P19 protein encoded with the tomato bushy stunt virus was used as a suppressor of any gene silencing (Voinnet *et al.*, 2003) by binding to siRNA and blocking the interaction between siRNA and viral RNA (Wydro *et al.*, 2006). *Agrobacterium tumefaciens* strain GV1301 carrying each binary vector and P19 plasmid was grown overnight at 28°C in LB liquid media with the appropriate antibiotics. Cultures were centrifuged at 13000 rpm for 15 min at RT and gently re-suspended in infiltration buffer (5 mM MES, 5 mM MgSO<sub>4</sub>, pH 5.7, 100 mM acetosyringone) to an optical density of OD<sub>600</sub>≈0.6. Prior to

infiltration, suspensions of *Agrobacterium* carrying binary plasmid including the eYFP gene were mixed in a 1:1 ratio with an *Agrobacterium* harbouring viral silencing suppressor (P19) in the binary plasmid. The final mixtures of *Agrobacterium* cells were infiltrated by the gentle squeezing of cultures from a 1 ml syringe barrel into the underside of fully-expanded leaves of 4-week-old *N. benthamiana* plants. Plants were housed in a 24°C plant growth room with overhead lighting using the light-dark cycle for three days.

#### **2.4.4 Microscopy observation**

After three days of infiltration, infiltrated plant leaves were imaged using a confocal microscope with a 63X oil immersion objective as described in Wei and Wang (2008). YFP was excited at 488 nm to 514 nm, and the emitted light was captured at 525 to 650 nm. Images were captured digitally and handled using the Leica LCS software.

#### **2.4.5 Histochemical GUS assays**

After three days of infiltration, GUS activities were assayed histochemically per the method described in Jefferson *et al.* (1987). Infiltrated and wild type *N. benthamiana* leaves were immersed in GUS reaction buffer (1 mM X-Gluc (5-bromo-4-chloro-3-indolyl- $\beta$ -D-glucuronide), 100 mM phosphate buffer pH 7.0, 0.1% Triton X-100, 5 mM K<sub>3</sub>Fe(CN)<sub>6</sub>, 5 mM K<sub>4</sub>Fe(CN)<sub>6</sub>, 10 mM EDTA and 20% methanol). Then they were incubated at 37°C overnight. Finally, they were washed with 100% ethanol to remove the chlorophyll several times with incubations at 37°C until the GUS blue spots were clearly observed.

#### **2.4.6 Gas exchange measurement**

Photosynthesis measurements were performed on the middle of fully mature leaves at different developmental stages (Zadoks growth stages 1.4-1.5 and 4.1-4.5). The response of assimilation rate of CO<sub>2</sub> (*A*) to range of concentrations of intercellular CO<sub>2</sub> (*C<sub>i</sub>*) was determined at a maintained level of saturated light at 2000 μmol m<sup>-2</sup> s<sup>-1</sup> using an open infrared gas exchange system and a 2 cm<sup>2</sup> leaf chamber with an integral blue-red LED light source (LI-COR 6400; LI-COR, Lincoln, Nebraska). Leaf temperature was fixed at 25°C, and the humidity was maintained around 20 mmol mol<sup>-1</sup>. The CO<sub>2</sub> was provided using an external gas cylinder. The measurements were performed at different CO<sub>2</sub> concentrations through the experiments starting from ambient CO<sub>2</sub> concentration (*C<sub>a</sub>* at 400 μmol mol<sup>-1</sup>) afterward the concentrations were decreased to 300, 200, 100, and 50 μmol mol<sup>-1</sup> and then retained back to 400 μmol mol<sup>-1</sup>. Following this, the *C<sub>a</sub>* was increased gradually in four steps to 1500 μmol mol<sup>-1</sup> (650, 900, 1200 and 1500 μmol mol<sup>-1</sup> respectively) to fit the curve. The *A/C<sub>i</sub>* readings were recorded after the stability of *A* to the new conditions. Subsequently, the maximum rate of Rubisco enzyme for carboxylation (*V<sub>cmax</sub>*), the maximum rate of electron transport require for RuBP regeneration (*J<sub>max</sub>*), the ambient CO<sub>2</sub> rate of photosynthesis (*A<sub>sat</sub>*) and the CO<sub>2</sub>-saturated rate of photosynthesis (*A<sub>max</sub>*) were solved by curve fitting as described by equations described in von Caemmerer and Farquhar (1981).

#### **2.4.7 The measurement of SBPase activity**

The total activity of SBPase enzyme was determined from wheat flag leaves by phosphate release, as described by Harrison et al., (1997) with replacing the classic Malachite green reagent by Biomol green reagent and was measured using micro-plate

reader. Two stages were carried out to measure the SBPase activity, starting with protein extraction as well as the determination of the activity.

#### **2.4.7.1 Protein extraction for SBPase activity measurement**

Immediately after gas exchange measurement (as described in the method 2.4.6), 5-6 cm<sup>2</sup> of flag leaves were isolated from the same area used for photosynthetic rate measurement, and frozen in N<sub>2</sub>. The leaf discs were grounded to a fine powder in N<sub>2</sub>, and 1.75 ml of the extraction buffer (50 mM HEPES [pH 8.2], 5 mM MgCl<sub>2</sub>; 1 mM EDTA; 1 mM EGTA; 10% glycerol; 0.1% Triton X-100; 2 mM benzamidine; 2 mM aminocaproic; 0.5 mM phenylmethylsulphonyl fluoride (PMSF); 10 mM dithiothreitol (DTT)) was added to the grounded tissues, centrifuged for 3 min at 14,000 g and at 4°C. Then 1 ml of the supernatant was applied to a pre-equilibrated desalting NAP-10 column (illustra NAP-10, GE Healthcare Life Sciences, Little Chalfont, UK) and eluted with 1.5 ml of desalting buffer (exactly the same as the extraction buffer except that it did not contain 0.1% Triton X-100), allowed to penetrate through the column fully. The proteins were then eluted with 1.5 ml desalting buffer and collected in new tubes on ice. Finally the samples were mixed and aliquoted into seven tubes (150-200 µl per tube), snap frozen in N<sub>2</sub>, and stored at -80°C until assay analysis.

#### **2.4.7.2 SBPase activity determination by phosphate release**

The assay reaction was started by adding 20 µL of extracted, desalted proteins to 66 µL of assay buffer (50 mM Tris, [pH 8.2]; 15 mM MgCl<sub>2</sub>; 1.5 mM EDTA; 10 mM dithiothreitol (DTT); 2 mM SBP) and incubated at 25°C for 10 min. Then, the reaction was immediately stopped by adding 50 µl of 1 M perchloric acid on ice, and centrifuged for 10 min at 14000 g and 4°C. The assay control reaction was started, in parallel for

samples, by the addition of the same assay buffer but already consisting of 1 M perchloric acid, incubated at 25°C for 10 min and spun down for 10 min at 14000 g and 4°C. After that, 15 µl of the Samples, 15 µl of controls, and 15 µl of standards ( $\text{PO}_4^{-3}$  0.125 to 8 nmol) were incubated (in triplicate in microtiter plate) for 30 min at RT with 300 µL of Biomol Green reagent (Enzo Life Sciences Ltd, Exeter, UK). Then the absorbance was measured at 620 nm using micro-plate reader ((SpectroStar Omega, BMC Labtech, Aylesbury, UK). The SBPase activity was determined by phosphate release using the standard curve established between 0.125 to 4 nmol  $\text{PO}_4^{-3}$ .

#### **2.4.8 Determination of total Biomass**

Plant biomass was determined when they all reached their maximum physiological maturity (Zadoks growth stage 9.1-9.2). Leaves, Stems, ears and seeds were harvested, counted, and dried at 70°C until a steady weight were obtained. Then the final dry weights of each were determined. Ears were afterward completely threshed and total seeds were all counted and weighed as well.

**Chapter 3: Increased SBPase activity improves  
photosynthesis and grain yield in wheat grown in  
greenhouse conditions**

### 3.1 Introduction

The Calvin–Benson cycle is the major pathway of carbon fixation occurring in the chloroplast's stroma. In addition, this cycle plays a key role in the metabolism of plants, as well as in carbon flux (Geiger and Servaites, 1994). Genetic manipulation approaches were used to produce transgenic plants with individually reduced activity levels of the Calvin–Benson cycle enzymes for the purpose of exploring and analysing the photosynthetic effects of these enzymes. Several experimental analysis studies have been carried out to manipulate these enzymes by the overexpression technique in model plants (tobacco and *Arabidopsis*) to produce transgenic plants with increased levels of these enzymes or by decreasing their levels, and then to investigate the effects of these manipulations on the plants' photosynthesis and biomass productions. Based upon these analyses, sedoheptulose 1,7-bisphosphatase (*SBPase*), transketolase (TK), and fructose 1,6-bisphosphate aldolase (aldolase) enzymes were identified as displaying significantly highly efficient flux control over the carbon fixation and on photosynthesis, compared with other enzymes within the cycle. As a result, they have been identified as significant targets for genetic engineering studies to improve plants' photosynthesis (Raines, 2003, 2011).

The *SBPase* enzyme acts to catalyse the SBP de-phosphorylation to sedoheptulose-7-phosphate (S7P), resulting in the transformation of two carbon skeleton groups from S7P to glyceraldehyde-3-phosphate, catalysed by TK enzyme, to form either xylulose-5-phosphate (X5P) or ribose-5-phosphate (R5P) (Martin et al., 2000). Additionally, it is essential to maintain the balance between carbon leaving the Calvin–Benson cycle and that necessary for the regeneration of RuBP (Raines, 2003). Its activity is found to increase in the light by more than 10-fold as a consequence of thioredoxin system through light-modulated activation. The level of  $Mg^{+2}$  and pH in stroma can also

regulate *SBPase* (Ölçer et al., 2001). Moreover, its importance is highlighted in some modelling studies as a controlled carbon flux enzyme in the Calvin–Benson cycle because of its regulatory features, as well as its localisation between two stages of the Calvin–Benson cycle: the assimilatory (the biosynthesis of starch and sucrose) and the regenerative (of RuBP) (Raines et al., 1999; Zhu et al., 2007; Rosenthal et al., 2011). It is clearly shown that the Calvin–Benson cycle is limited by the Rubisco enzyme under the conditions of light saturation and with increasing CO<sub>2</sub> concentrations through RuBP regeneration. Previous studies have shown that increased levels of the RuBP regeneration enzymes such as *SBPase* and fructose 1, 6-bisphosphate aldolase (FBPA) could stimulate photosynthesis rates and improve plants' growth as well as total biomass (Lefebvre et al., 2005; Uematsu et al., 2012).

It was found that reducing *SBPase* activity in tobacco led to a negative effect on plant photosynthesis (Harrison et al., 1997, 2001). In contrast, increased levels of *SBPase* activity have resulted in improved photosynthetic rates and biomass production in tobacco plants grown under controlled greenhouse conditions (Lefebvre et al., 2005), and also in field conditions under higher CO<sub>2</sub> (Rosenthal et al., 2011). Feng and his co-workers have produced transgenic rice plants through the overexpression of *SBPase* cDNA from rice cultivar 9311 (*Oryza sativa* ssp. *indica*) into rice cultivar zhonghua11 (*Oryza sativa* L. ssp. *Japonica*) under salt conditions. As a result, plants with increased *SBPase* activity were generated with high tolerance to salt conditions at the young seedling stage. Hence, it has been shown that the *SBPase* overexpression has led to an enhancement in the tolerance of plants against the salt condition during their growth (Feng et al., 2007a). Furthermore, the *SBPase* cDNA of rice plants (*Oryza sativa* L.) was overexpressed in rice plants zhonghua11 (*Oryza sativa* L.) to produce plants with enhanced activity of *SBPase* under high temperature conditions during young seedling

growth. This study has resulted in producing transgenic rice plants with significantly enhanced photosynthesis and improved tolerance to heat conditions compared to wild type plants (Feng et al., 2007b). However, the regenerative phase *SBPase* enzyme of the Calvin–Benson cycle has not yet been the subject of enough studies in wheat crops. Consequently, transgenic wheat plants expressing the *Brachypodium SBPase* gene were produced to investigate and study the effect of *SBPase* overexpression on wheat photosynthesis, growth and biomass production under controlled greenhouse conditions.

The major aims of this chapter are: 1. To screen and analyse transgenic wheat plants with increased *SBPase* activity levels to enhance regeneration of the Calvin–Benson cycle and to enhance wheat yields; this was carried out in collaboration with Dr. Steven Driever. 2. To study the effects of these increased *SBPase* activity levels on wheat photosynthesis and growth rates.

## **3.2 Results**

Construct was transformed into wheat using a bombardment approach and transgenic T0 plants were generated at Rothamsted, West Common, Harpenden, UK. To identify transgenic wheat plants with increased *SBPase* expression, 11 lines were screened at both the molecular and physiological levels in collaboration with Dr. Steven Driever. Out of these 11 lines, two independent transgenic *SBPase* lines that showed notable increases in *SBPase* activity are discussed in this chapter.

### **3.2.1 Gene expression analysis of the *SBPase* construct in transgenic wheat plants using qPCR**

To analyse the expression of the *Brachypodium SBPase* construct as well as the native *SBPase* wheat gene in transgenic wheat T3 progeny, total RNA from the flag leaf of three plants from different independent transgenic lines was extracted and cDNA was synthesised. The cDNA of the different plants within these independent lines was amplified using qPCR. The results showed a significant increase in introduced *SBPase* construct expression levels in two independent lines, SOX2 and SOX3, compared to the WT line (Figure 3.1).

To examine the expression of the native *SBPase* gene, the cDNA of the different plants within these independent lines was amplified using qPCR. Consequently, as can be seen in Figure 3.2, different increases in native *SBPase* gene expression levels between SOX2 and SOX3 lines compared to the WT line.

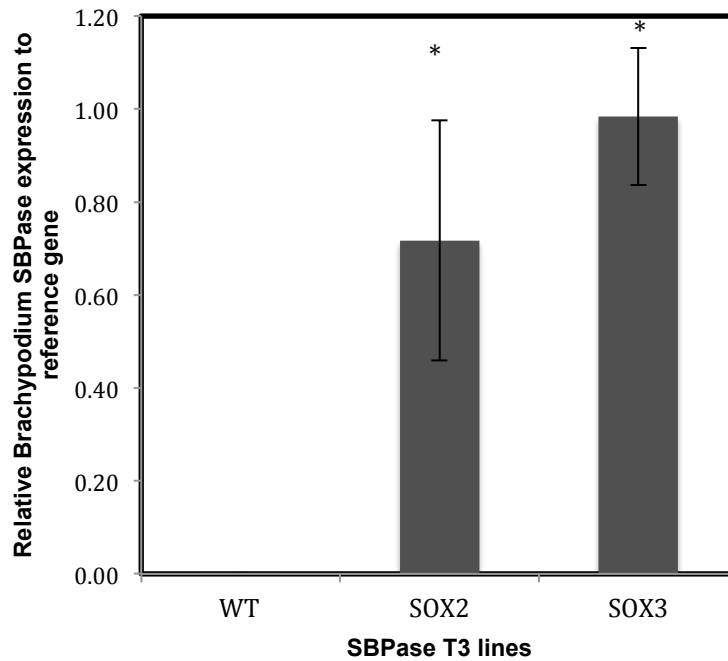


**Figure 3.1: Determination of *Brachypodium SBPase* gene expression in transgenic wheat plants.**

The RNA was extracted from the flag leaf from T3 plants. *Brachypodium SBPase* construct was amplified using specific primers (chapter 2, Table 2.1). The expression was normalised against actin reference gene. Values represent the average of five plants from two individual transgenic lines compared to the WT line. Stars indicate significant differences from WT ( $P < 0.05$ ).

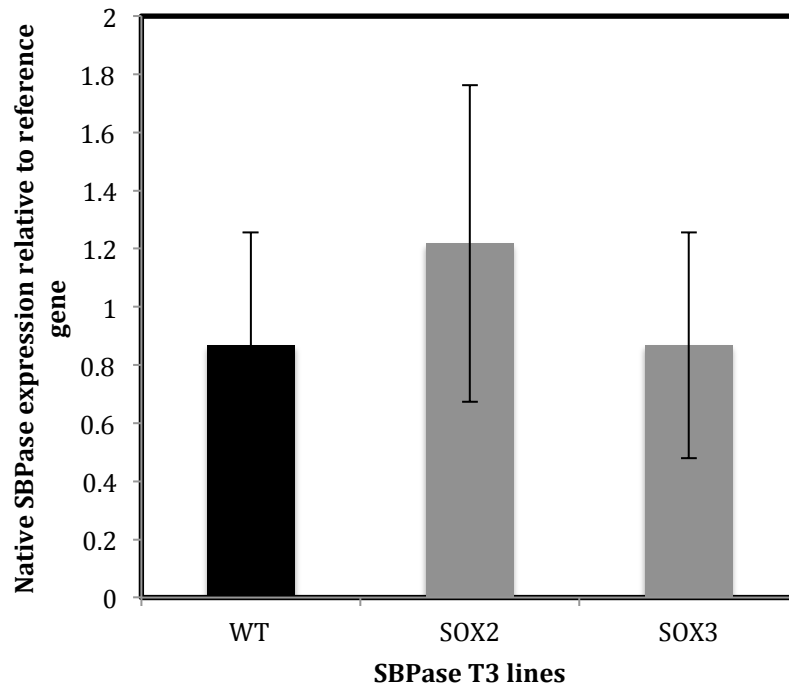


**Figure 3.2: Determination of native *SBPase* gene expression in transgenic wheat plants.**

The RNA was extracted from the flag leaf from T3 plants. Native wheat *SBPase* gene was amplified using specific primers (chapter 2, Table 2.1). The expression was normalised against actin reference gene. Values represent the average of five plants from two individual transgenic lines compared to the WT line. Stars indicate significant differences from WT ( $P < 0.05$ ).

### **3.2.2 SBPase activity in transgenic T3 wheat plants**

Total extractable *SBPase* enzyme activity of the flag leaves of T3 progeny was spectrophotometrically determined by phosphate released determine. The results revealed that significantly increased levels of *SBPase* activity were observed in two independent transgenic lines (SOX2 and SOX3) as a result of overexpression of *Brachypodium* *SBPase* in wheat plants compared to the wild type plants ( $P < 0.05$ ) (Figure 3.3); this corresponded to the increases found in the *SBPase* gene construct expression previously shown.

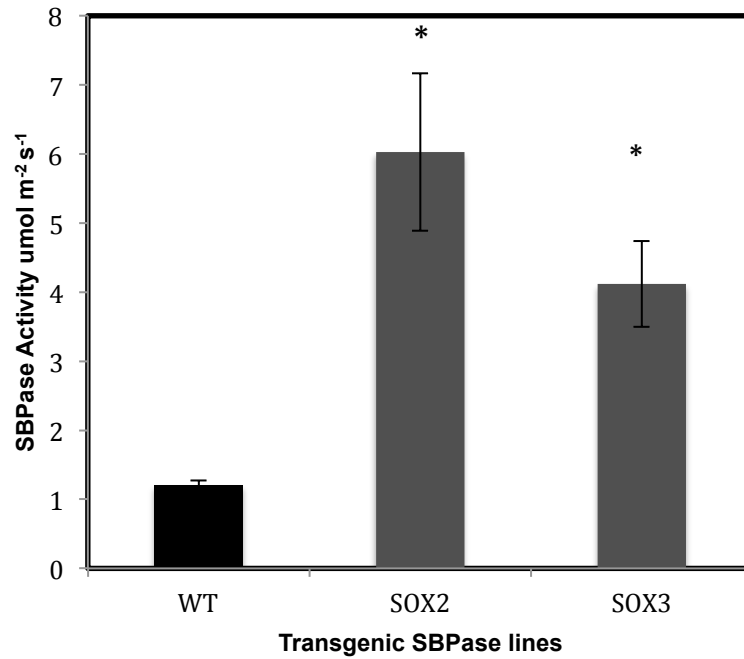


**Figure 3.3: Increase in total extractable *SBPase* activity in transgenic *SBPase* wheat plant T3 progeny.**

The plants were grown in a controlled conditioned greenhouse. Total extractable *SBPase* activity was assayed using a spectrophotometer. Values represent the average of four transgenic plants per line compared to the average of four WT plants. Stars indicate significant differences from WT ( $P < 0.05$ ).

### **3.2.3 The effects of increased levels of *SBPase* activity on photosynthesis and growth in transgenic wheat T3 plants grown in greenhouse conditions**

#### **3.2.3.1 The effects of increased levels of *SBPase* activity on CO<sub>2</sub> assimilation (*A/C<sub>i</sub>* analysis)**

To identify the effects of the increased levels of *SBPase* activity on wheat photosynthesis, the response of photosynthetic rates to changes in intercellular CO<sub>2</sub> concentrations (*A/C<sub>i</sub>*) was measured under a light-saturated level of 2,000 mmol m<sup>-2</sup> s<sup>-1</sup> for different independent overexpressing *SBPase* lines at the developmental growth stage of Zadoks scale (flag leaf; Z3.9-Z4.1). After the germination of seedlings in a control room for three weeks, selected seedlings showing higher levels of *SBPase* gene expression were transferred to a controlled greenhouse and allowed to complete their growth. The results showed small differences in photosynthesis between transgenic SOX3 line with larger *SBPase* activity compared to the WT; however, significant differences were found ( $P < 0.05$ ), particularly when measured under saturating CO<sub>2</sub>, compared to the WT plants (Figure 3.4).

From the *A/C<sub>i</sub>* response curves, the maximum rate of carboxylation allowed by the Rubisco enzyme ( $V_{c,max}$ ) and the maximum electron transport required for the regeneration of RuBP ( $J_{max}$ ) were determined via the equations of von Caemmerer and Farquhar (1981). Consequently, increases in these parameters were observed in the SOX3 line with the largest increases in the levels of *SBPase* activity compared to the WT, but no differences between SOX2 line and the WT line (Table 3.1).

A further analysis of the *A/C<sub>i</sub>* curves showed that the ambient CO<sub>2</sub> rate of photosynthesis ( $A_{sat}$ ) and the CO<sub>2</sub>-saturated rate of photosynthesis ( $A_{max}$ ) were also

slightly increased in the two overexpressed *SBPase* lines with increased levels of *SBPase* activity compared to the WT line (Figures 3.5a and 3.5b).

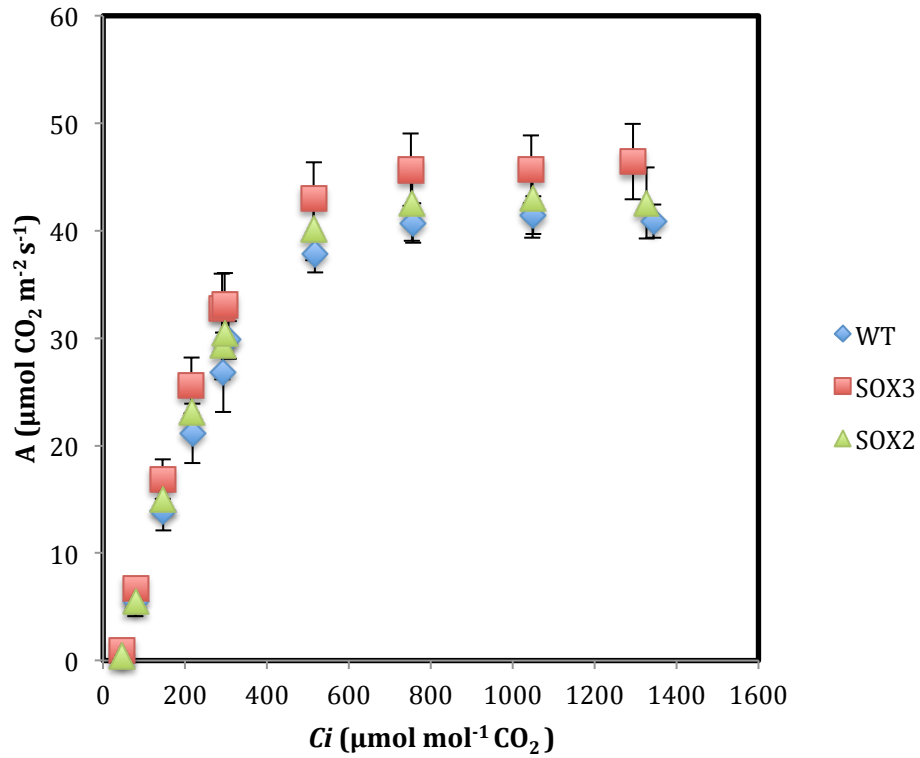


**Figure 3.4: Photosynthetic  $\text{CO}_2$  assimilation ( $A$ ) response to different internal concentrations of  $\text{CO}_2$  ( $C_i$ ) ( $A/C_i$  curve) of two independent overexpressed *SBPase* T3 lines compared to the WT line.**

Plants were grown in an environmentally controlled greenhouse. Gas exchange measurements were performed on flag leaf at Zadoks scale of Z3.9-Z4.1, with a light-saturated rate of  $2,000 \mu\text{mol m}^{-2} \text{ s}^{-1}$  using an open infrared gas exchange system. Values represent three plants from two independent lines compared to the WT line.

**Table 3.1: Maximum rate of carboxylation allowed by rubisco enzyme ( $V_{c, \max}$ ) and the maximum electron transport required for RuBP regeneration ( $J_{\max}$ ).**

$V_{c, \max}$  and  $J_{\max}$  were both solved from the  $A/C_i$  measurements shown in Figure 3.4 by using the equations published by von Caemmerer and Farquhar (1981). Values represent the average of three plants from two independent *SBPase* overexpressed lines compared to the WT line. Stars indicate significant differences from WT ( $P < 0.05$ ).

	$V_{c, \max}$ ( $\mu\text{mol m}^{-2} \text{s}^{-1}$ )	$J_{\max}$ ( $\mu\text{mol m}^{-2} \text{s}^{-1}$ )
WT	63.8	184
SOX2	63.1	185
SOX3	70.0 <sup>*</sup>	203 <sup>*</sup>

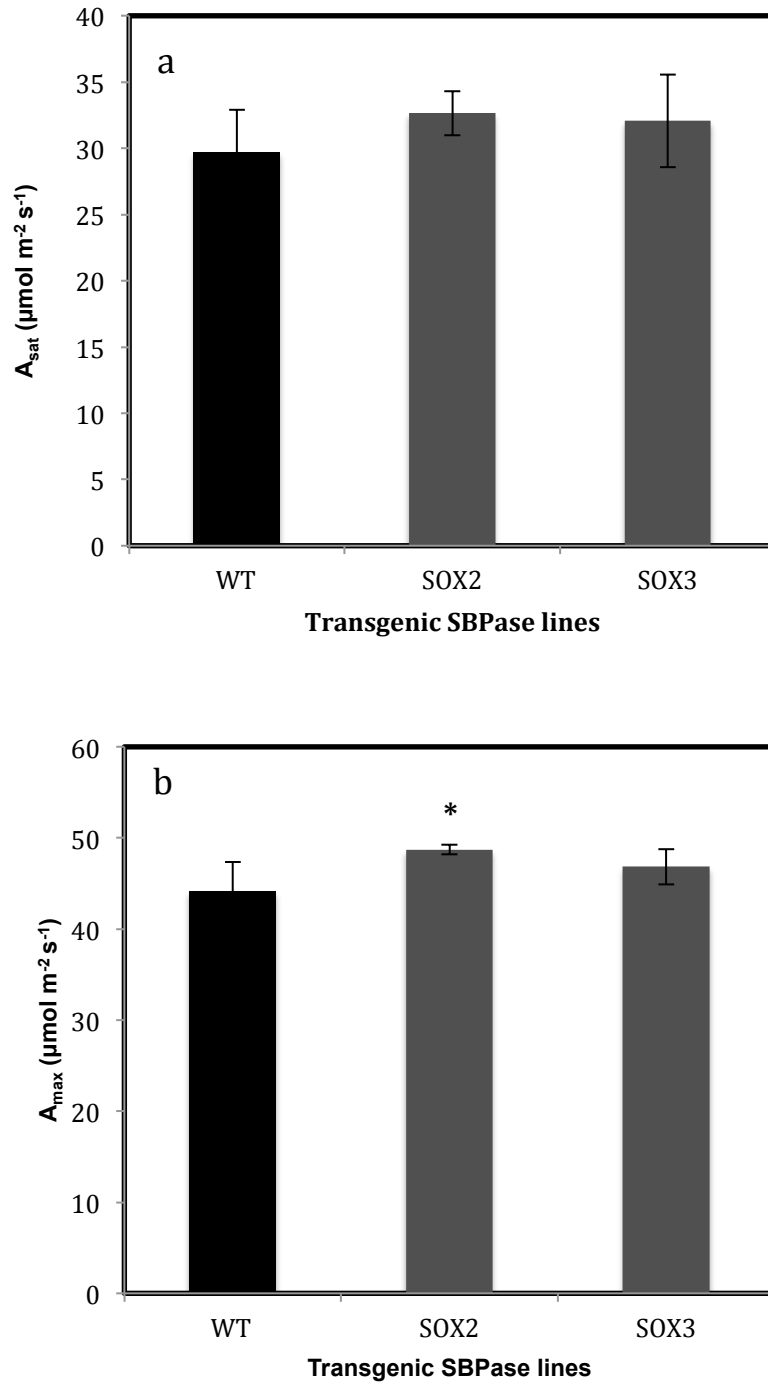
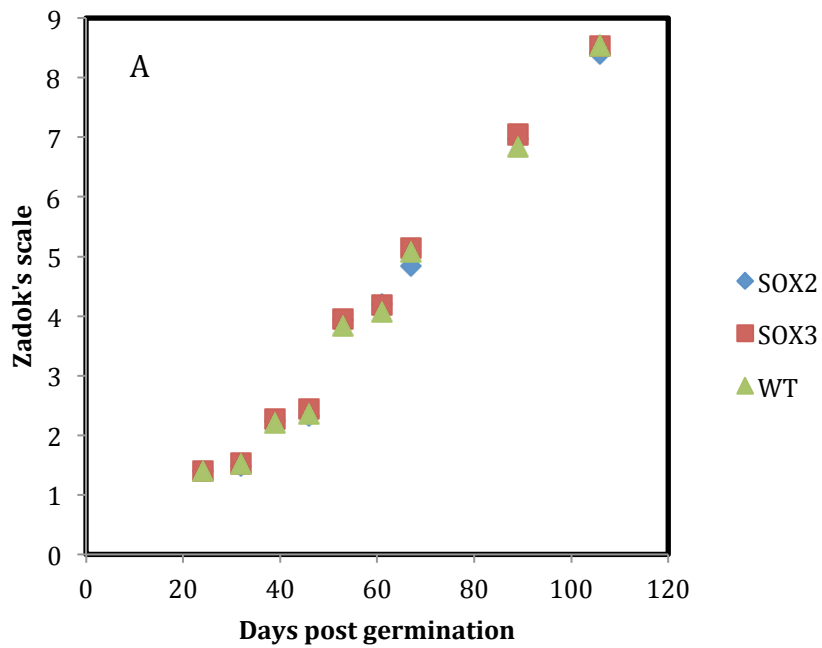


**Figure 3.5: CO<sub>2</sub> assimilation rates at ambient ( $A_{\text{sat}}$ ) and saturating CO<sub>2</sub> ( $A_{\text{max}}$ ) of transgenic overexpressed *SBPase* T3 wheat plants.**

Plants were grown in an environmentally controlled greenhouse.  $A_{\text{sat}}$  (a) and  $A_{\text{max}}$  (b) were derived from the  $A/C_i$  response curves shown in Figure 3.4, at flag leaf (Zadoks growth Z3.9-Z4.1). Values represent three plants from two independent overexpressed *SBPase* lines compared to the WT line. Stars indicate significant differences ( $P < 0.05$ ) compared to the WT.

### **3.2.3.2 The effect of increased SBPase activity on transgenic wheat plants' growth and visual phenotypes**

To assess the growth rate, the Zadoks growth scale was used every week to count the leaves, tillers and ears and also to observe the nodes and flowers on plants grown in an environmentally controlled greenhouse. The results revealed that the transgenic overexpressed *SBPase* plants with the largest increases in the levels of *SBPase* activity showed developmental growth rates clearly more rapid compared to the WT. Moreover, the overexpressed plants with significantly higher levels of *SBPase* activity were clearly bigger, taller and had more green leaves compared to the WT plants as phenotypic effects as a result of the increases in *SBPase* activity levels (Figure 3.6).



B

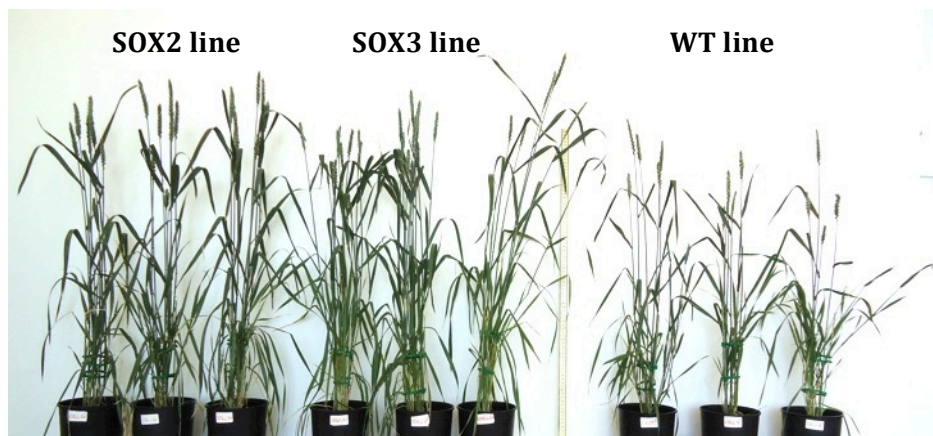


**Figure 3.6: Growth analysis and Visual phenotypes of *SBPase* transgenic T3 lines and WT plants.**

Plants were grown in an environmentally controlled greenhouse. **A.** Growth measurements were done using Zadoks scale by counting leaves, tillers (stems), ears and observing the flowering development regularly every week. **B.** Visual phenotype pictures are of *SBPase* transgenic plants compared to the WT plants at Zadoks scale of Z6.9-Z7.0.

### **3.2.3.3 The effect of higher levels of *SBPase* activity on plant biomass and seed production**

To determine the total biomass seed production of transgenic wheat T3 overexpressing *SBPase*, plants were harvested when they reached Zadoks growth stage 9. The plants with the higher levels of *SBPase* activity had a significantly higher total biomass than the WT plants (Figure 3.7a). Also, a significant increase in the average weigh of dried ears was evident in the plants with the highest *SBPase* activity compared to the WT plants (Figure 3.7b), despite of no effect on the number of ears (Figure 3.7c) and significantly higher weight per seed compared to the WT plants (Figure 3.7d).

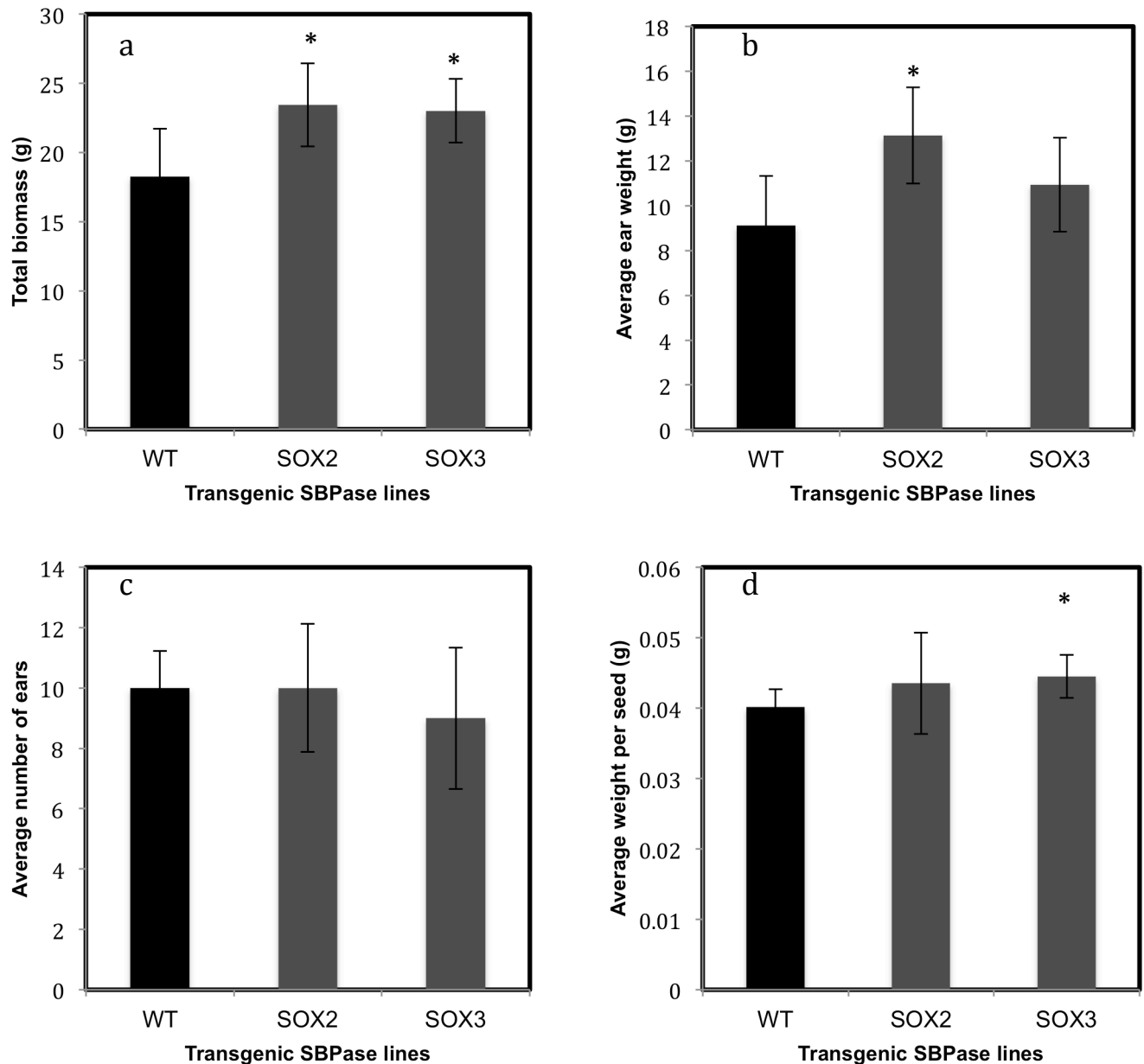


**Figure 3.7: Biomass analysis of transgenic *SBPase* lines and WT lines.**

Plants were grown in an environmentally controlled greenhouse. Plants were harvested when they reached Zadoks growth stage of 9 and they were completely dry. The following were measured and are shown above: **a.** plant total biomass, **b.** average ear weight, **c.** average number of ears, and **d.** average weight per seed. Values represent the average of 5-6 plants from two independent *SBPase* transgenic lines compared to the WT line. Stars indicate significant differences from the WT ( $P < 0.05$ ).

### 3.3 Discussion

Evidence has shown that increased levels of regeneration phase enzymes, such as *SBPase*, could stimulate the rate of photosynthesis and improve plant growth and total biomass. Therefore, it has been the target for genetic manipulations in wheat in this study.

Out of several transgenic *SBPase* wheat lines, two lines of T3 progeny have proven to have a significantly overexpressed *SBPase* gene, at the transcript level, compared to the WT line; this resulted in an increase in its activity. Moreover, this increase in *SBPase* activity clearly led to improved photosynthetic rates, in particular under higher concentrations of CO<sub>2</sub>. This also led to clearly visible phenotypes in the transgenic overexpressed *SBPase* plants with the largest increases in the levels of *SBPase* activity, as they exhibited a noticeably faster developmental growth rate compared to the WT, as well as being clearly bigger, taller and having more green leaves compared to the WT plants as a result of an increase in the *SBPase* activity. Moreover, significant increases in total biomass, number and weight of leaves and number and weight of ears were all observed, which can mainly be explained by significant increases in the total seed weight and number compared to the WT plants. These findings are all similar to the results previously shown for some studies on tobacco (Lefebvre et al., 2005; Rosenthal et al., 2011). In contrast, rice plants with increased *SBPase* did not lead to increases in total biomass production compared to the WT plants under both ambient and controlled conditions (Feng et al., 2007a; Feng et al., 2009), which indicates clear differences between the species of crops (wheat and rice). However, the *SBPase* overexpression has led to the rice plants with increased tolerance to the salt condition (Feng et al., 2007a) and heat stress (Feng et al., 2007b) during their growth; hence,

this needs to be further investigated in wheat plants. Therefore, this could be applicable to wheat plants, which need further investigations.

These results support the hypothesis that increasing the level of *SBPase* activity in wheat could improve photosynthetic performance and total biomass production (Parry et al., 2011). Resource use efficiency could also be improved as a result of increased *SBPase* activity, as shown in Rosenthal et al. (2011). Modelling studies suggest that an underinvestment of the enzymes *SBPase* and *FBPaldolase* is currently observed. Nevertheless, the carboxylation reaction that happens with the Rubisco enzyme increases along with the continuous increase in the atmospheric CO<sub>2</sub>, which would need an increase in the *SBPase* activity. Under elevated CO<sub>2</sub>, increases in leaf photosynthesis through increased levels of *SBPase* activity would potentially require a reallocation of several enzymes of the Calvin-Benson cycle. This could include a small decrease in the Rubisco amount and activity with no negative effect on plant photosynthesis and yield in order to improve nitrogen use efficiency (NUE), as it represents about 25-30% of total leaf N (Mae et al., 1993), whereas *SBPase* represents only less than 1% of total leaf N (Zhu et al., 2007).

#### Summary:

- This preliminary study shows that the increase in *SBPase* led to improved photosynthesis and enhanced growth.
- The results showed that an increase in *SBPase* activity clearly led to improved photosynthetic rates, and also results in clearly visible phenotypes in the transgenic overexpressed *SBPase* plants.

- The increase in SBPase activity also led to a significant increase in total biomass and seed production.
- Therefore, these results prove the hypothesis that increasing *SBPase* activity in wheat could improve photosynthetic performance and total biomass production.
- Further studies need to be implemented to explore and investigate the effect of this increase in *SBPase* on wheat photosynthesis under some stress conditions such as salt and heat conditions.

**Chapter 4: Effect of decreased Rubisco by *RbcS* RNAi on wheat photosynthesis, growth and grain quality under natural sunlight in the UK spring/ summer seasons**

## 4.1 Introduction

The rapid and continuing growth of the global population has significantly increased the demand for food that increases the global demand for high cereal yield production (FAO, 2012), and subsequently, increased the fertilization Nitrogen (N) inputs. N has an important role in plants productions involving in photosynthetic process as well as determining the content of protein and quality of grains. Although N fertilization would be necessary in high N rate inputs for the productivity and grain quality of cereals, managing efficient capture and use will need to be optimized for great important of economic and environmental issues (Shewry, 2009), because high amount of non-absorbed N could lead to oxygen depletion in the soils which as a result, preventing the functional role of microorganisms in the soils to metabolize the non-absorbed N (eutrophication) and reduce the soils fertility. These eutrophic soils could contribute to release some toxic gaseous and ammonia (NH<sub>3</sub>) emissions into the atmosphere (Ramos, 1996). Therefore, improving the efficiency of nitrogen uptake, assimilation and also utilization need to be understood in order to improve the nitrogen use efficiency (NUE) together with increasing yield is significant for maintaining the N inputs (Shewry, 2009; Hawkesford, 2014). Whilst the great importance of N for the cereals productivity, this could effect on grain quality negatively if it is highly available. High rate of N supplement could lead to an increase in grain proteins in which this results in altering the balance between the glutenin grain protein and other main grain storage proteins; for example, an accumulation of gliadin together with a decrease in the glutenin. Therefore, this would effect negatively in grain quality resulting in an increase in the strength of dough and reducing grain quality (Abrol *et al.*, 1971; Shewry *et al.*, 1995).

It has been shown that approximately 80% of all N is to be found in the form of proteins

in plant chloroplast (Adam *et al.*, 2001). Moreover, among these proteins in the chloroplast, Rubisco is the most abundant protein in plant chloroplast, and it represents approximately 50% of the total protein in leaves and about 30% of leaf nitrogen (Mae *et al.*, 1993). Hence, it is considered as a key investment and means for storage of nitrogen in crops (Millard, 1988; Evans, 1989). Rubisco is classified as a slow catalytic rate enzyme that can be found in the chloroplast stroma acting to catalyse two competitive pathways: carboxylation and oxygenation reactions. Therefore, it is required in large amounts for maintaining a sufficient rate of photosynthesis. It is also found to be a limiting factor of the maximum photosynthetic rate (Evans, 1989). Furthermore, it consists of two different subunit polypeptides: eight dimeric large subunits (55 kDa) and eight tetrameric small subunits (15 kDa). The large subunits are encoded as the *rbcL* gene in the chloroplast and include the catalytic site and binding sites of the enzyme. However, the small subunits are encoded by the nuclear *rbcS* gene, and they do not carry the enzyme catalytic site (Spreitzer, 2003).

A small reduction in the Rubisco enzyme content in crops is an important opportunity to reduce the requirement for total leaf N in order to improve NUE for sustaining and improving wheat yield with reduced N fertilizer inputs. It was found that there is an over-investment of N in Rubisco for maintaining the photosynthetic process in wheat (Mitchell *et al.*, 2000). Transgenic studies on plants with reduced levels of Rubisco grown in high CO<sub>2</sub> environments show that a reduction of 15–20% in the levels of the Rubisco protein can definitely cause a slight reduction in the demand for N by approximately 10% without any negative impact on the photosynthetic efficiency of plants (Parry *et al.*, 2013). It has been identified as an important target for genetic

engineering using RNAi technology to the small subunit in order to investigate the limitations imposed by it on photosynthetic capacity as well as growth performance attempting to improve NUE (Rodermel *et al.*, 1988; Hudson *et al.*, 1992). It was found that both the rates of photosynthesis and growth were not significantly affected under low light conditions ( $340 \mu\text{mol m}^{-2} \text{s}^{-1}$ ) when the activity of Rubisco was reduced to about half of what is found in the WT (Quick *et al.*, 1991b). On the other hand, under high light ( $1,050 \mu\text{mol m}^{-2} \text{s}^{-1}$ ), the photosynthetic capacity in and the growth of tobacco antisense plants were significantly affected (Stitt *et al.*, 1991; Hudson *et al.*, 1992).

In this study, the genetic engineering approach employing the technology of RNAi was used to produce wheat plants with less Rubisco. These transgenic *RbcS* RNAi plants were used to evaluate the Rubisco contribution and effect on wheat photosynthesis, growth and grain yields quality in an air-conditioned greenhouse under ambient UK spring/summer natural sunlight conditions in an attempt to improve NUE in wheat without any negative impact on photosynthesis.

The aim of this chapter was to 1. Identify transgenic lines with a range of reductions in Rubisco content throughout different generations (T0, T1 and T2), and 2. To carry out preliminary physiology and growth analyses on identified transgenic T1 lines with a range of reductions in Rubisco content to evaluate the photosynthetic capacity and biomass productions. 3. Leaf photosynthetic rates were measured in two different developmental growth stages with Zadoks growth scale of 1.5 and 4.5 (flag leaf) under UK spring/summer natural sunlight in the greenhouse under conditions as close to natural as possible. Additionally, total extractable Rubisco activity was determined in *RbcS* RNAi plants and WT plants. The total N and C contents were also analysed in

both grains (seeds) and leaves as a response to different ranges of decreased levels of Rubisco activity. Finally, the growth rate was investigated to determine the response of the transgenic plants' growth to different decreased levels of Rubisco activity.

## 4.2 Results

### 4.2.1 Construction and transformation of *RbcS* RNAi into wheat leaf

A following strategy was adopted for the use of the RNAi technology (built by Dr. Steven Dreiver). After the identification of the most conserved region sequences between wheat *RbcS* isoforms cDNA sequences, the start and stop codons were deleted because this fragment would not be translated. Then, the *RbcS* RNAi construct, containing a 345 bp of the codon sequence fragment, was designed with antisense and sense orientation at the 5' and 3' ends, respectively, and separated or spliced by an intron derived from the wheat TAK14 gene as described in Travella et al. (2006) with the addition of EcoRV and XmaI restriction sites. It was sent to the Invitrogen Company to be synthesised and cloned into a basic vector at DraIII sites and to generate plasmid at level 0. When it was returned, a functional construct of RNAi was first digested from the level 0 plasmid, using XmaI and EcoRV restriction enzymes, and cloned into an expression vector into the XmaI and EcoRV sites (pRRes14.101; Rothamsted, West Common, Harpenden, UK) under the control of a maize ubiquitin promoter. The BAR gene for phosphinothricin resistance was used for plant selections, and the ampicillin resistance gene was used in the vector for selection of bacteria (Figure 4.1). The recombinant *RbcS* RNAi plasmid was introduced into wheat cv. Cadenza by the use of particle bombardment of the wheat embryos, as described by Sparks and Jones (2009). Following biolistic transformation and tissue culture, which were regenerated in a medium containing Carbencillin antibiotic ( $100 \mu\text{g ml}^{-1}$ ) and were transformed to soil at at Rothamsted, West Common, Harpenden, UK.

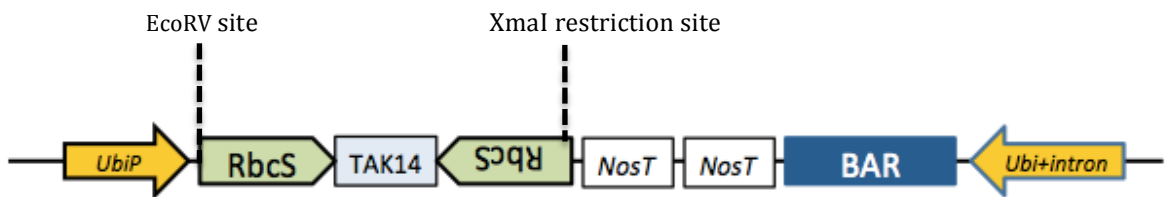


**Figure 4.1: Rubisco small subunit RNAi construct used for particle bombardment transformation into wheat.**

The most conserved region between the isoforms of wheat Rubisco small subunit (345 bp) was cloned in antisense and sense orientation at the 5' and 3' ends, respectively, and spliced by an intron derived from the wheat TAK14 gene, with the addition of EcoRV and XmaI restriction sites.

#### **4.2.2 Selection of primary transformants wheat plants (T0): Expression of Rubisco small subunit (*RbcS*) cDNA using a quantitative polymerase chain reaction (q-PCR)**

The leaf tissues of T0 transformed *RbcS* wheat plants were screened in order to identify the transformants with reduced *RbcS* gene expression. Total RNA was extracted from leaf tissues and cDNA were prepared for expression analysis using qPCR. Specific wheat *RbcS* primers were designed for *RbcS* CDS amplification (Chapter 2, Table 2.4). As a result, relative transcriptional levels were found to be decreased to different levels in different independent lines compared to those of the actin reference gene. Out of 13 T0 plants tested, there were decreased expression levels in 10 different independent transformant plants (RSS2, RSS3, RSS6, RSS7, RSS8, RSS9, RSS10, RSS11, RSS12 and RSS13) compared to the wild type (Figure 4.2).

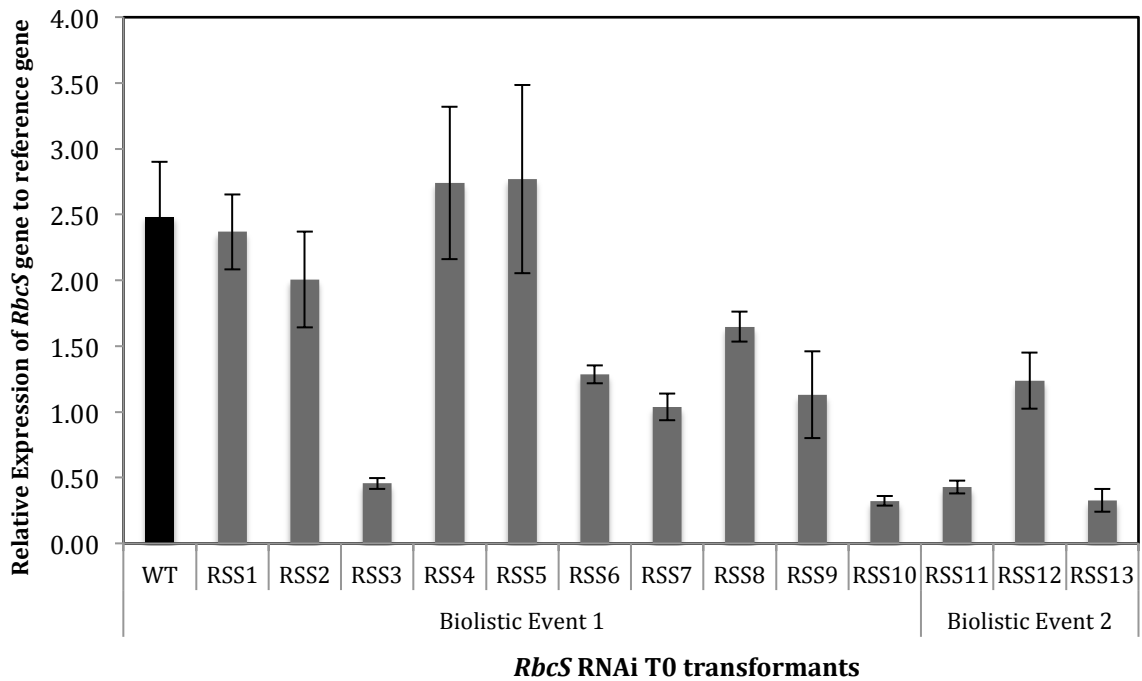


**Figure 4.2: Relative gene expression analysis of the wheat *RbcS* gene in transformant T0 wheat plants using q-PCR.**

RNA was extracted from the second leaf at the seedling stage from T0 plants. Wheat *RbcS* genes were all amplified by qPCR using specific primers (chapter 2, Table 2.4). The expression was relative to the gene expression of a stable actin reference gene.

In this study, primary transformants wheat plants were screened, and a low level of *RbcS* expression was confirmed. The main part of this preliminary screening was done on T1 and T2 progenies. The primary transformants were allowed to self-fertilize and then seeds were collected for further analyses.

#### **4.2.3 Preliminary screening of T1 progeny**

The preliminary analyses of the T1 transgenic wheat plants consisted of two different processes: molecular and physiological analyses. The molecular screenings were done in three different approaches: DNA screening using PCR, gene expression analysis using qPCR and protein expression analysis using the Western blot. Plants confirmed to have a reduced *RbcS* protein levels were subject to physiological analyses to examine whether the reductions of the *RbcS* level had had an impact on photosynthesis or biomass production.

##### **4.2.3.1 Confirming the presence of transgenic *RbcS* in transgenic wheat T1 plants using PCR**

To confirm the stable presence of the *RbcS* RNAi construct in the T1 generation, 10–14 seeds each from seven lines of transgenic wheat T0 (80 transgenic plants and 20 wild type plants) were germinated, and seedlings were allowed to grow in a controlled room for three weeks. The first leaf of each was harvested for DNA extractions and PCR screening using primers for the unique sequence of the construct (Chapter 2, Table 1). As a result, five lines of seven were shown to have the *RbcS* RNAi construct at about 750 bp size, including the RSS2, RSS7, RSS8, RSS11 and RSS13 lines compared to the wild-type (WT) line. However, three lines did not have the construct (Figure 4.3).

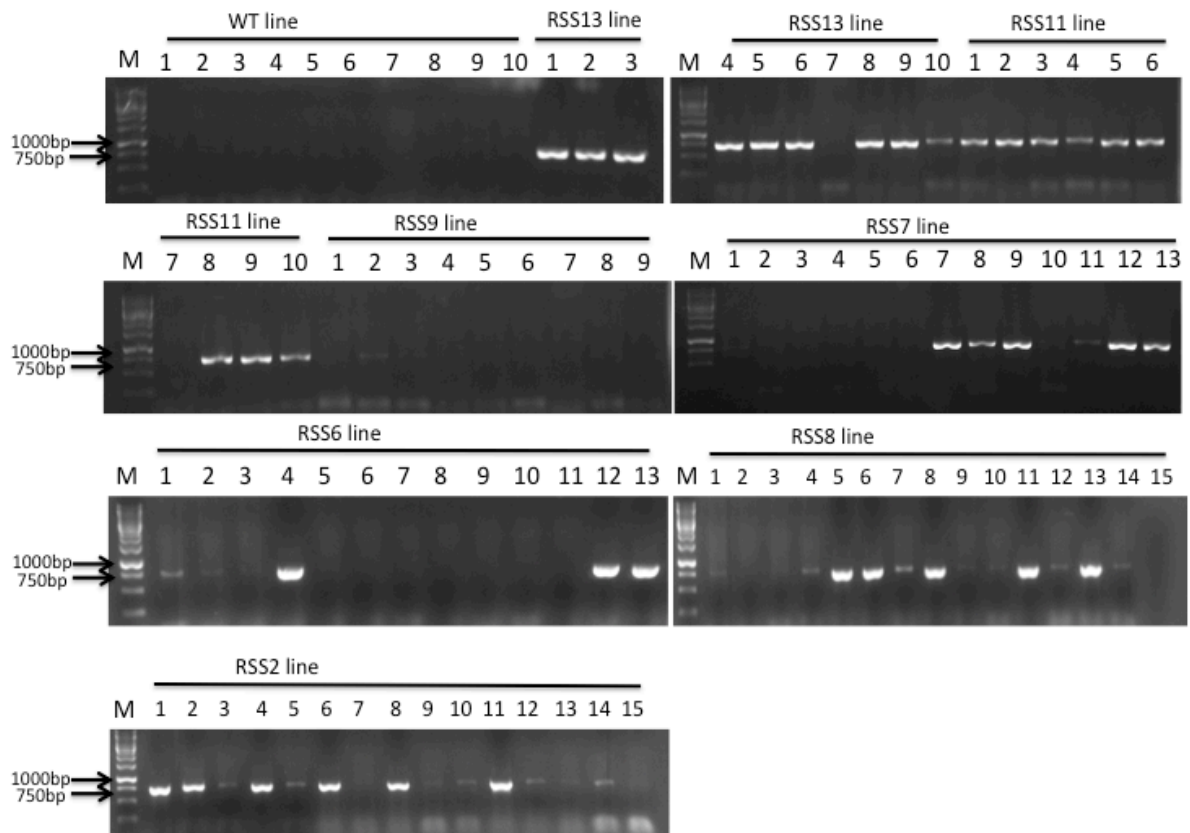


**Figure 4.3: PCR analysis of genomic DNA to confirm the presence of the *RbcS* RNAi construct in T1 wheat leaves.**

DNA was extracted from the first leaves of T1 transgenic and WT wheat plants. *RbcS* RNAi construct was amplified by PCR using specific designed primers shown in chapter 2, Table 2.1, the PCR products were separated on a 1% agarose gel. The condition of the electrophoresis was 110 V for 30 min, with 5  $\mu$ l of DNA ladder used as a DNA marker along with 0.5 $\times$  TBE buffer. M, molecular size marker (1 kb gene ruler).

#### **4.2.3.2 Gene expression analysis of coding sequence *RbcS* in transgenic wheat plants T1 using q-PCR**

To analyse the expression of *RbcS* gene into transgenic wheat T1, the second leaves were harvested in liquid N<sub>2</sub> from the plants that had the construct within the five independent lines plus the WT. Total RNAs from the second leaves of 6 to 10 plants, within five independent lines, were isolated and the cDNAs were synthesised. Then, *RbcS* cDNAs were amplified using qPCR specific designed primers (shown in Chapter 2, Table 2.4).

Figure 4.4 shows the different decreased expression levels of *RbcS* in some plants in five independent lines compared to the wild-type (WT). This confirms that the *RbcS* gene has down-expressed at a transcription level in different plants within different independent transgenic *RbcS* RNAi lines (Table 4.4).

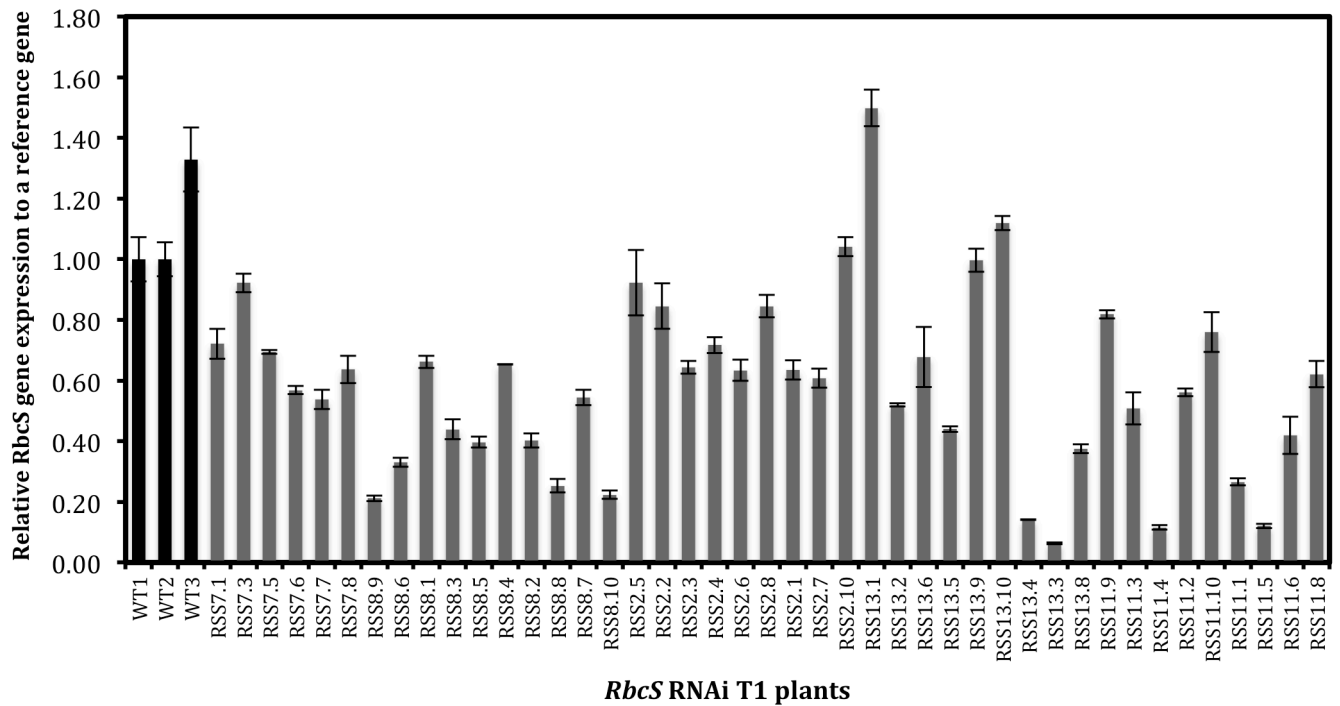


**Figure 4.4: Determination of the transcript levels of the *RbcS* transcript in T1 transgenic wheat plants.**

RNA was extracted from the second leaf at the seedling stage from 6-10 plants that showed to have the construct in Figure 4.3. Wheat *RbcS* genes were amplified and detected by qPCR using specific primers shown in chapter 2, Table 2.1. The expression was relative to the gene expression of a stable Ta2291 reference gene.

**Table 4.2: Transgenic *RbcS* RNAi wheat T1 lines with reduced expression compared to WT plants.**

<b><i>RbcS</i> RNAi lines</b>	<b>Positive transgenic Plants</b>
<b>RSS13</b>	2, 6, 5, 4, 3 and 8
<b>RSS11</b>	1, 2, 3, 4, 5, 6, 8, 9 and 10
<b>RSS7</b>	1, 3, 5, 6, 7 and 8
<b>RSS8</b>	1, 2, 3, 4, 5, 6, 7, 8, 9 and 10
<b>RSS2</b>	1, 3, 4, 6 and 7

#### **4.2.3.3 Protein expression analysis of *RbcS* in transgenic T1 wheat plants using Western blot**

To investigate whether *RbcS* protein expression is reduced, proteins were extracted from leaves of the plants shown to have reduced gene expression levels, and were analysed using immunoblotting. First, to determine the optimal and sufficient concentration of protein needed for the analysis of *RbcS* protein expression, different dilutions of protein (from 0.1 µg to 3 µg) were used for Western blot and antibody raised against Rubisco enzyme. Consequently, protein concentrations ranging from 0.8 µg to 1.5 µg were used to determine the level of the *RbcS* protein (Figure 4.5).

Immunoblotting was carried out using total extractable protein of 1.5 µg and loaded into 12% SDS-polyacrylamide gels. The proteins were run and separated by electrophoresis, transferred into PVDF membranes, probed and rinsed with Rubisco antibody. A band was recognised at about 15 kDa indicating the Rubisco small subunit (Figure 4.6). The protein levels of Rubisco were shown to vary between the five different transgenic T1 lines compared to the WT: RSS13 line (2, 6, 2, 5, and 4), RSS11 line (5, 6, 8, 3, and 2), RSS8 line (9, 1, 5, 4 and 2), RSS7 line (5, 6, 7, and 8) and RSS2 line (1, 2, 3, 4, 6, 7, and 8). This reduction in protein levels correlated with the gene expression results of the *RbcS* gene.

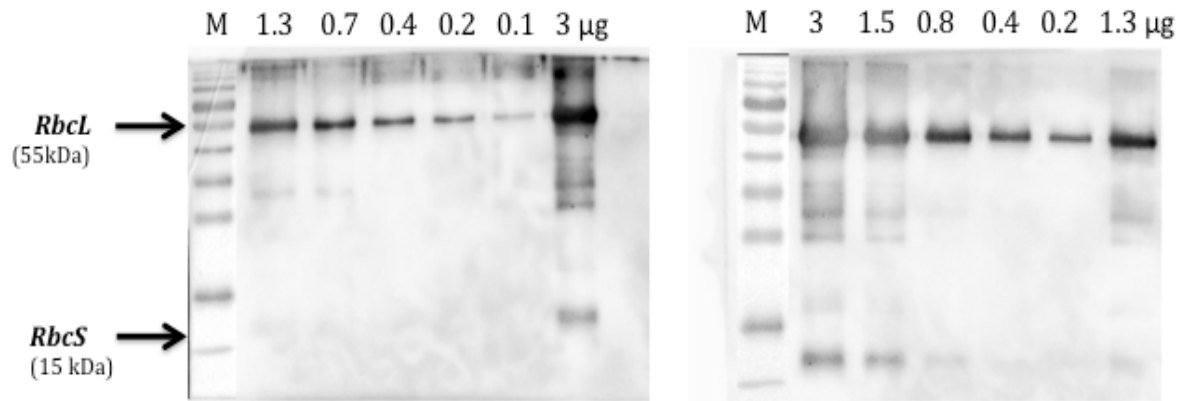


**Figure 4.5: Optimizing the protein dilution to detect *RbcS* in T1 wheat plants.**

Total extractable proteins between 0.1 to 3 μg were loaded into 12% polyacrylamide gels and blotted to PVDF membrane. Antibody raised against Rubisco protein was used to detect the small subunit enzyme.

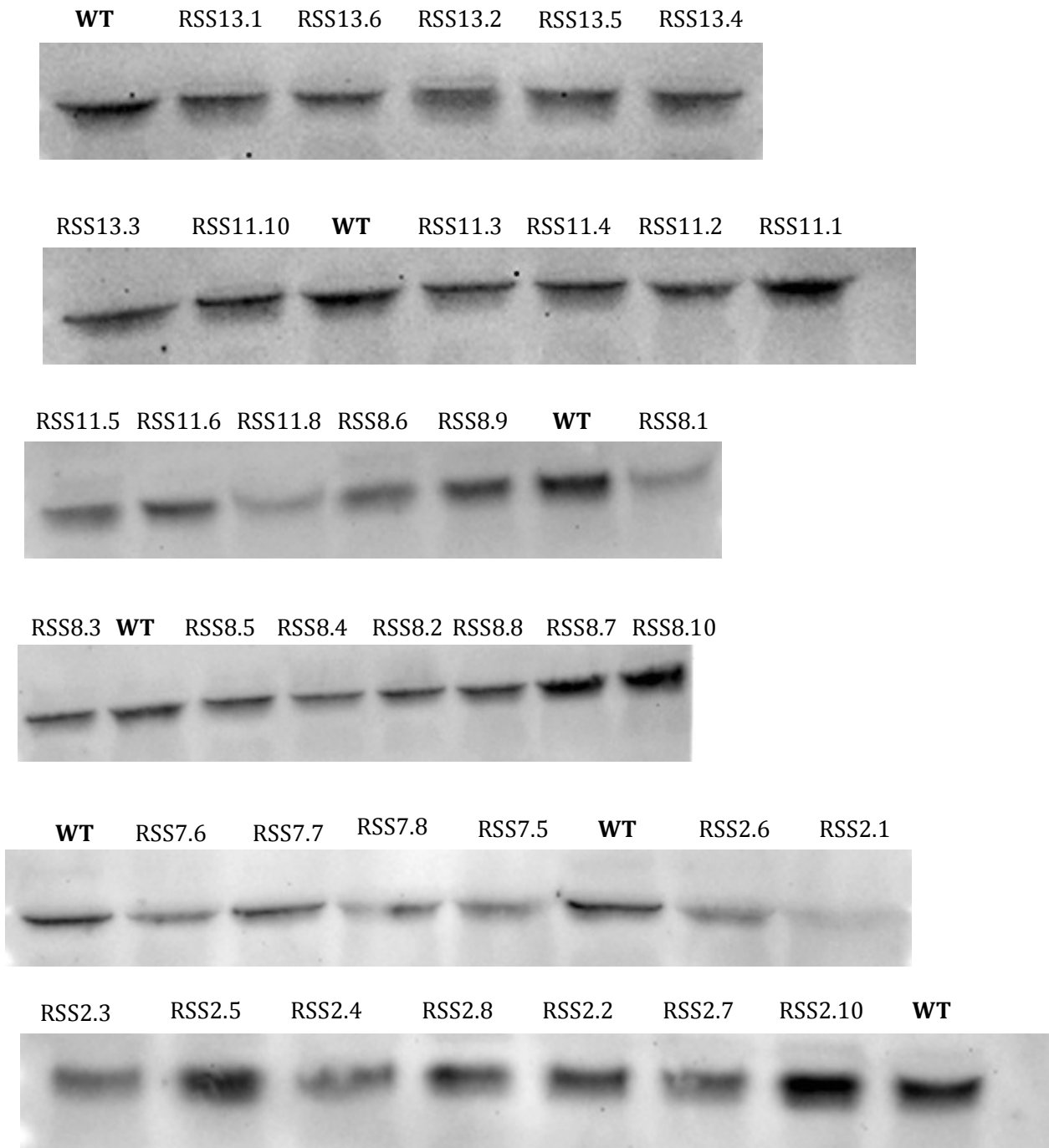


**Figure 4.6: Immunoblot analysis of transgenic *RbcS* RNAi T1 wheat plants.**

Western blot analysis in the third leaves from five independent transgenic lines compared to the WT. A total extractable leaf protein of 1.5  $\mu$ g, of individual *RbcS* RNAi plants with five independent transgenic T1 lines and wild type (WT), were loaded and separated into 12% polyacrylamide gels and blotted to PVDF membrane. Antibody raised against Rubisco protein was used to detect the small subunit enzyme.

At this stage, the previous molecular results indicated that there were clearly different levels of reduction in the *RbcS* in several plants within the five different independent transgenic lines compared to the WT plants. Therefore, in order to test the hypothesis that this *RbcS* reduction affects the photosynthetic capacity and growth of wheat plants, preliminary physiological and biomass analyses were needed to examine the effect of these different levels of reduction on the photosynthesis capacity of wheat T1 plants.

#### **4.2.3.4 $A/C_i$ photosynthetic gas exchange measurement**

To explore the impact of the decreased level of *RbcS* protein on leaf photosynthetic rate, the response of light saturated photosynthesis to increasing  $\text{CO}_2$  concentrations ( $A/C_i$  curve) was determined for the five T1 lines of transgenic *RbcS* RNAi wheat compared to the WT plants. After germination of the seedlings in a control room for three weeks, selected seedlings that showed reduced levels of SSU gene and protein expression were transferred to a controlled greenhouse (25–32 °C day/18 °C night, 16 h photoperiod of natural irradiance supplemented with high-pressure sodium lamps [minimum light level:  $175 \mu\text{mol m}^{-2} \text{s}^{-1}$  PAR]) for further analysis. The gas exchange measurements were done on a fully mature flag leaf using Zadoks scale of 4.1–4.5. The results clearly showed that significant decreases in photosynthesis were observed in three of the *RbcS* RNAi lines (RSS7, RSS8 and RSS13) particularly when measured under saturating  $\text{CO}_2$  compared to WT line. In *RbcS* RNAi lines with small reductions in Rubisco showed only (RSS2 and RSS11), a slightly lower photosynthetic  $\text{CO}_2$  assimilation was observed compared to that in the WT line (Figure 4.7).

From the  $A/c_i$  response, both the maximum rate of carboxylation of the Rubisco enzyme ( $V_{c, \text{max}}$ ) and the maximum electron transport required for the regeneration of

ribulose-1, 5-bisphosphate (RuBP) ( $J_{\max}$ ) were determined and solved using the equations of von Caemmerer and Farquhar (1981). As a consequence, both  $V_{c, \max}$  and  $J_{\max}$  were significantly lower in three different independent transgenic lines (RSS7, RSS8 and RSS13) than in the WT plants. However, they were lower in the other two independent transgenic lines (RSS2 and RSS11) than in the WT plants, but not significant (Figures 4.8a and 4.8b).

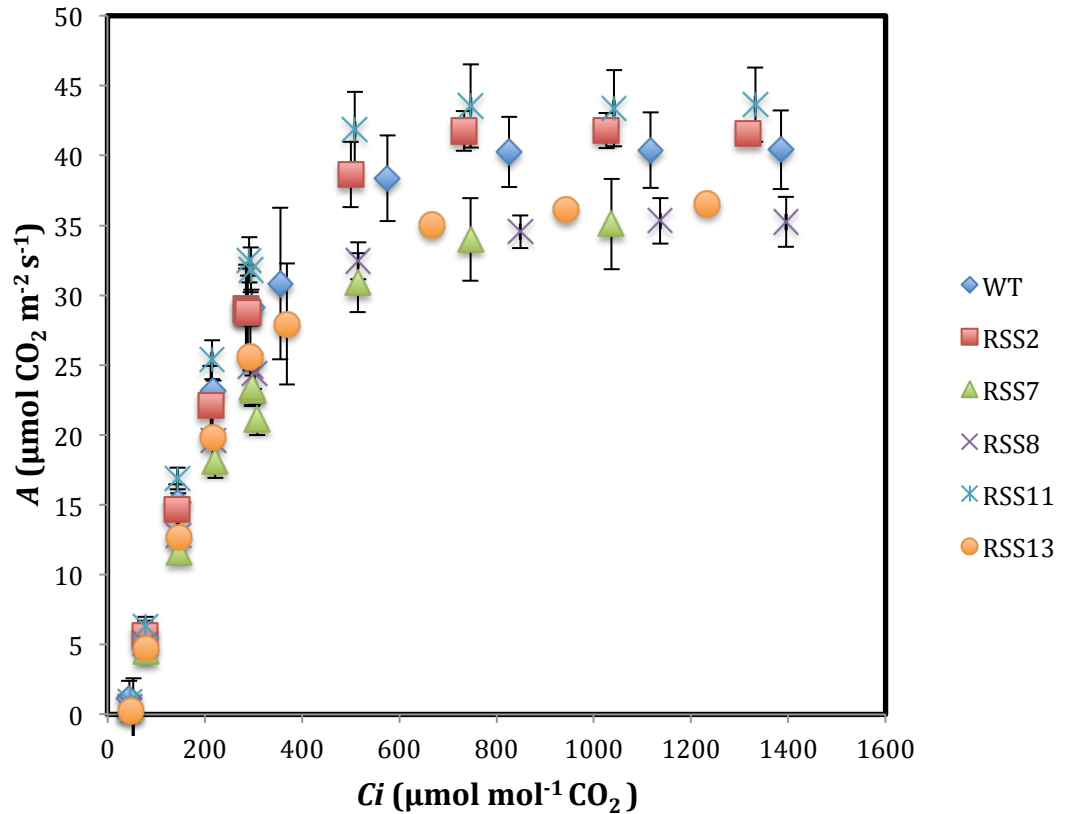


**Figure 4.7: Photosynthetic  $\text{CO}_2$  assimilation ( $A$ ) response to increasing internal concentration of  $\text{CO}_2$  ( $C_i$ ) ( $A/C_i$  curve) for five independent *RbcS* RNAi T1 lines compared to the WT plants.**

Plants were grown in an environmental controlled greenhouse (25-32 °C day/ 18 °C night, 16h photoperiod of natural irradiance supplemented with high-pressure sodium lamps (minimum light level: 175  $\mu\text{mol m}^{-2} \text{s}^{-1}$  PAR). Photosynthetic measurements were performed on a fully mature flag leaves at Zadok's scale of 4.1-4.5, with a light-saturated rate of 2000  $\mu\text{mol m}^{-2} \text{s}^{-1}$  using an open infrared gas exchange system. Value represents the average of three plants per line.

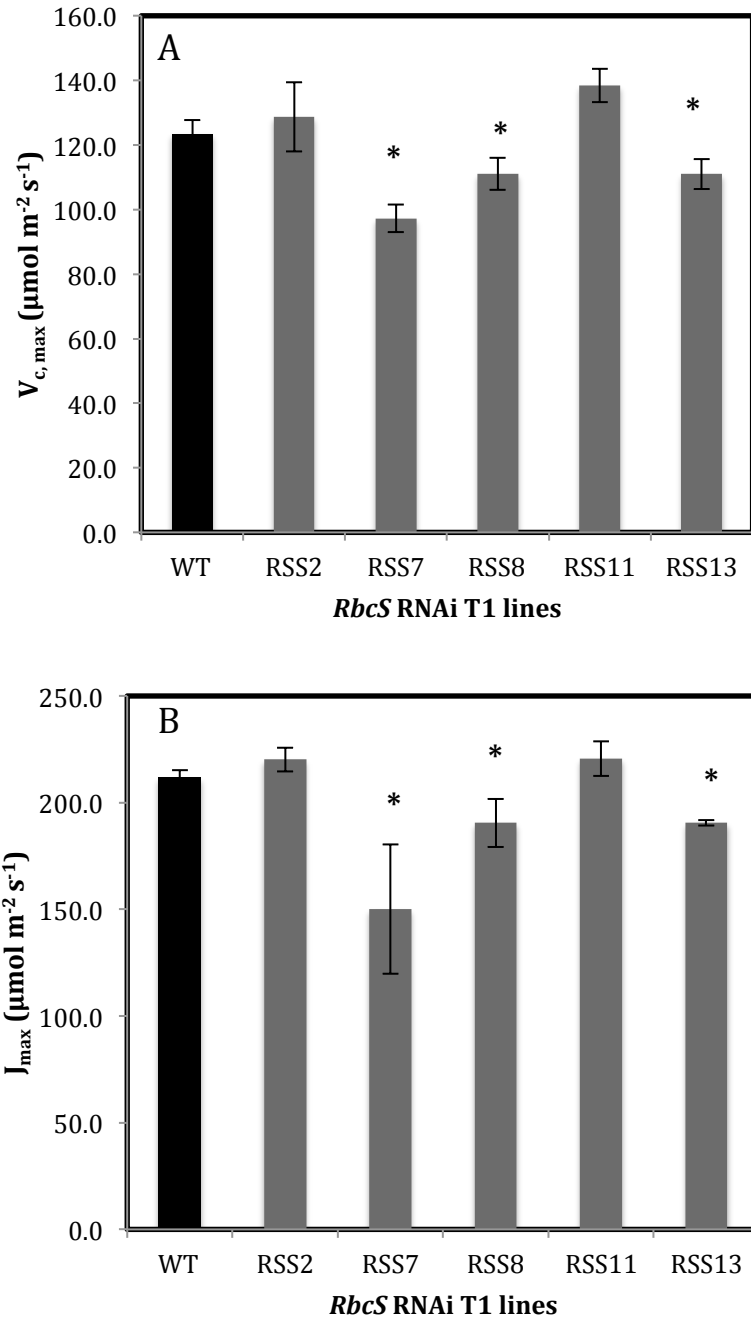


**Figure 4.8: Maximum rate of carboxylation allowed by the Rubisco enzyme ( $V_{c,max}$ ) and the maximum electron transport required for RuBP regeneration ( $J_{max}$ ).**

$V_{c,max}$  and  $J_{max}$  were both solved from the  $A/C_i$  measurements shown in Figure 4.7, by the use of the equations of von Caemmerer and Farquhar (1981). **A.** Maximum *in vivo* rate of carboxylation allowed by RuBisCO enzyme ( $V_{c,max}$ ). **B.** Maximum electron transport required for RuBP regeneration ( $J_{max}$ ). Value represents the average of three plants per line. Stars indicate significant differences from WT ( $P < 0.05$ ).

#### **4.2.3.5 The effect of decreased level of Rubisco protein on T1 plant biomass**

To determine the total biomass of transgenic T1 wheat with reduced level of *RbcS* protein, the leaves, stems, ears and seeds were harvested and dried when all seeds were hardened and all plants had reached Zadoks growth stage of 9.2. By this time, three independent T1 lines, which showed less Rubisco protein and lower photosynthetic rate, had exhibited significantly lower total biomass (RSS7, RSS8 and RSS13) compared to the WT plants; while the other two *RbcS* RNAi lines (RSS2 and RSS11), which showed less Rubisco protein but not clear reduction in photosynthesis, were not significantly different than the WT line (Figure 4.9).

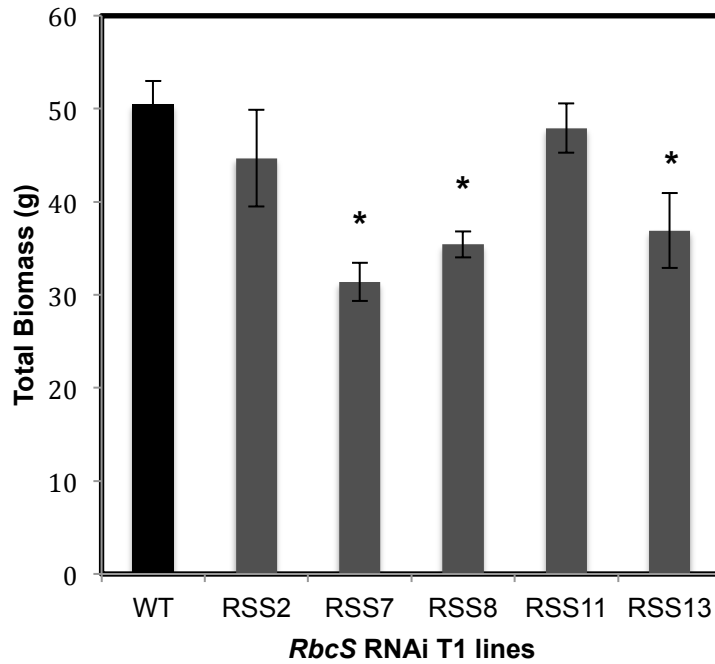


**Figure 4.9: Total biomass analysis of *RbcS* RNAi wheat T1 plants grown in a controlled-environment greenhouse.**

Plants were grown in same conditions as for Figure 4.7 and were all harvested when all seeds had hardened and plants reached Zadoks growth stage of 9.2; and dried at 70°C for three days. Values represent the average of at least three plants per line of *RbcS* RNAi wheat plants and wild type (WT). Stars indicate significant differences from WT (P < 0.05).

#### 4.2.3.6 The effect of decreased content of Rubisco protein on individual plant photosynthesis

To identify the effect of the decreased content of Rubisco protein on individual plants, the response of photosynthetic rates to changes in intercellular CO<sub>2</sub> concentrations ( $A/C_i$ ) was measured under the condition of a light-saturated level of 2,000  $\mu\text{mol m}^{-2} \text{s}^{-1}$  for different individual plants within different lines of transgenic *RbcS* RNAi wheat T1 progeny at the developmental growth stage 4.1 of the Zadoks scale. After the germination of three week old seedlings which showed lower levels of gene and protein expressions, were transferred to the greenhouse and allowed to complete their growth. The results clearly showed that decreased Rubisco protein content did not impact negatively on photosynthetic CO<sub>2</sub> assimilation in those *RbcS* RNAi lines that had only small reductions in Rubisco protein content (RSS2 and RSS13) than in the WT plants (Figure 4.10).

From the  $A/C_i$  responses, the maximum rate of carboxylation allowed by the Rubisco enzyme ( $V_{c,\text{max}}$ ) and the maximum electron transport required for the regeneration of RuBP ( $J_{\text{max}}$ ) were determined via the equations of von Caemmerer and Farquhar (1981). Consequently, no significant differences were found in the other two lines with small reductions of Rubisco protein compared to the WT plants (Figure 4.11).

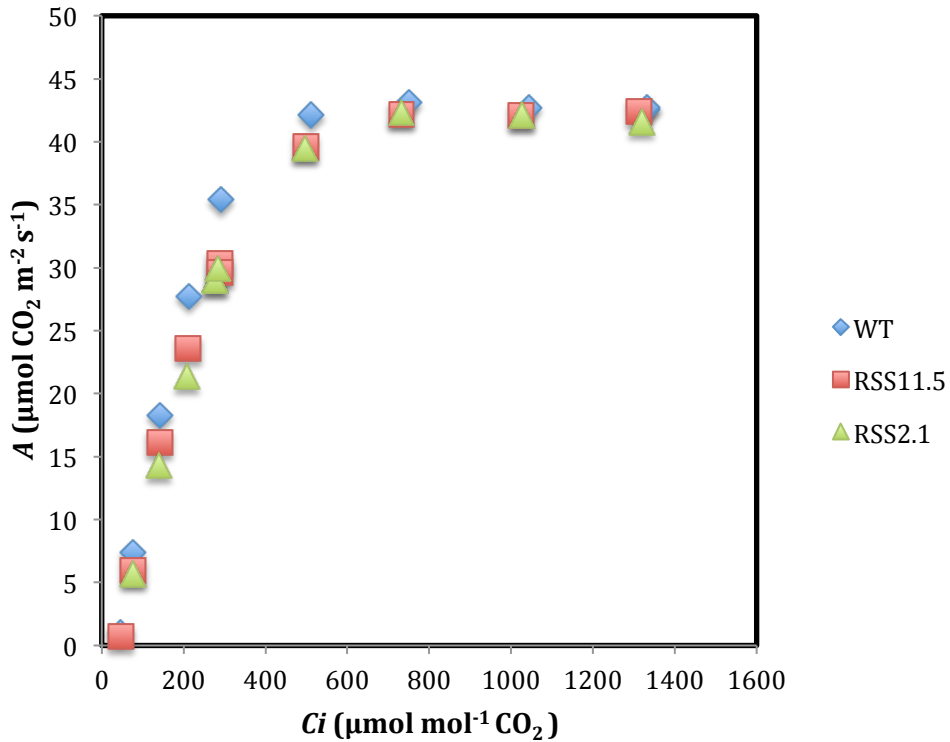


**Figure 4.10: Photosynthetic  $\text{CO}_2$  assimilation ( $A$ ) response to different internal concentrations of  $\text{CO}_2$  ( $C_i$ ) ( $A/C_i$  curve) for two individual *RbcS* RNAi T1 plants compared to the WT plant.**

Plants were grown in an environmental controlled greenhouse (25-32 °C day/ 18 °C night, 16h photoperiod of natural irradiance supplemented with high-pressure sodium lamps (minimum light level: 175  $\mu\text{mol m}^{-2} \text{ s}^{-1}$  PAR). Photosynthetic measurements were performed on a fully mature flag leaves at Zadok's scale of 4.1-4.5, with a light-saturated rate of 2000  $\mu\text{mol m}^{-2} \text{ s}^{-1}$  using an open infrared gas exchange system.

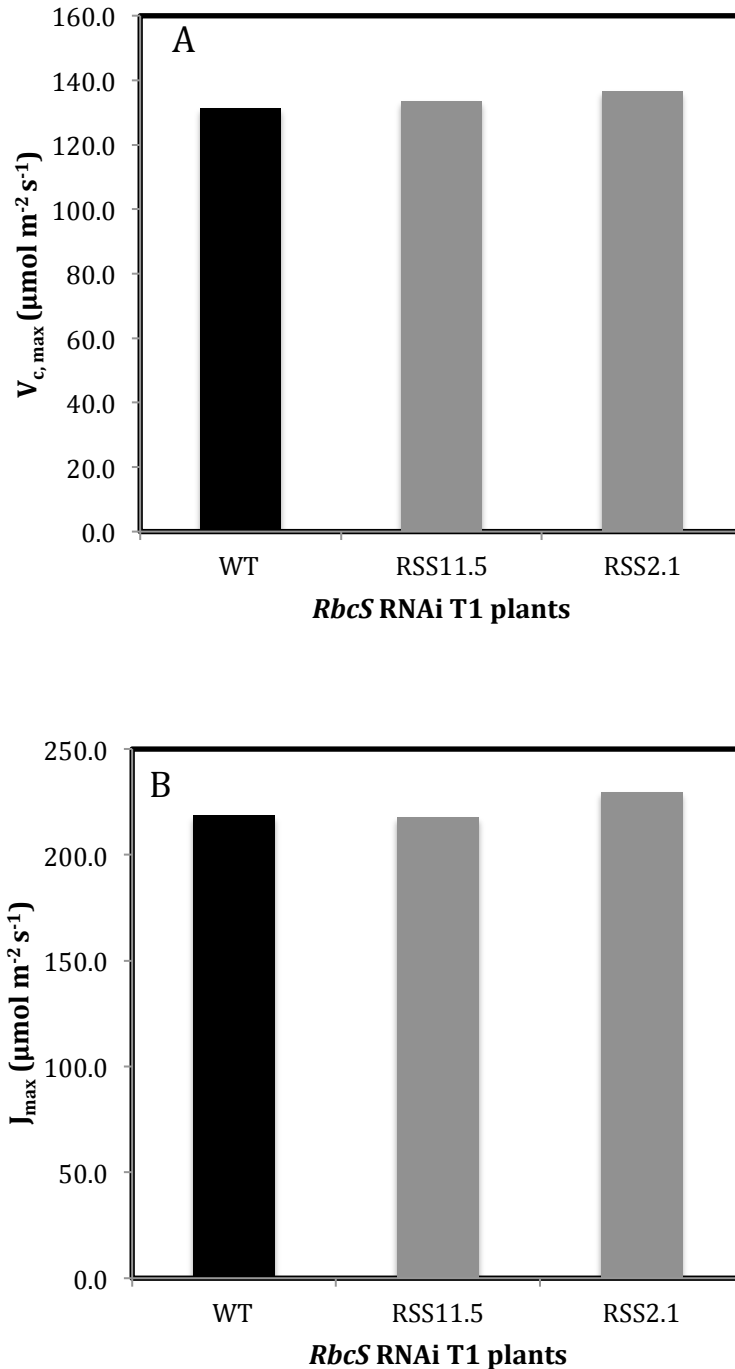


**Figure 4.11: Maximum rate of carboxylation allowed by the Rubisco enzyme ( $V_{c,max}$ ) and the maximum electron transport required for RuBP regeneration ( $J_{max}$ ).**

$V_{c,max}$  and  $J_{max}$  of two individual *RbcS* RNAi transgenic plants from two different lines compared to the WT plant, were all solved from the *A/Ci* measurements shown in Figure 3.10, by the use of the equations of von Caemmerer and Farquhar (1981). **A.** Maximum *in vivo* rate of carboxylation allowed by RuBisCO enzyme ( $V_{c,max}$ ). **B.** Maximum electron transport required for RuBP regeneration ( $J_{max}$ ).

#### **4.2.4 Molecular analyses of T2 progeny: DNA screening, *RbcS* gene expression and *RbcS* protein content**

##### **4.2.4. 1 Confirming the presence of transgenic *RbcS* RNAi in wheat T2 plants using PCR**

To confirm the presence of the *RbcS* RNAi construct in the T2 generation, 10–13 seeds of each plant from each of the independent eight lines (that showed less *RbcS* proteins in T1 generation) were planted, and the first leaf of each was harvested for DNA extractions and PCR screening. As a result, several positive bands were identified at approximately 750 bp, which indicated the presence of the *RbcS* RNAi construct compared to the WT line with no bands (Figure 4.12).

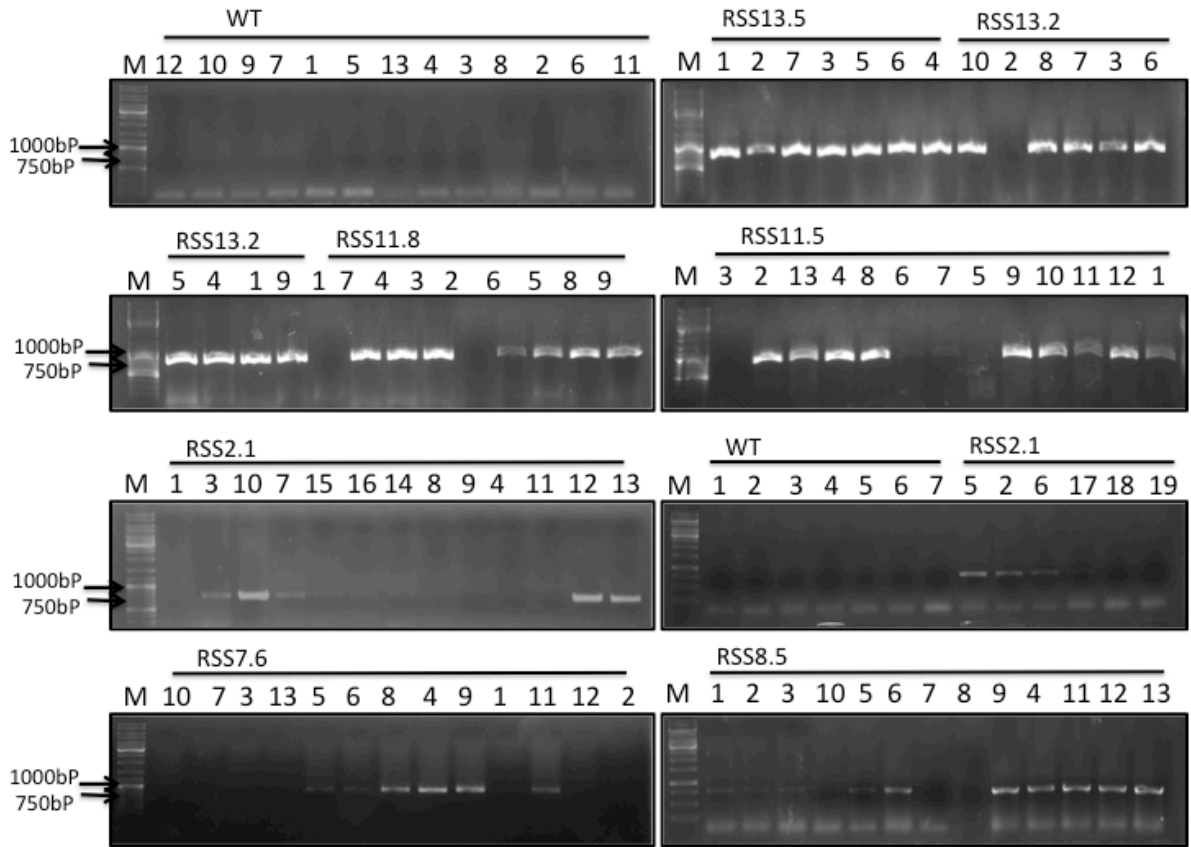


**Figure 4.12: PCR analysis of genomic DNA to confirm the presence of the *RbcS* RNAi construct in T2 wheat leaves.**

Plants were grown in an environmental controlled greenhouse under natural sunlight. DNA was extracted from the first leaves of T2 transgenic and WT plants. *RbcS* RNAi construct was amplified by PCR using specific designed primers shown in chapter 2, Table 2.4. The plants expressing the *RbcS* RNAi construct represent a band at approximately 750 bp compared to the wild type (WT). M, molecular size marker (1 gene ruler mix). The condition of the 1% agarose gel electrophoresis was 110 V for 30 min, with 5  $\mu$ l of DNA ladder used as a DNA marker along with 0.5 $\times$  TBE buffer.

#### **4.2.4.2 Gene expression analysis of the coding sequence of the *RbcS* gene in transgenic wheat plants (T2) using q-PCR**

To analyse the expression of the *RbcS* RNAi construct in transgenic wheat T2, total RNA from the second leaf of 4 to 10 plants within the five independent transgenic lines: RSS2.1, RSS7.6, RSS8.5, RSS11.5 and RSS13.2, was extracted cDNA synthesised. The *RbcS* cDNA of the different plants within the five independent lines was amplified using qPCR. The results showed that the relative expression levels were decreased in several individual *RbcS* RNAi plants within the lines compared to the WT individual plants (Figure 4.13A), and that a range of reductions in *RbcS* gene expression levels was evident in the different independent *RbcS* RNAi lines compared to the WT lines (Figure 4.13B).

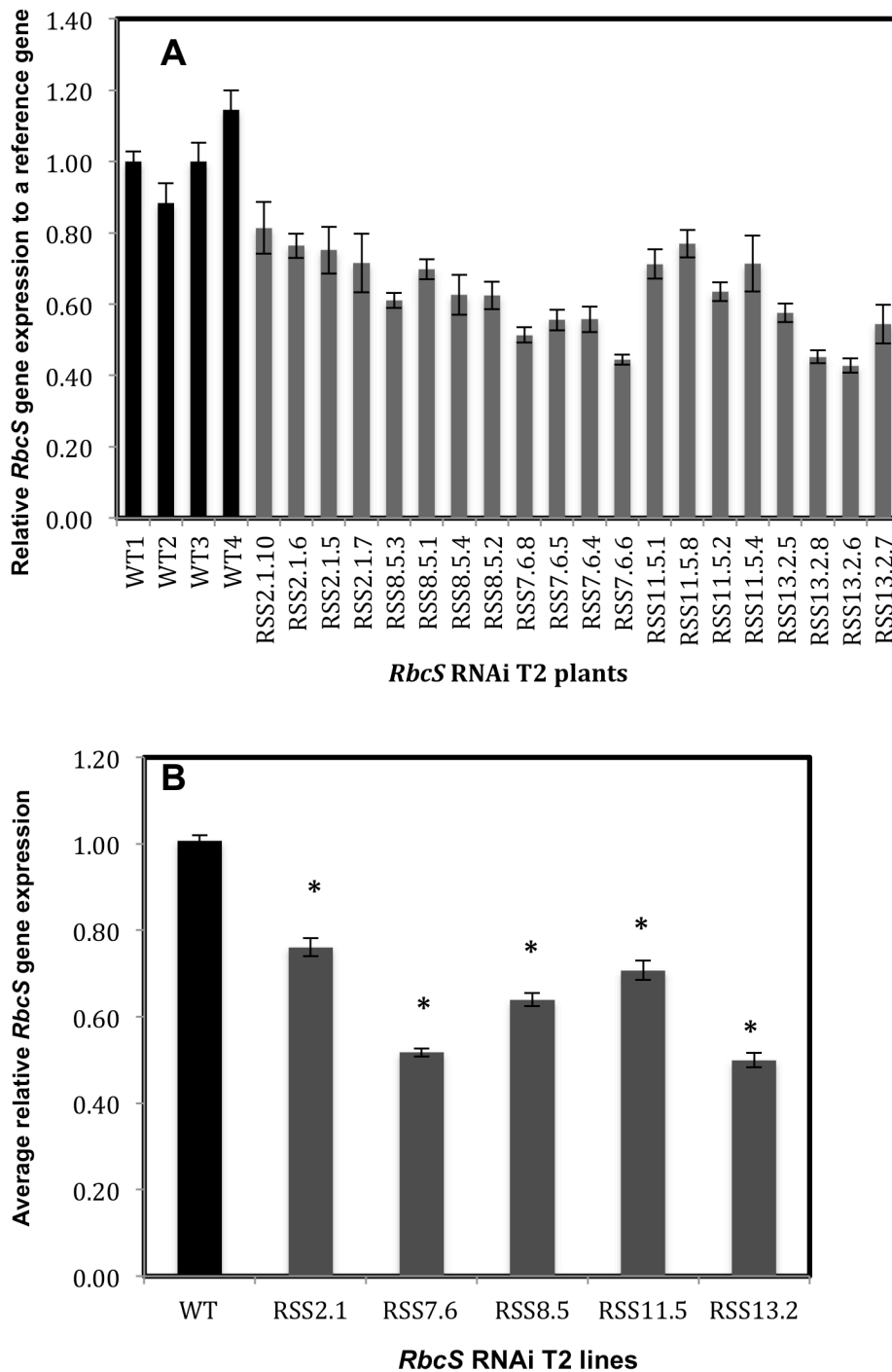


**Figure 4.13: Determination the level of *RbcS* gene expression in transgenic T2 wheat plants.**

The RNA was extracted from the second leaf at the seedling stage from T2 plants. *RbcS* RNAi construct was amplified using specific primers (chapter 2, Table 2.4) that detect all *RbcS* genes in the wheat genome. The expression was normalized against actin reference gene. **A.** *RbcS* gene expression in individual *RbcS* RNAi plants into five independent lines compared to the wild type (WT). **B.** Average of *RbcS* gene expression per line compared to the wild type (WT), Values represent average of four plants from five individual transgenic lines compared to WT line. Stars indicate significant differences from WT ( $P < 0.05$ ).

#### **4.2.4.3 Protein expression analysis of *RbcS* in transgenic wheat plants (T2) using the Western blot approach**

To investigate whether the expression of the *RbcS* protein level is reduced in the subsequent T2 plants, the third leaf was harvested from 3–4 plants of five independent lines and the WT control. Next, the protein was extracted and quantified using the Bradford assay as a preparation for Western blotting. The Rubisco protein was screened using Western blotting and consequently, it was confirmed that there were plants with decreased levels of the Rubisco small subunit protein among the five different transgenic lines compared to the WTs. This *RbcS* reduction led to a corresponding decrease in Rubisco large subunit protein compared to the WT, whereas the level of PRK proteins remained constant (Figure 4.14). This confirmed that the functionality of the introduced RNAi construct in the wheat leaves had resulted in some independent lines with varying reductions in Rubisco protein content.

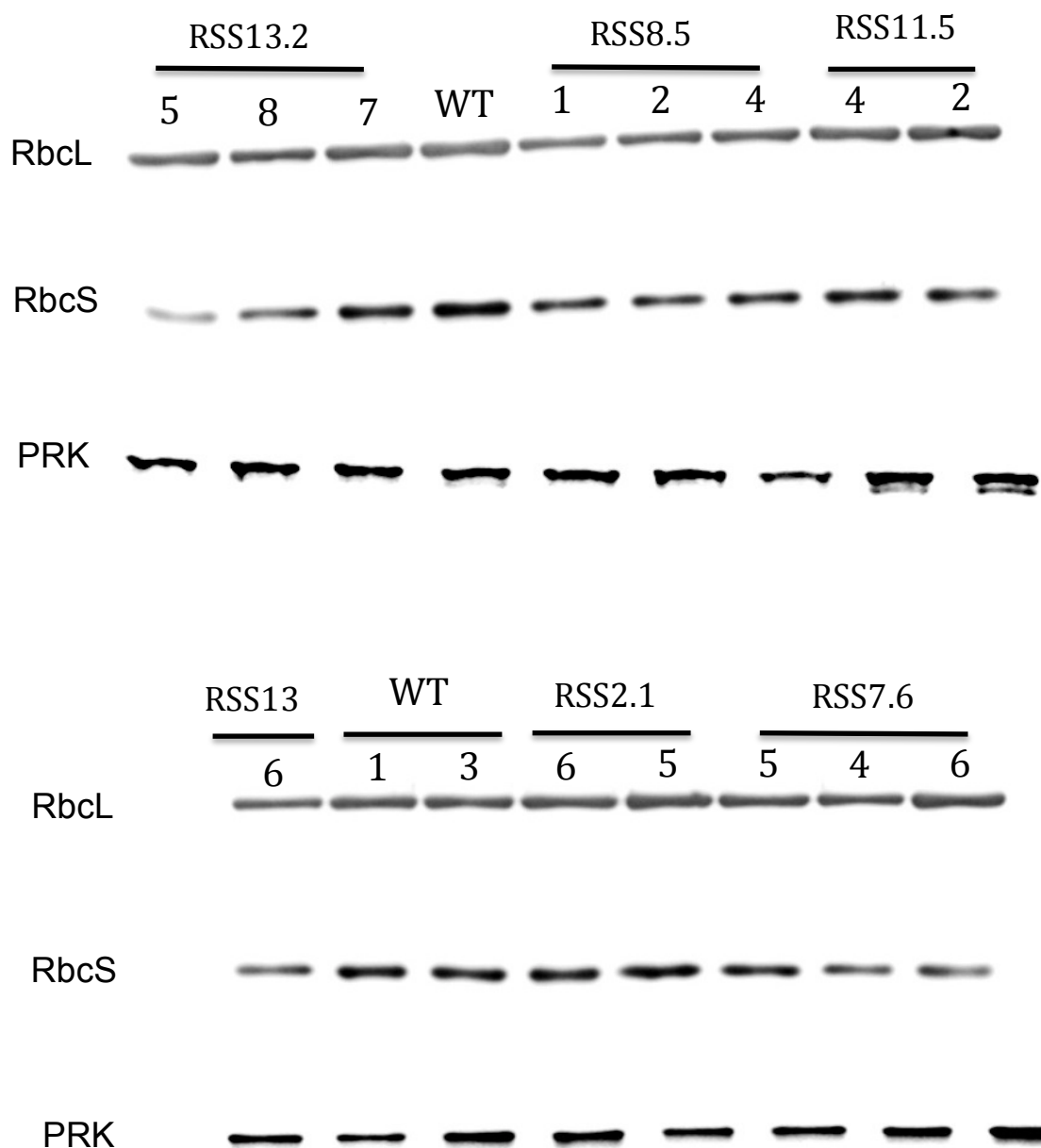


**Figure 4.14: Immunoblot analysis of transgenic *RbcS* RNAi T2 wheat plants.**

Western blot analysis in the third leaves from five independent *RbcS* RNAi T2 lines compared to the wild type line (WT). A total extractable leaf protein of 0.8  $\mu\text{g}$ , of individual transgenic plants within five independent transgenic lines and WT, were loaded into 12% polyacrylamide gels and blotted to PVDF membrane. Antibody raised against Rubisco protein was used to detect the small subunit enzyme.

#### **5.2.1.4 Rubisco activity in *RbcS* RNAi wheat plants**

For the selected *RbcS* RNAi lines and the WT line, plants were grown in an air-conditioned greenhouse under conditions as close to UK spring/summer natural sunlight conditions as possible. Total extractable Rubisco enzyme activity of the flag leaves of T2 progeny was spectrophotometrically determined. The results revealed that *RbcS* RNAi plants with a range of decreased Rubisco activity was observed, and this corresponded to the decrease found in both the *RbcS* gene expression as well as the protein content levels, respectively. The average Rubisco activity of the three transgenic lines (RSS7.6, RSS8.5 and RSS13.2) was significantly lower than the average of the WT line at approximately 30% to about 48%, respectively ( $P < 0.05$ ), and significant differences were observed in the other two transgenic lines (RSS2.1 and RSS11.5) compared to the WT plants at around 25% to about 28%, respectively ( $P > 0.05$ ) (Figure 4.15).

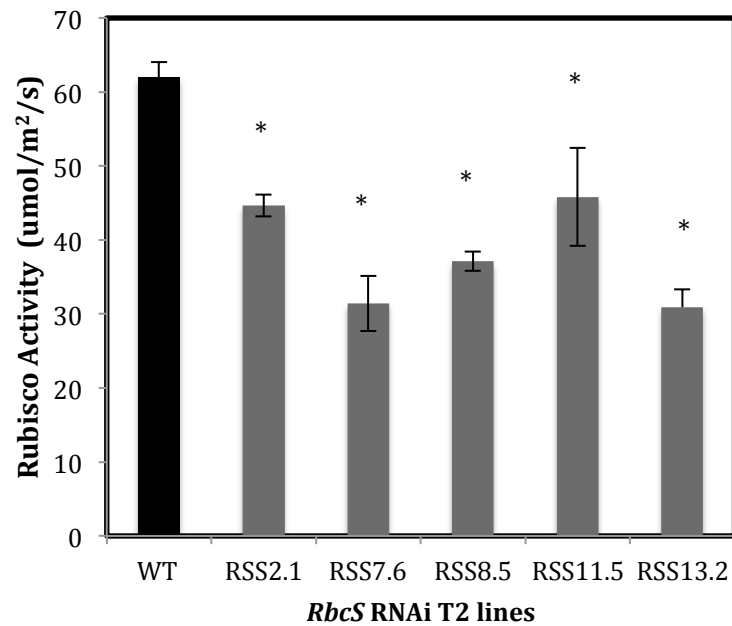


**Figure 4.15: Decrease in total extractable Rubisco activity in *RbcS* RNAi wheat plant T2 progeny.**

The plants were grown in an air-conditioned greenhouse in conditions as close to natural as possible under the UK spring/ summer sunlight. Protein was extracted from the flag leaves and total extractable Rubisco activity were assayed using spectrophotometer and was calculated by observing the reduction of NADH absorbance at the wavelength of 340 nm after the reaction initiation by RuBP substrate. Values represent the average of four transgenic plants per line compared to the average of four WT plants. Stars indicate significant differences from WT (P<0.05).

#### **4.2.5 The effect of different decreased levels of Rubisco activity on photosynthesis and growth in wheat *RbcS* RNAi transgenic plants grown under natural sunlight in the UK spring/ summer seasons.**

##### **4.2.5.1 CO<sub>2</sub> assimilation in leaves at different developmental growth stages of Zadoks scale**

To identify the effect of the decreased level of Rubisco activity on wheat photosynthesis, the response of photosynthetic rates to changes in intercellular CO<sub>2</sub> concentrations ( $A/C_i$ ) was measured under the condition of a light-saturated level of 2,000  $\mu\text{mol m}^{-2} \text{s}^{-1}$  for the five different independent lines of transgenic *RbcS* RNAi wheat T2 progeny at two developmental growth stages of Zadoks scale (Z1.5 and flag leaf or Z3.9–4.1). After the germination of seedlings in a control room for three weeks, selected seedlings, which showed lower levels of gene and protein expressions, were transferred to a controlled greenhouse under natural sunlight and allowed to complete their growth. The results showed clearly that significant decreases in photosynthetic rate were observed in three *RbcS* RNAi lines (RSS7.6, RSS8.5 and RSS13.2), particularly when measured under saturating CO<sub>2</sub> compared to the WT plants. Whereas a slightly lower photosynthetic CO<sub>2</sub> assimilation was observed in the other two transgenic lines (RSS2.1 and RSS11.5) than in the WT plants (Figure 4.16).

From the  $A/C_i$  response curves, the maximum rate of carboxylation allowed by the Rubisco enzyme ( $V_{c,\text{max}}$ ) and the maximum electron transport required for the regeneration of RuBP ( $J_{\text{max}}$ ) were determined via the equations of von Caemmerer and Farquhar (1981). Consequently, significant decreases in these parameters were observed in the three *RbcS* RNAi lines with the largest decrease in the level of Rubisco activity in both the early stage leaves and the flag leaves. However, no significant

differences were found in the other two transgenic lines with small reductions of Rubisco activity compared to the WT plants (Table 4.2).

A further analysis of the  $A/C_i$  curves showed that the ambient  $\text{CO}_2$  rate of photosynthesis ( $A_{\text{sat}}$ ) and the  $\text{CO}_2$ -saturated rate of photosynthesis ( $A_{\text{max}}$ ) were also significantly lower in three RNAi lines with decreased levels of Rubisco activity in the young leaves (Figure 4.17A and B) and flag leaves (Figure 4.17C and D), with the exception of the other transgenic line that had a slightly decreased level of Rubisco activity (RSS2 line) with lower rates of  $A_{\text{sat}}$  and  $A_{\text{max}}$  that were not significant.

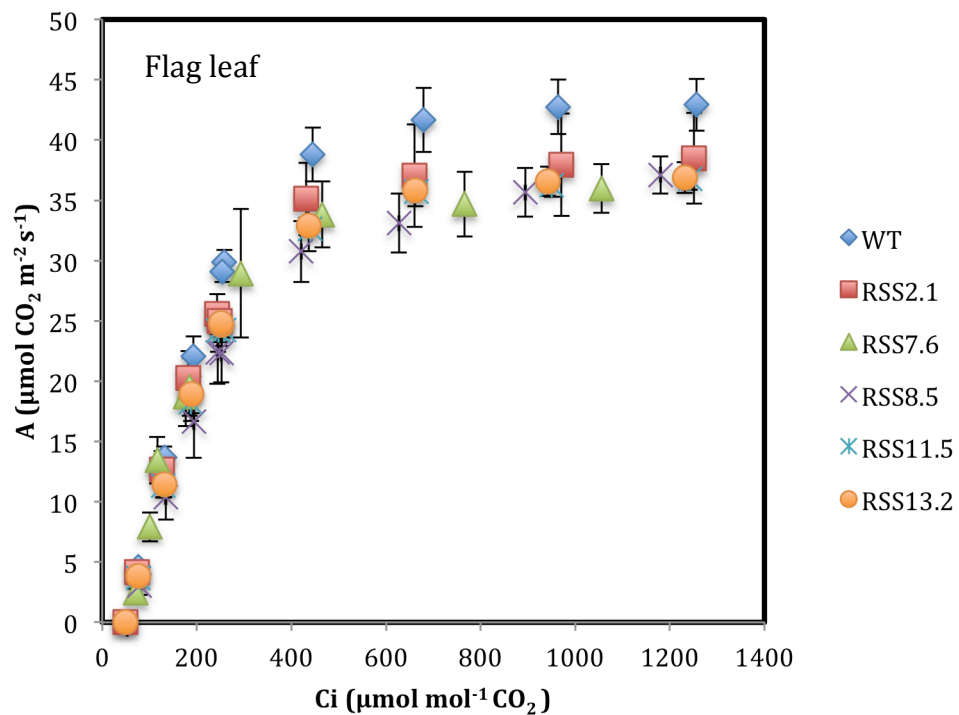
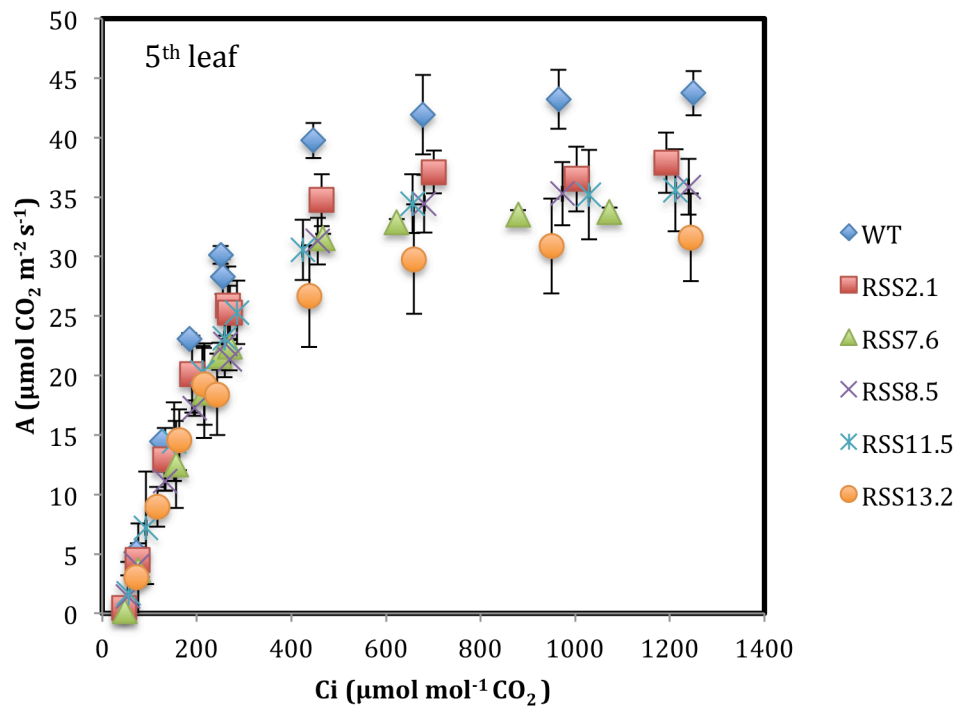


**Figure 4.16: Photosynthetic  $\text{CO}_2$  assimilation (A) response to different internal concentrations of  $\text{CO}_2$  ( $\text{C}_i$ ) (A/ $\text{C}_i$  curve) of five independent *RbcS* RNAi T2 lines compared to the WT line.**

Plants were grown in an environmental controlled greenhouse under natural sunlight. Gas exchange measurements were performed on 4<sup>th</sup> or 5<sup>th</sup> leaves at a Zadoks growth scale of Z1.5 and flag leaf at Zados scale of Z3.9-4.1, with a light-saturated rate of  $2,000 \mu\text{mol m}^{-2} \text{ s}^{-1}$  using an open infrared gas exchange system. Values represent three plants from five independent lines compared to the WT line.

**Table 4.2: Maximum rate of carboxylation allowed by Rubisco enzyme ( $V_{c, \max}$ ) and the maximum electron transport required for RuBP regeneration ( $J_{\max}$ ).**

$V_{c, \max}$  and  $J_{\max}$  were both solved from the  $A/C_i$  measurements shown in Figure 5.5 by using the equations published by von Caemmerer and Farquhar (1981). The fourth or fifth leaves (Zadoks growth scale 1.4–1.5) and flag leaves (Zadoks growth scale 3.9–4.1) are shown. Values represent the average of three plants from five independent RNAi lines compared to the WT line. Stars indicate significant differences from WT ( $P < 0.05$ ).

	5 <sup>th</sup> Leaf		Flag Leaf	
<i>RbcS</i> Lines	$V_{c, \max}$ ( $\mu\text{mol m}^{-2} \text{s}^{-1}$ )	$J_{\max}$ ( $\mu\text{mol m}^{-2} \text{s}^{-1}$ )	$V_{c, \max}$ ( $\mu\text{mol m}^{-2} \text{s}^{-1}$ )	$J_{\max}$ ( $\mu\text{mol m}^{-2} \text{s}^{-1}$ )
<b>WT</b>	154.16	229.22	145.769	231.02
<b>RSS13.2</b>	118.69 <sup>*</sup>	169.29 <sup>*</sup>	127.63 <sup>*</sup>	199.7 <sup>*</sup>
<b>RSS7.6</b>	104.67 <sup>*</sup>	181.05 <sup>*</sup>	132.398 <sup>*</sup>	191.88 <sup>*</sup>
<b>RSS8.5</b>	107.79 <sup>*</sup>	187.176 <sup>*</sup>	115.25 <sup>*</sup>	199.36 <sup>*</sup>
<b>RSS11.5</b>	120.826 <sup>*</sup>	186.2 <sup>*</sup>	140.70	211.82
<b>RSS2.1</b>	128.05 <sup>*</sup>	198.82	142.79	206.386

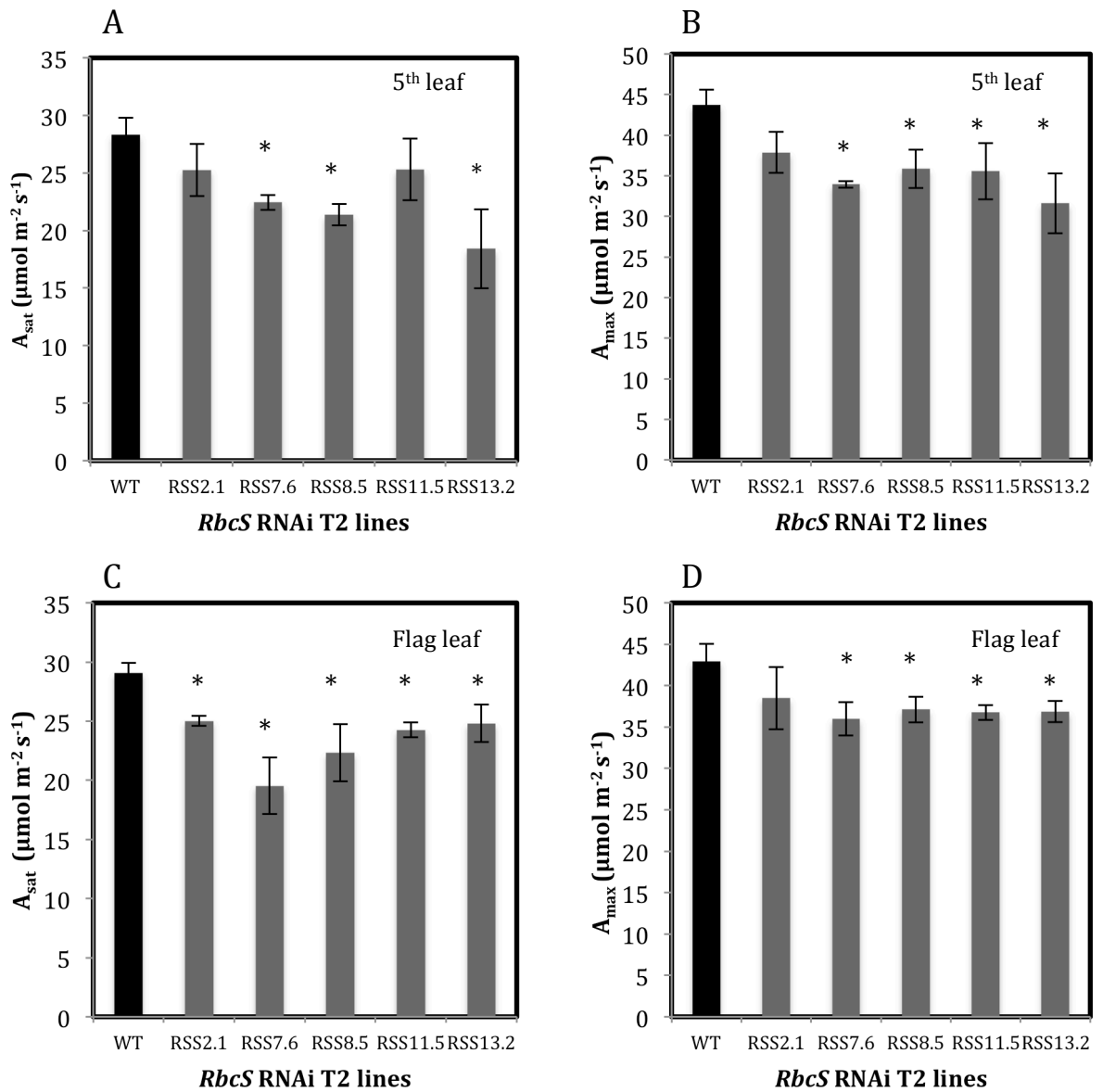
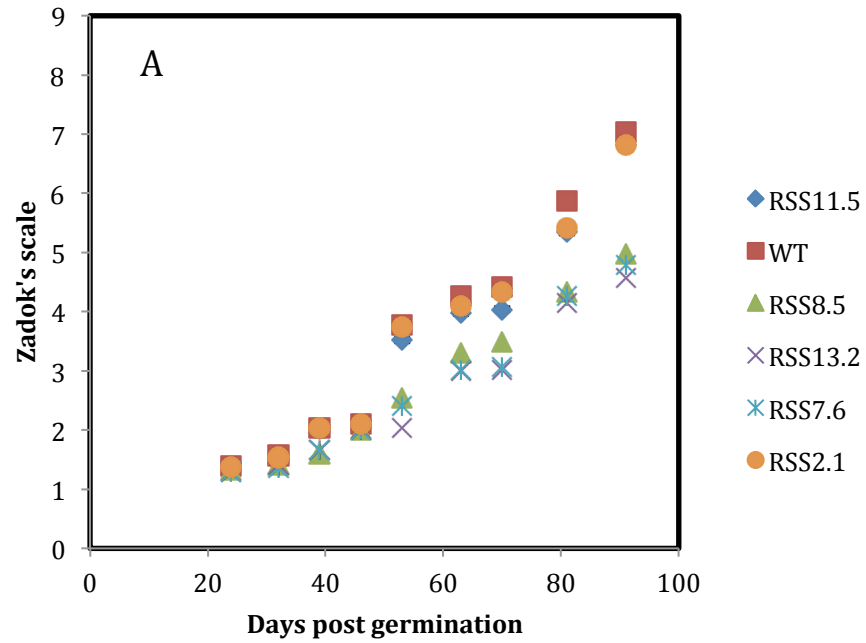


**Figure 4.17: The  $\text{CO}_2$  assimilation rates at ambient ( $A_{sat}$ ) and saturating  $\text{CO}_2$  ( $A_{max}$ ) of transgenic *RbcS* RNAi T2 wheat plants.**

Plants were grown in an environmental controlled greenhouse under natural sunlight.  $A_{sat}$  and  $A_{max}$  were derived from  $A/C_i$  response curves shown in Figure 5.2, at both Fourth or fifth leaves (Zadok's growth 1.4-1.5) (A and B), and flag leaves (Zadok's growth 3.9-4.1) (C and D). Values represent three plants from five independent *RbcS* RNAi lines compared to the WT line. Star indicate significant differences (<0.05) compared to the WT.

#### **4.2.5.2 The effect of decreased Rubisco activity on plants growth and visual phenotypes**

To assess the growth rate over the entire plant life cycle the Zadoks growth scale was used regularly every week to count the leaves, tillers and ears and also to observe the nodes and flowers on plants grown in an environmentally controlled greenhouse under natural sunlight. The results revealed that the *RbcS* RNAi plants with the largest reduction in the levels of Rubisco activity showed a notable delay in the developmental growth rate at the level of the whole plant, whereas there was no effect on the growth in the plants with a slight decrease in Rubisco activity (Figure 4.18A). The *RbcS* RNAi plants with a significantly lower level of Rubisco activity were clearly smaller compared to the WT plants, whereas the plants with a slightly decreased level of Rubisco activity were similar to the WT plants with no observed phenotypic effects. Plants with low Rubisco activity were also visibly shorter, with fewer green leaves and with no ears, as a result of a delay in reaching the flowering growth stage compared to the WT plants (Figure 4.18B).



B

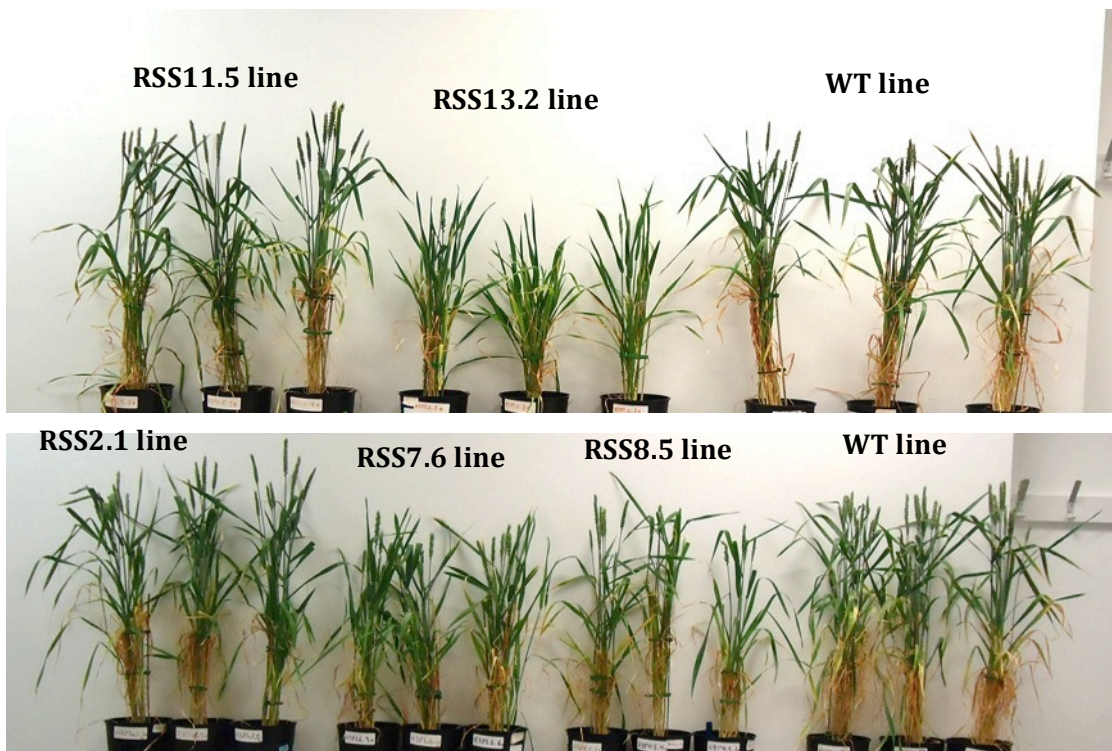


**Figure 4.18: Growth analysis and visual phenotypes of *RbcS* RNAi transgenic T2 lines and WT plants.**

Plants were grown in an environmental controlled greenhouse under natural sunlight. **A.** growth measurements were done using Zadoks scale by counting leaves, tillers (stems), ears and observing the flowering development regularly every week. **B.** Visual phenotypes pictures of *RbcS* RNAi transgenic plants compared to the WT plants at Zadoks scale of 6.9-7.0.

#### **4.2.5.3 The effect of different levels of decreased Rubisco activity on plant biomass and seed production**

To assess the plants' biomass and seed production, plants were harvested when they reached Zadoks growth stage 9. The plants with the lowest level of Rubisco activity had a significantly lower total biomass than the WT plants (Figure 4.19a). Also, a significant decrease in the total number of dried leaves was evident in the plants with the lowest Rubisco activity compared to the WT plants (Figure 4.19b), as well as a lower number of ears (Figure 4.19c) and significantly reduced ear weight compared to that found for the WT plants (Figure 4.19d).

The total average weight of the seeds per line was also significantly lower in plants with a more greatly decreased level of Rubisco activity compared to the WT plants (Figure 4.20a), which was a result of the significantly lower number of seeds per plant (Figure 4.20b) as well as a significantly lower number of seeds per ear (Figure 4.20c). However, the weight per seed was significantly higher in plants with different levels of Rubisco activity compared to the WT plants (Figure 4.20d).

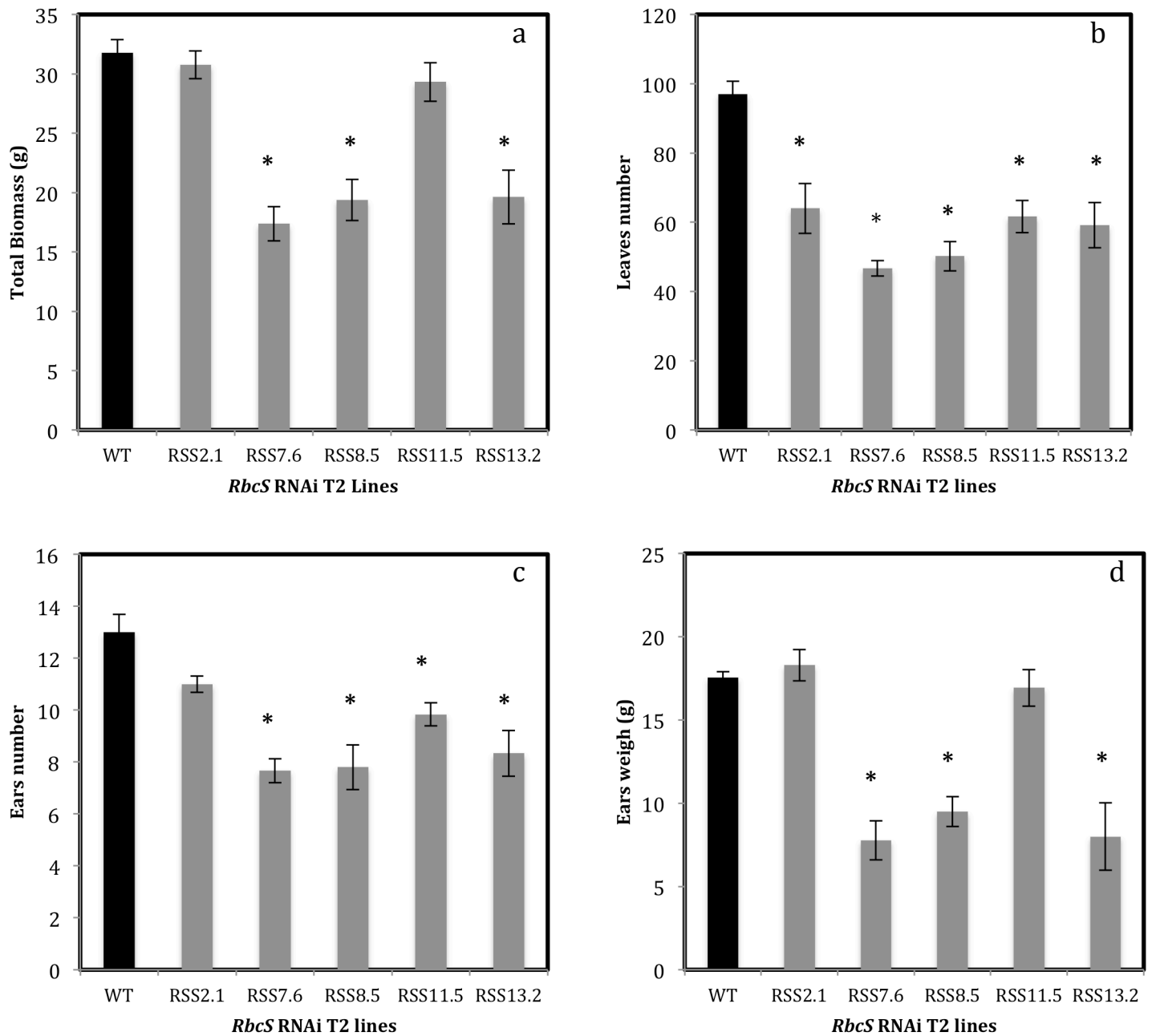


**Figure 4.19: Biomass analysis of *RbcS* RNAi lines and WT lines.**

Plants were grown in an environmental controlled greenhouse under natural sunlight. Plants were harvested when they reached to Zadok's growth stage of 9 and they were completely dry; **a.** plant biomass, **b.** average leaves number, **c.** average ears number, **d.** average ears weights. Values represent average of 5-6 plants from five independent *RbcS* RNAi lines compared to the WT line. Stars indicate significant difference from the WT (P < 0.05).

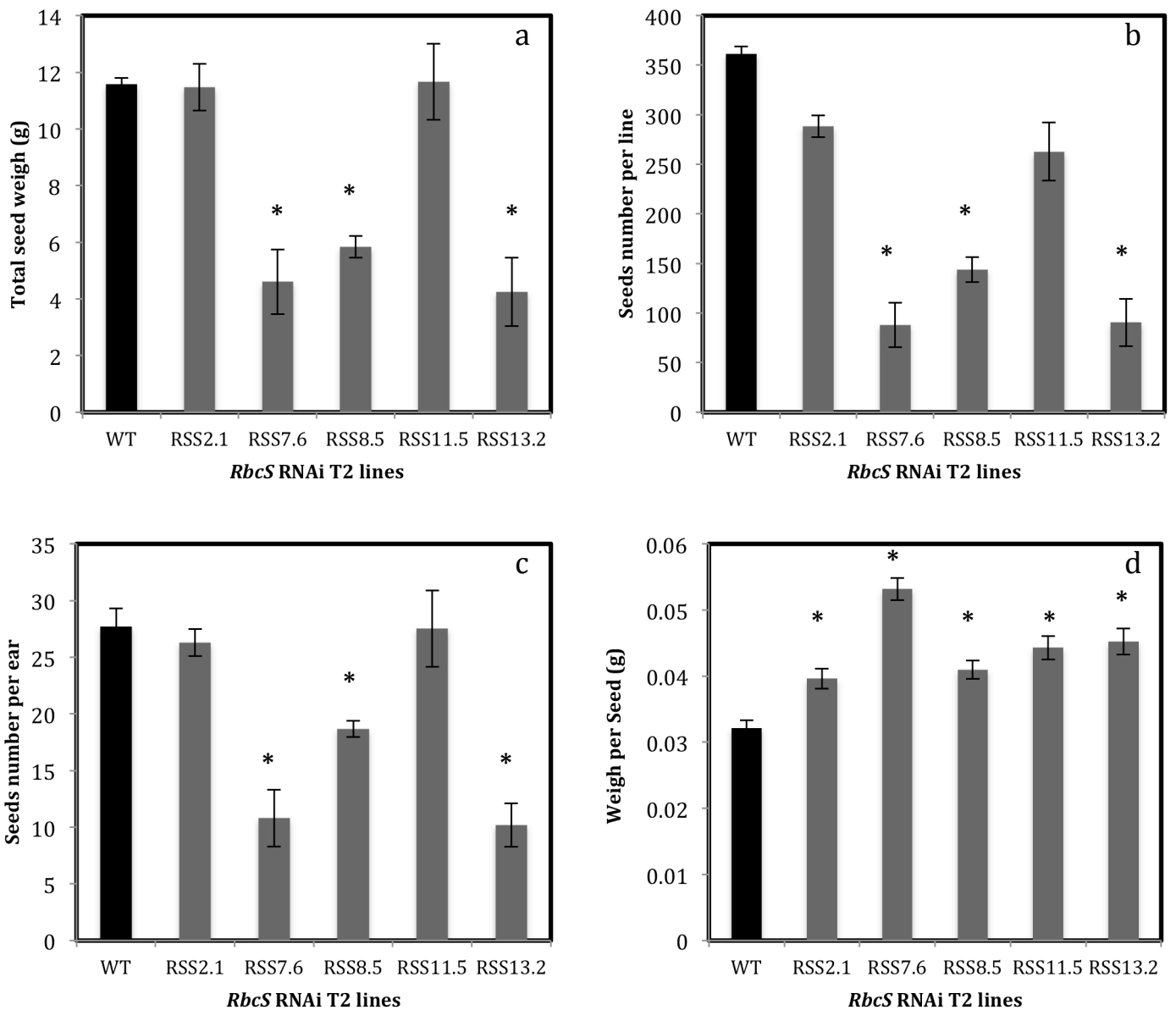


**Figure 4.20: Seed analysis of *RbcS* RNAi T2 transgenic lines and WT lines.**

Plants were grown as described in Figure 4.19. Plants were harvested when they reached to Zadok's growth stage of 9 and they were completely dry; total seed yield (a), total seeds weight (b), seeds number per ear (c), and weight per seed (d). Values represent average of 5-6 plants from five individual *RbcS* RNAi transgenic lines compared to the WT line. Stars indicate significant difference from WT (P < 0.05).

#### **4.2.5.4 The effect of different levels of decreased Rubisco activity on carbon and nitrogen distributions in leaves and seeds**

To evaluate the levels of N and C in the leaves and seeds of *RbcS* RNAi transgenic and WT plants, plants were harvested when they reached to Zadoks growth stage of 9, and then they were completely dried. After the biomass analyses, 1 g of leaf and also seeds of each of the plants within the independent transgenic and WT lines were sent to the Chemical Biological Laboratory at Wageningen University in the Netherlands for N and C content analyses. The raw data was received and analysed. As a result, it was found that the plants with the lowest level of Rubisco activity had significantly higher totals of leaf and seed N than those found for the WT plants. On the other hand, the N of the plants with slight reductions in the level of Rubisco activity was similar to the WT plants (Figure 4.21a and b). Furthermore, it was observed that the C content was not affected in all *RbcS* RNAi plant leaves as well as seeds compared to the WT plants (Figure 4.21c and d).

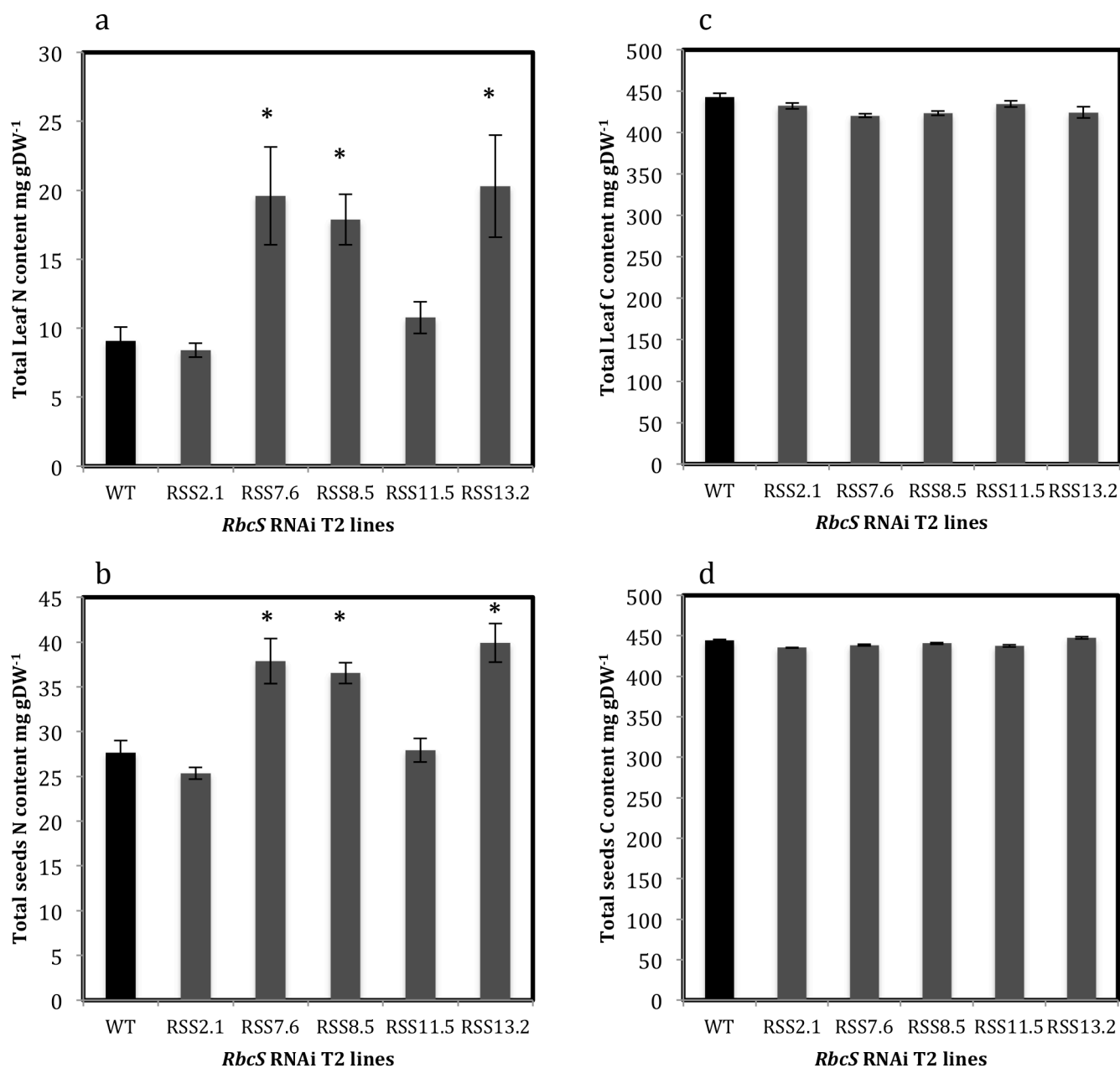


**Figure 4.21: Nitrogen and carbon analysis into leaves and seeds of *RbcS* RNAi T2 lines and WT lines.**

Plants were grown as described in Figure 4.19. They were harvested when they reached to Zadok's growth stage of 9 and they were completely dry; total leaf N content (a), total seeds N content (b), total leaf C content (c), and total seeds C content (d). Values represent average of five plants from five individual *RbcS* RNAi lines compared to the average of five WT plants. Stars indicate significant difference from WT ( $P < 0.05$ ).

### 4.3 Discussion

The Rubisco protein is a major N investment in crops but it has also been shown that under some environmental conditions that there may be an excess of Rubisco over that needed to maintain photosynthesis. This raises the question - can a small reduction in amount of Rubisco enzyme be used to improve nitrogen use efficiency (NUE) without any negative effect on plant yield? Previous studies showed that decreased activity levels of Rubisco enzymes were obtained using a genetic antisense technique in tobacco plants to assess the involvement of Rubisco in controlling the rates of both photosynthesis and growth under the CO<sub>2</sub> enrichment conditions (Rodermeil et al., 1988; Hudson et al., 1992; Stitt and Schulze, 1994). In addition, an antisense RNAi approach was used with tobacco and plants with reduced Rubisco enzymes in order to investigate the photosynthetic N economy and growth rate under the condition of ambient CO<sub>2</sub> (Masle et al., 1993). The technology was also applied to rice, targeting the RbcS subunit, to produce plants with less Rubisco, and this resulted in an improvement in NUE in rice (Makino et al., 1997); yet, this did not lead to an improvement in NUE of the whole plant (Makino et al., 2000). However, this technology has not yet been applied to the wheat crop.

To address the question - can a small reduction in amount of Rubisco enzyme be used to improve nitrogen use efficiency (NUE) in wheat without any negative effect on plant yield? Wheat plants with decreased Rubisco were produced, by transformation with a wheat *RbcS* RNAi construct under the control of the Ubiquitin promoter. Transgenic wheat plants with reduced Rubisco gene and protein expressions were identified and confirmed in T0 and T1 generations. Therefore, several molecular screenings were performed on the five T2 transgenic plant lines that had showed a wide range of Rubisco protein reductions and effects on wheat photosynthesis and biomass in order

to select the most positive, stable down-expressed *RbcS* lines. First, the existence of *RbcS* RNAi in T2 generation was confirmed using PCR. As a result, several lines were shown to contain the construct in five independent lines compared to the WT plants. Next, the *RbcS* genes expression was analysed using q-PCR to confirm whether the gene was still expressed at the transcript level in the T2 generation. Consequently, the analysis showed a significant decrease in the *RbcS* genes in different transgenic wheat plants within different lines compared to the WT plants. Afterward, a Western blot approach was used to investigate the *RbcS* expression at the protein level, revealing a decrease in the *RbcS* protein in some of the T2s of five different independent lines compared to the WT. Subsequently, the molecular analysis results confirmed the stability of the level of Rubisco down-expression in five independent lines within the T2 generation; therefore, its activity as well as its impact on wheat photosynthesis, growth and grain yield quality need to be further examined in an attempt to improve NUE.

Moll *et al.*, (1982) described the NUE as the yield of dry grain per the available unit of N in the soil. It divided into two activities: the efficient ability of plant to take up the N from the soil (uptake efficiency process); and the ability of plant to utilize and use the uptaken N efficiently (utilization efficiency) (Hirel *et al.*, 2007; Gaju *et al.*, 2014). In wheat, the accumulation and allocation processes of N are both play a central and significant role to determine the yield of grain as well as grain quality (Simpson *et al.*, 1983; Gaju *et al.*, 2014; Taulemesse *et al.*, 2016). Moreover, it is found that the major grain N in wheat comes from the accumulation of N before anthesis and N remobilized from shoots and roots. However, the majority of grain N in wheat derived from the vegetative organs, leaves and stems (Pelta and Fillery, 1995; Critchley, 2001; Kichey *et al.*, 2007). Thus maintaining the balance between the allocation of N to support photosynthesis and the N reallocation to other organs such as seeds is necessary for

optimization of NUE (Sage *et al.*, 1987; Lawlor, 2002).

In this study, we have investigated the effect of decreased Rubisco activity by *RbcS* RNAi lines on photosynthesis, growth rate and grain quality under conditions of UK spring/summer natural sunlight. The results clearly show that largest decrease in Rubisco activity results in clear reductions in leaf CO<sub>2</sub> assimilation rates under saturated CO<sub>2</sub> measurements.  $V_{c,max}$  and  $J_{max}$  were also clearly affected as a result of a large decrease in the level of Rubisco activity. It was noted that a large decrease in Rubisco activity (about 40% to around 67%) results in significant decreases in total biomass, leaf weight and number, and ear number and weigh, which can mainly be explained by significant reductions in total seed weigh and number compared to WT plants. This reduction in seed production was not only due to the small number of ears produced per plant within the lines but also to the small number of seeds produced per ear. However, the weight per seed was higher in plants with lower levels of Rubisco activity, which could be a result of an increase in the N content level of the seeds. Wheat plants, as well as rice, have a greater Rubisco content than that found in tobacco plants. It was found that, in wheat, approximately 30% of N content was present in Rubisco (Makino *et al.*, 1992; Mae *et al.*, 1993) compared to about 18% found in Rubisco in tobacco plant (Evans *et al.*, 1994). Therefore, a reduction of Rubisco activity could effect on the allocation of N into other photosynthetic components. Consequently, in this study, the N allocations in seeds and leaves were clearly observed in the *RbcS* RNAi plants with the largest reductions in Rubisco activity, as it is higher than in the WT plants. It was observed that there were strong positive correlations between total N content in seeds and leaves and total biomass and total seed production. Additionally, it was clear that the growth of plants with a large reduction in Rubisco activity was affected compared to the WT plants, as they

were found to grow much more slowly and produced fewer leaves, stems and ears, as well being delayed in their flowering, all of which is similar to the results shown in a previous study on antisense tobacco plants (Masle *et al.*, 1993). Therefore, this means that a 40% to 67% reduction in Rubisco activity negatively affects photosynthesis performance; growth rate and grain yield quality at ambient conditions that are as close to natural as possible.

On the other hand, decreased Rubisco activity between about 10% and 25% does not affect photosynthetic rate, growth, biomass production and grain quality, and this supports the hypothesis that slight reductions in the content of Rubisco protein in photosynthetic leaves could increase NUE without compromising photosynthetic performance (Parry *et al.*, 2013). The N allocations in seeds and leaves were also clearly the same in the transgenic plants with slight reductions in Rubisco activity (approximately 10% to 25%) relative to the WT. Also, the plants' growth was not affected compared to the WT. Similarly, it was found that, at the individual plant level, the photosynthesis, biomass production and grain yield were not affected by the slight reductions in the level of Rubisco within the three different independent lines, including one plant of the RSS8.5 line which, interestingly, showed a large reduction in Rubisco activity. A previous study on rice by Makino *et al.* (1997) showed that a 35% reduction in Rubisco in rice led to an improvement in the photosynthetic NUE under saturated CO<sub>2</sub> conditions. Therefore, this could be applicable to wheat, as a slight reduction in Rubisco activity (up to 25%) in wheat, shown in this study, did not significantly affect photosynthetic capacity, growth rate and grain quality. The main goal of this study was to attempt to improve NUE by identifying transgenic wheat plants that can experience a slight reduction in Rubisco activity without suffering significant and negative effects on their photosynthetic rate. Thus, this study establishes the next steps toward crossing

these transgenic plants with stable and reduced Rubisco levels with wheat plants that have stable and higher SBPase levels in order to increase yield together with improved NUE.

#### Summary:

- The Rubisco RNAi lines with reductions in the Rubisco protein of more than 40% showed a significant decrease in photosynthesis, growth and grain yield.
- Interestingly, the plants with the lowest level of Rubisco activity had significantly higher levels of leaf and seed N when compared to WT plants.
- In contrast, small reductions in Rubisco protein of between about 26% did not have an adverse effect on photosynthesis, growth or grain yield in two independent transgenic wheat lines.

## **Chapter 5: Genetic Engineering Tools to Improve Photosynthetic Efficiency in Wheat Leaf**

## 5.1 Introduction

A promoter is a 1–2 kb DNA fragment sequence upstream of the coding region sequence of a particular gene. It consists of various *cis*-acting elements, which are specific binding sites for RNA polymerase and proteins involved in controlling transcription regulation and gene expression (Peremarti *et al*, 2010). Two elements can be found at promoter regions: core and promoter regulatory components. The core element of the promoter is responsible for the specific pattern expression of a gene and is located ~40 bp upstream from the transcriptional start site of the gene. It includes the TATA box (the binding site for the transcriptional initiation protein), which participates in orientating RNA polymerase II in the process of mRNA synthesis. The promoter regulatory component plays a role in activating, repressing and modulating gene expression located upstream of the core components. It consists of a variety of regulatory elements, such as *cis*-acting enhancers and silencers elements, including two types of motifs: either CAAT or AGGA boxes (which act to regulate the transcriptional level). The promoter also contains the transcription factor elements that are an essential requirement for enhancing gene transcription through binding to the regulatory elements of the promoter. Both the availability of active transcription factors around the promoter and the type and number of regulatory elements in the promoter are essential for efficient transcriptional regulation (Hughes, 1996; Hernandez-Garcia and Finer, 2014; Jones *et al*, 2012).

Three categories of promoters can be identified: constitutive, spatiotemporal and inducible. The constitutive promoter is identified as an active promoter in most or all species tissues during all periods of growth and development. The activation of the spatiotemporal promoter can be observed in specific tissues, such as photosynthetic

plant tissues, and at specific developmental times. The inducible promoter is inactive until induced by a chemical application (biotic factors) or in response to abiotic factors, such as light and heat; therefore, the timing of the expression can be controlled. A number of promoters have been identified from different organisms and are used for several study purposes in plant genetic engineering, for example to express a given gene of interest. It is critical in plant molecular biology to choose the correct promoters for effective transformation of a gene of interest into plants and its subsequent level of expression in the targeted plant tissue and developmental growth stage in order to avoid undesirable consequences (Dale *et al*, 2002; Chen *et al*, 2006; Peremarti *et al*, 2010).

The Calvin–Benson cycle enzymes, including sedoheptulose 1,7-bisphosphatase (SBPase) and fructose 1,6-bisphosphate aldolase (FBPaldolase), are mainly located and expressed in the leaves' chloroplast. Their regulation activity is driven by light and other environmental changes, and they have demonstrated to participate significantly in the photosynthesis process (Raines *et al*, 1999; Lefebvre *et al*, 2005). The transcriptional nuclear gene-encoding protein of the Calvin–Benson cycle is activated directly by light. This can be mediated by the presence of *cis*-acting elements, which are sensitive to light. For example, the promoters of all different enzymes encoded by different genes of the Calvin–Benson cycle contain the G-box (Hughes *et al*, 2000), which is necessary for the expression activity at the transcription level (Gilmartin *et al*, 1990). The SBPase enzyme is known to be regulated highly by light and is expressed completely in the leaves' chloroplast. In addition, it is found as a single gene in the majority of higher plants (Willingham *et al.*, 1994). Therefore, the chances are high that its promoter will drive strong expression in wheat mesophyll cells.

The major aim of this project is to identify and analyse new native promoters of the Calvin–Benson cycle enzymes with the desired features and characteristics being used to drive the strong desired expression level in wheat mesophyll cells.

## 5.2 Results

### 5.2.1 Identification of *Brachypodium distachyon* SBPase and FBPaldolase

To identify the promoter sequences from the *Brachypodium distachyon* SBPase (Bradi2g55150) and FBPaldolase (Bradi4g24367) genes, a phytozome database (<https://phytozome.jgi.doe.gov/pz/portal.html>) was used to isolate the promoter sequences 2kb upstream of the start codon (ATG) (Figure 5.1). The isolated promoter sequences were analysed using PlantCare software (<http://bioinformatics.psb.ugent.be/webtools/plantcare/html/>) to identify and characterise the elements present in the promoters. The results revealed the present of motifs elements boxes that are characteristic to both promoters (Figure 5.2 and Figure 5.3) and motifs sequences are represented in SBPase promoter in Table 6.1 and FBPaldolase in Table 6.2. Both promoters have the similar motifs of I Box, G box and TATA box.

Then, these two *Brachypodium* promoters of the genes' SBPase and FBPaldolase were used in the construction of the chimeric expression vectors GUS and eYFP to examine the expression pattern of the Calvin–Benson cycle gene promoters *in vivo* to drive expression in the mesophyll cells of both *Nicotiana benthamiana* leaves (dicots) and wheat (*Triticum aestivum*) (monocots). Two types of molecular cloning strategies were used: gateway cloning for transient analysis of *N. benthamiana* and traditional cloning for transient and stable transformation of wheat.

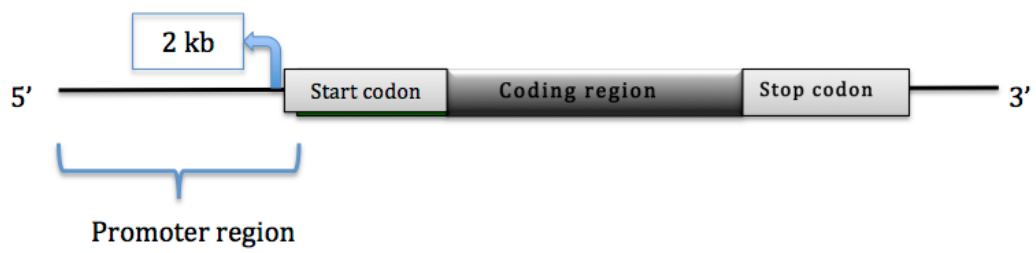


**Figure 5.1:** The structure of the gene showing the 2-kb region that taken from *Brachypodium* SBPase and FBPaldolase genes to make the constructs.

+ TTGATATGCA GCCCAACACA TGGTATCTTT TGTTTGTTAC GGAGGATAGA ATGCATTAAA CTGAAGGATA  
 - AACTATACGT CGGGTTGTGT ACCATAGAAA ACAAACAATG CCTCCTATCT TACGTAATTT GACTTCCTAT  
 + GACTGTGCTT CCTGTGCTTC ATTACAAGTT AGCTTCAGAT GTGATGAATT TATGTGCTGG CAGCAAAGGA  
 - CTGACACGAA GGACACGAAG TAATGTTCAA TCGAAGTCTA CACTACTTAA ATACACGACC GTCGTTTCTT  
 + AATAATTGTC TGTGCAAACC TATCTTCTGC CTGAACTGAT GAAAGAAATG ATACAGCTGC ACAGTAGATG  
 - TTATTAACAG ACACGTTTGG ATAGAAGACG GACTTGACTA CTTTCTTTAC TATGTGACG TGTGATCTAC  
 + CATTAAACGA TGGTGATCAG AGTTAAGGTC TGGTGCATAT GAAGCTTGTG ATAGTGGATG TTTTTCACCTT  
 - GTAATTTGCT ACCACTAGTC TCAATTCCAG ACCACGTATA CTTGGAACAC TATCACCTAC AAAAAGTGAA  
 + TTTTGTTCAG GCATGCTCAT ACTCTTTACA GAAAAGGCA CATAACCAC AGCAGGGAGT CTTGGATGTA  
 - AAAACAAGTC CGTACGAGTA TGAGAAATGT CTTTTTCCGT GTATGTGGTG TCGTCCCTCA GAACCTACAT  
 + TTTCTCCCGA GTTATAGGAG ATCATCTGAT TTAAGTAGGC CAACCTTGTG TACTTGTGAA CAATTTGTAA  
 - AAAGAGGGCT CAATATCTC TAGTAGACTA AATTCATCCG GTTGAACAC ATGAACACTT GTTAAACATT  
 + CTATCAGCTT TTGTTATTCA ATAGTAGTAA AATCCCTTC ATGGTACTCT GTGTCCTTTT TCATTGAGGG  
 - GATAGTCGAA AACATAAGT TATCATCATT TTAGGGAAAG TACCATGAGA CACAGGAAA AGTAACTCCC  
 + CAGTAGGTC CATATACCAA CTTGCTCTGT GATGTTAATG TTTTGGTGA TTAGTGACAA GGGTGCCTAA  
 - GTCATCCAAG GTATATGGTT GAACGAGACA CTACAATTAC AAAAACCCT AATCACTGTT CCCACGGATT  
 + TTTCTTTTCT GATGTTAATA TTTTGAAAGA TCTTCACTCT GAAAAAAA TGCATGTTCA TATCCATGTT  
 - AAAGAAAAGA CTACAATTAT AAACTTTCT AGAAGTGAGA CTTTTTTTTT ACGTACAAGT ATAGGTACAA  
 + TCTCTAAAAA TAATCCATAG CCAGTGTGTG ATACTTTCTA CTAGTCCCA CTAATGCAT TGTGAAATTA  
 - AGAGATTTT ATTAGGTATC GGTCACACAC TATGAAAGAT GATCAAGGGT GATTTACGTA AACTTTAAT  
 + AATCTATAA AATTTGTAA TTTCTAATAT TTAGTAAGGG TAGAAACAGA GATTTTTTTC TTAATTTTAA  
 - TTAAGATATT TTA AACATT AAAGATTATA AATCATTCCC ATCTTTGTCT CTA AAAAAG AATTAAAT  
 + ATCATCATGT ATCAGGAGTC GCAAAGGTC AGGAATGATA TGCAAGATTG CTACATGGTT GGTATCCTCT  
 - TAGTAGTACA TAGTCTCAG CGTTCCAGG TCCTTACTAT ACGTCTAAC GATGTACCAA CCATAGGAGA  
 + TAATGTCATC CTTGGCAGGG AGTTGTGGTG GATATGCCTT CTGCTGCCAG GCACTGGGGC ACAAGAAGAA  
 - ATTACAGTAG GAACCGTCCC TCAACACCAC CTATACGGAA GACGACGGT CCGTACCCCG TGTCTTCTT  
 + TGGTGTCTGC CACACAAGCC ACCCTGCACC CTACAAACA CTCACAGCTG GAATGGTTAT CACCAAACCA  
 - ACCACAGACG GTGTGTTCCG TGGGACGTGG GATGTTTGTG GAGTGTGAC CTTACCAATA GTGGTTTGGT  
 + ATGACAGAAA AAAGTGTGTA TTCCACGTAA TTGATGGTTA CTGGCAAAT TCATGGATGT AATACATCAG  
 - TACTGTCTTT TTTGACACAT AAGGTGCATT AACTACCAAT GACCGTTTA AGTACCTACA TTATGTAGTC  
 + GGCATCTCAA CCGTCGAAAG ATGCTCATGG GCACTACTCC TCGGCGAAAT GCGCCACAG AAACCCAGAA  
 - CCGTAGAGTT GGCAGCTTTC TACGAGTACC CGTGATGAGG AGCCGCTTTA CGCGGGTGTG TTTGGGTCTT  
 + TTGTTTATCA GCCAAGACCA TCCTTAAGGT CAAGAATGTC CAGATAATAT TTATGGACGG TGCAGCGCAA  
 - AACAAAGTAG CGGTTCTGGT AGGAATTCCA GTTCTTACAG GTCTATTATA AATACCTGCC ACGTCGCGTT  
 + ACGATAAAAT TCCAGTATTG CAGATTTTAC ATGGTACACA GAGAAGCTAA GGAATCATA GAGACAAGCA  
 - TGCTATTTTA AGGTCATAAC GTCTAAAATG TACCATGTGT CTCTTCGATT CCTTTAGTAT CTCTGTTCTG  
 + TGTGGCAGAG CCAGGACAAA AACAGAAGGT GGCAAGAGGA TTGGAGCAAC CAAATCACAG CCATTATAT  
 - ACACCGTCTC GGTCTGTTT TTGTCTTCCA CCGTCTCTCT AACCTCGTTG GTTTAGTGTG GGTAAGTATA  
 + CCAGAAGGCC AGCCTCCACC TCACAACCTA TATCCTTTGT ACTCAGGTAC TCACCCTTAA ATCTGAGCAG  
 - GGTCTTCCGG TCGGAGGTGG AGTGTGAGT ATAGGAAACA TGAGTCCATG AGTGGGAATT TAGACTCGTC  
 + GCGCTTCACT TCTCACCACC CCTAAGGAAA GGCTGCAATT GCAAGCTTGT GTCAAAGAAG AGGGTAGCAC  
 - CGCGAAGTGA AGAGTGGGGG GGATTCCTTT CCGACGTTAA CGTTGGAACA CAGTTTCTTC TCCCATCGTG  
 + CTGATCCTCT TGCCTTTGGA GCCAGAAAC ATG  
 - GACTAGGAGA ACGGAAACCT CGGTCTTTG

**Figure 5.2: Brachypodium FBPaldolase promoter motif sequences.**

The different coloured boxed sequences represent the promoter motifs. The arrow showed that the start of 2 kb promoter sequence upstream from the start codon region ATG. The motifs was analysed using Plant Care software.

+ ATTTGTCGAA CCGAGTCAAC CTGTGGTGAT TTATAACCTC TCTAAATTC CGATTCTCAA AATGAAAAAC  
 - TAAACAGCTT GGCTCAGTTG GACACCAC TA AATATTGGAG AGATTTAAAG GCTAAGAGTT TTA CTTTTTGG  
 + CTCTCTAAAT TTCC TAAAAA ACCACTATAA ATAAGGCAAA TGAGTGAAAA CAGGCTGAGA ACTCTCGCTC  
 - GAGAGATTTA AAGGATTTTT TGGTGATATT TATTCCGTTT ACTCACTTTT GTCCGACTCT TGAGAGCGAG  
 + CATATCCCGC CATATTTTTT CTCTTACAGC TCGTTTGACA CCAATCATCT GGGTTTAGAA TTCTGAAATT  
 - GTATAGGGCG GTATAAAAAA GAGAATGTGC AGCAAAC TGT GGT TAGTAGA CCCAAATCTT AAGACTTTAA  
 + CATTTTCAAA AATCAACTTA TTTGATTGGC GCAAGATTGG CCACGGAAAT TCAATCTCAA AAATTT CATA  
 - GTAAAAGTTT TTAGTTGAAT AAAC TAACCG CGTTCTAACC GGTGCCTTTA AGTTAGAGTT TTTAAAGTAT  
 + AAGTCACACT ATAAAGTCCA ATTCCAAAAA TGGACGGTTA AATGGACGGC TAAGAAATAT CCACTCCATT  
 - TTCAGTGTGA TATTT CAGGT TAAGGTTTTT ACCTGCCAAT TTACCTGCCG ATTCTTTATA GGTGAGGTAA  
 + CCACCCTGTA CGAAAGCACA GTGGTGATCA ACAAGACAAC AAAGCTGGAT CAAATCCCTT GTCACGAACT  
 - GGTGGGACAT GCTTTCGTGT CACCAC TAGT TGTTCTGTTG TTTGCACCTA GTTTAGGGAA CAGTGCTTGA  
 + ACTGCGGGCG GTGCCACGAA AAGCCA ACTT GCAAAGTAAG GTCCGGATGA AACCTCCTAA CTCCTAAGGC  
 - TGACGCCCGC CACGGTGCTT TTCGGTTGAA CGTTTCATTC CAGGCCTACT TTGGAGGATT GAGGATTCCG  
 + TAAGGGGCTG TTAAA ACTTA ATGTGGATGC ACCGTCTGAT GTAGATGAAC TCCGAGGAAC AGACGTTGTG  
 - ATTCCCGAC AATTTTGAAT TACACCTACG TGGCAGACTA CATCTACTTG AGGCTCCTTG TCTGCAACAC  
 + TCATTATFTC CGGACTCCAA GGGCGATTTT GTGGTGGCTA CCTATAAGAA GTTTGCGGGC TGTCTTGACG  
 - AGTAATAAAG GCCTGAGGTT CCCGCTAAAA CACCACCGAT GGATATTCTT CAAACGCCGC ACAGAACTGC  
 + TTCATGTTCC GGAAGCTTCT GCACTACACT TCGGACTCCT CGCACAAATG GTGGGATGTA ACAGGATGGT  
 - AAGTACAAGG CCTTCGAAGA CGTGATGTGA AGCCTGAGGA GCGTGTTTAC CACCCTACAT TGTCTACCA  
 + CATCGGTGGG TTGCACAACC AGGAAATGAT TGGTACCGCG AGCCAGCAGG AGCGATGAGG TACGGTGGAG  
 - GTAGCCACCC AACGTGTTGG TCCTTTACTA ACCATGGCGC TCGGTGCTGC TCGCTACTCC ATGCCACCTC  
 + CTGCGATCTA CGGAAACTCA AGTTTCAGGC AGACGAGTCC GTGGACATTC GTGGACATAT CCTTCCAACA  
 - GACGCTAGAT GCCTTTGAGT TCAAAGTCCG TCTGCTCAGG CACCTGTAAG CACCTGTATA GGAAGGTTGT  
 + TGCGCACCGC GAGTCAAACA TGGTGGCACA CGAACTTGCT CCGATGGCAA AGCATTC TCC CTCCGCTACT  
 - ACGCGTGGCG CTCAGTTTGT ACCACCGTGT GCTTGAACGA GGCTACCGTT TCGTAAGAGG GAGGCGATGA  
 + TGGATCGAAA CCCCACTTGG TAACATTATA CCTCTGCTCT TGGAAAGATGT AACGGCTATT GAAGCCTGGT  
 - ACCTAGCTTT GGGGTGAACC ATTGTAATAT GGAGACGAGA ACCTTCTACA TTGCCGATAA CTTCCGACCA  
 + AAAATGGTAT TTGTGTCAA AACAAGACA ACAAAGCTCG ATCTCTACAC CTTAGGAATT CAGTTGATGA  
 - TTTTACCATA AACACAGTTT TTGTTTCTGT TGTTTCGAGC TAGAGATGTG GAATCCTTAA GTCAACTACT  
 + AAATAGCAGG ACACTTCACT GAATTTTTTT GACGAGTACA CTTCACTGAA TTTAATCCGA TGTGTTACGA  
 - TTTATCGTCC TGTGAAGTGA CTTAAAAAAA CTGCTCATGT GAAGTGACTT AAATTAGGCT ACACAATGCT  
 + CTTACAAGTC GCGACTAATT AATCTGCCCC TCCCTTGCAA GCGCGCACAT ACGTACGGAC CCGATTGATC  
 - GAATGTT CAG CGCTGATTAA TTAGACGGGG AGGGAACGTT CCGCGGTGTA TGCATGCCTG GGC TAAC TAG  
 + ACGTCCCAGG AGGGCCACAC AACCCACGGA CGGTGCTCGC GC G C C C C G G G ACGCTCCCGG CGCGCTCTAT  
 - TGCAGGGTCC TCCCGGTGTG TTGGGTGCCT GCCAGCAGCG CGCGGGGCCC TGCAGGGCC GCGCGAGATA  
 + CTTCTCCCGC GC CACGTGGG CGCCCGGCTT ATCTGGTCCA GTCGTGCCTC CGCCGTGTGT GATCCCAAAT  
 - GAAGAGGGCG CCGTGCAGCC GCGGGCCGAA TAGACCAGGT CAGCACGGAG GCGGCACACA CTAGGGTTTA  
 + CCCCCATCCG AGCTTAGCTG CAGCCGCAGG TAGGTCGCTC ACCACGCAAC GTAAAATCGT ATGACA ACTA  
 - GGGGGTAGGC TCGAATCGAC GTCGGCGTCC ATCCAGCGAG TGGTGCGTTG CATT T T TAGCA TACTGTTGAT  
 + AATAACACAC TCCCCCTCC AAAGAAAAGC TTAAGCTCAG TCCGCCTCGG TCACCTCGTC GCGGTCTACC  
 - TTATTGTGTG AGGGGGGAGG TTTCTTTTCG AATTCGAGTC AGGCGGAGCC AGTGGAGCAG CCGCAGATGG  
 + AGAGATTACG GCGGCAGCTC GCATCGCAG ATG  
 - TCTCTAATGC CGCCGTCGAG CGTAGCGTC

**Figure 5.3: Brachypodium SBPase promoter motif sequences.**

The different coloured boxed sequences represent the promoter motifs. The arrow showed that the start of 2 kb promoter sequence upstream from the start codon region ATG. The motifs was analysed using Plant Care software.

**Table 5.1: The motifs boxes of *Brachypodium* SBPase promoter.** The *Brachypodium* SBPase promoter was analysed and its characteristic motifs boxes were identified using PlantCare software.

Motifs name	Organisms	Position	Strand	Sequence	Function
A-box	Oryza sativa	1401	+	AATAACAAACTCC	Sequence conserved in alpha-amylase promoters
	Petroselinum crispum	312, 324, 1218	-	CCGTCC	cis-acting regulatory element
ABRE	Arabidopsis thaliana	1271		ACGTGGC	cis-acting element involved in the abscisic acid responsiveness
ATCT-motif	Pisum sativum	1099	+	AATCTAATCC	Part of a conserved DNA module involved in light responsiveness
Box I	Pisum sativum	214	+	TTTCAA	Light responsive element
CAAT-box	Brassica rapa	107,230, 401, 675, 989, 1326	+, -	CAAAT and CAAT	Common cis-acting element in promoter and enhancer regions
	Arabidopsis thaliana	181, 235, 246, 298, 729	+, -	CAAAT and CAAT	Common cis-acting element in promoter and enhancer regions
CATT-motif	Zea mays	892	+	GCATTC	Part of a light responsive element
G-box	Zea mays	1190, 1273, 1301	+, -	CACGTC	cis-acting regulatory element involved in light responsiveness
GC-motif	Zea mays	1233	+	GCCCCGG	Enhancer-like element involved in anoxic specific inducibility
	Oryza sativa	1248	-	AGCGCGCCG	
TATA-box	Lycopersicon esculentum	85, 502, 980	-	TTTTA	Core promoter element around -30 of transcription start
	Arabidopsis thaliana	30,31, 32,290 601,603, 936, 937	+,-	TATAA, TATA	
	Nicotiana tabacum	94	+	tcTATAAAta	
	Brassica napus	935	+	ATTATA	
GATA-motif	Solanum tuberosum	486	+	AAGGATAAGG	part of a light responsive element

**Table 5.2: The motifs boxes of *Brachypodium* FBPA promoter.** The

Brachypodium FBPA promoter was analysed and its characteristic motifs boxes were identified using PlantCare software.

Motifs name	Organisms	Position	Strand	Sequence	Function
A-box	Petroselinum crispum	1175	-	CCGTCC	cis-acting regulatory element
ABRE	Arabidopsis thaliana	1004	-	TACGTG	cis-acting element involved in the abscisic acid responsiveness
ACA-motif	Pisum sativum	1313	+	AATTACAGCCATT	part of gapA in (gapA-CMA1) involved with light responsiveness
Box I	Pisum sativum	582	-	TTTCAA	light responsive element
CAAT-box	Glycine max	144, 411, 1009, 1119, 1436, 1437	+, -	CAATT	common cis-acting element in promoter and enhancer regions
	Hordeum vulgare	145, 439, 483, 689, 817, 1120, 1207, 1438	+,-	CAAT	
	Arabidopsis thaliana	978, 1300	+, -	CCAAT	
CATT-motif	Zea mays	49	-	GCATTC	part of a light responsive element
G-box	Brassica napus	1003	+	CCACGTAA	cis-acting regulatory element involved in light responsiveness
	Solanum tuberosum	17	+	CACATGG	
	Daucus carota	1004	-	TACGTG	
CCGTCC-box	Arabidopsis thaliana	1175	-	CCGTCC	cis-acting regulatory element related to meristem specific activation
TATA-box	Lycopersicon esculentum	448, 708, 765, 1215, 1195	+,-	TTTTA	core promoter element around -30 of transcription start
	Arabidopsis thaliana	362, 635, 706, 363, 503	+	TATAA, TATA	
	Nicotiana tabacum	633, 1168	+,-	tcTATAAAta	
	Oryza sativa	713	-	TACAAAA	
O2-site	Zea mays	841	-	GATGACATGA	cis-acting regulatory element involved in zein metabolism regulation

### **5.2.2 Building transcriptional fusion constructs of *Brachypodium* SBPase and FBPaldolase promoters for transient expression analysis into *N. benthamiana* leaves**

In order to isolate the DNA fragment of the SBPase promoter from the *B. distachyon* genome, specific primers (Table 2.1) designed from a region upstream of the start codon of SBPase (Gene ID: Bradi2g55150) were used to amplify the extracted DNA sample from the *Brachypodium* leaf. Next, it was cloned into the Gateway entry vector pENTR™ Directional TOPO® (supplied by Invitrogen) through a BP reaction (entry clone), and then, the colony PCR was performed, as well as sequencing. The binary expression vectors pGWB3 (GUS) and pGWB40 (eYFP) were constructed separately to carry the newly isolated SBPase promoter fragment driving the GUS (Figure 5.4) and eYFP reporter genes (Figure 5.5) and were transformed into agrobacterium cells as a preparation for agroinfiltration assay into the leaves of *N. benthamiana*. The colony PCRs were performed to select the positive ones that carry the constructs (Figures 5.6). The p19 promoter was used as a negative control.

The DNA fragment of the *B. distachyon* genome's FBPaldolase promoter was isolated from a region upstream of the start codon of FBPaldolase (Gene ID: Bradi4g24367) and cloned using gateway cloning technology as described above into pENTRY vector. The binary expression vectors pGWB3 (GUS) and pGWB40 (eYFP) were constructed separately to carry the newly isolated FBPaldolase promoter fragment driving the GUS (Figure 5.7) and eYFP reporter genes (Figure 5.8) and were transformed into agrobacterium cells as a preparation for agroinfiltration assay into the leaves of *N. benthamiana*. The colony PCRs were performed to select the positive ones that carry the constructs (Figures 5.9).

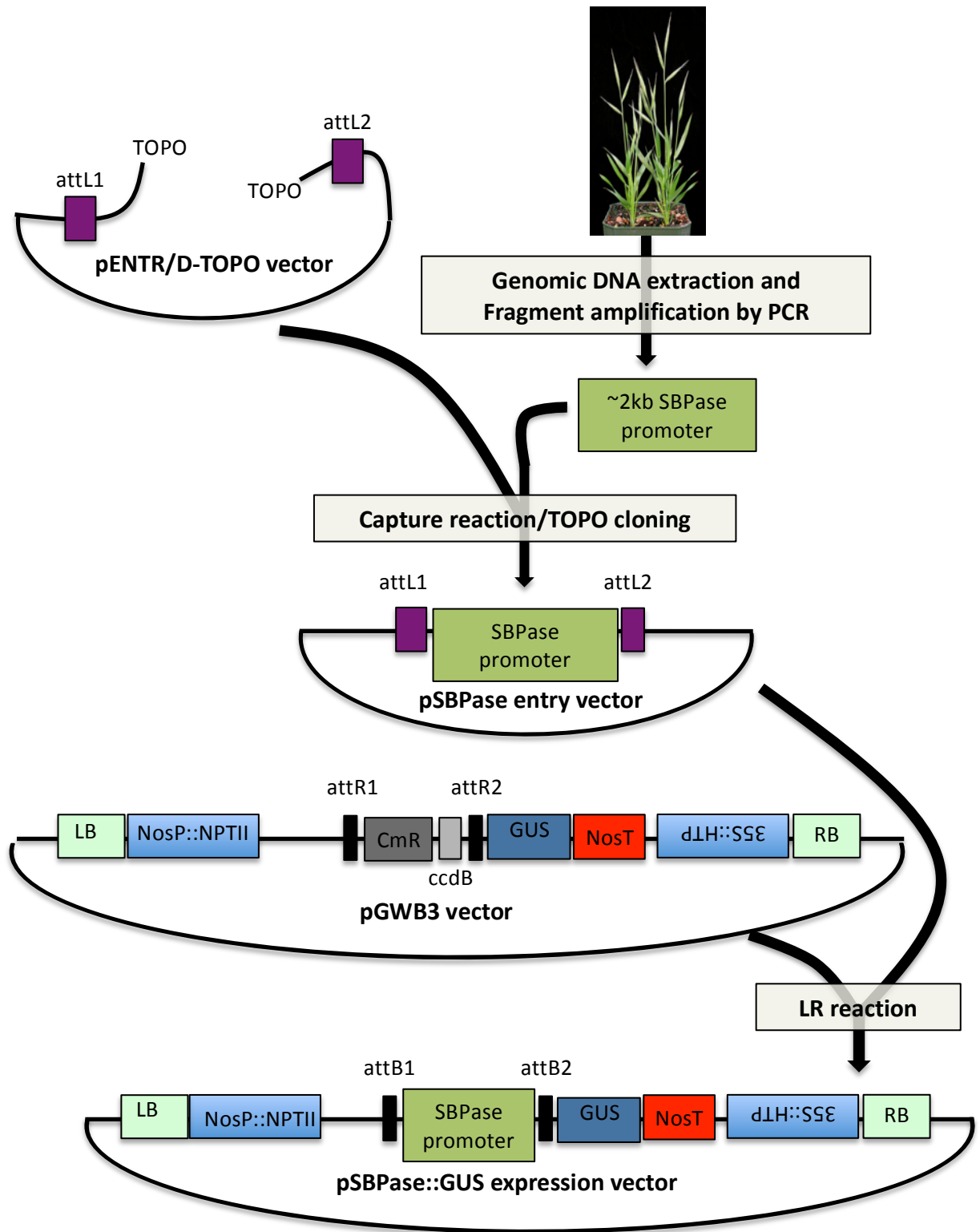


**Figure 5.4: Building transcriptional fusions of *Brachypodium* SBPase construct to the  $\beta$ -glucuronidase (GUS) for expression analysis into *N. benthamiana* leaves.** Genomic DNA of *Brachypodium* leaves was used to amplify the native promoters of SBPase. Then the promoter fragment was cloned into pENTR/D-TOPO vector before sub-cloned into pGWB3 vector (GUS).

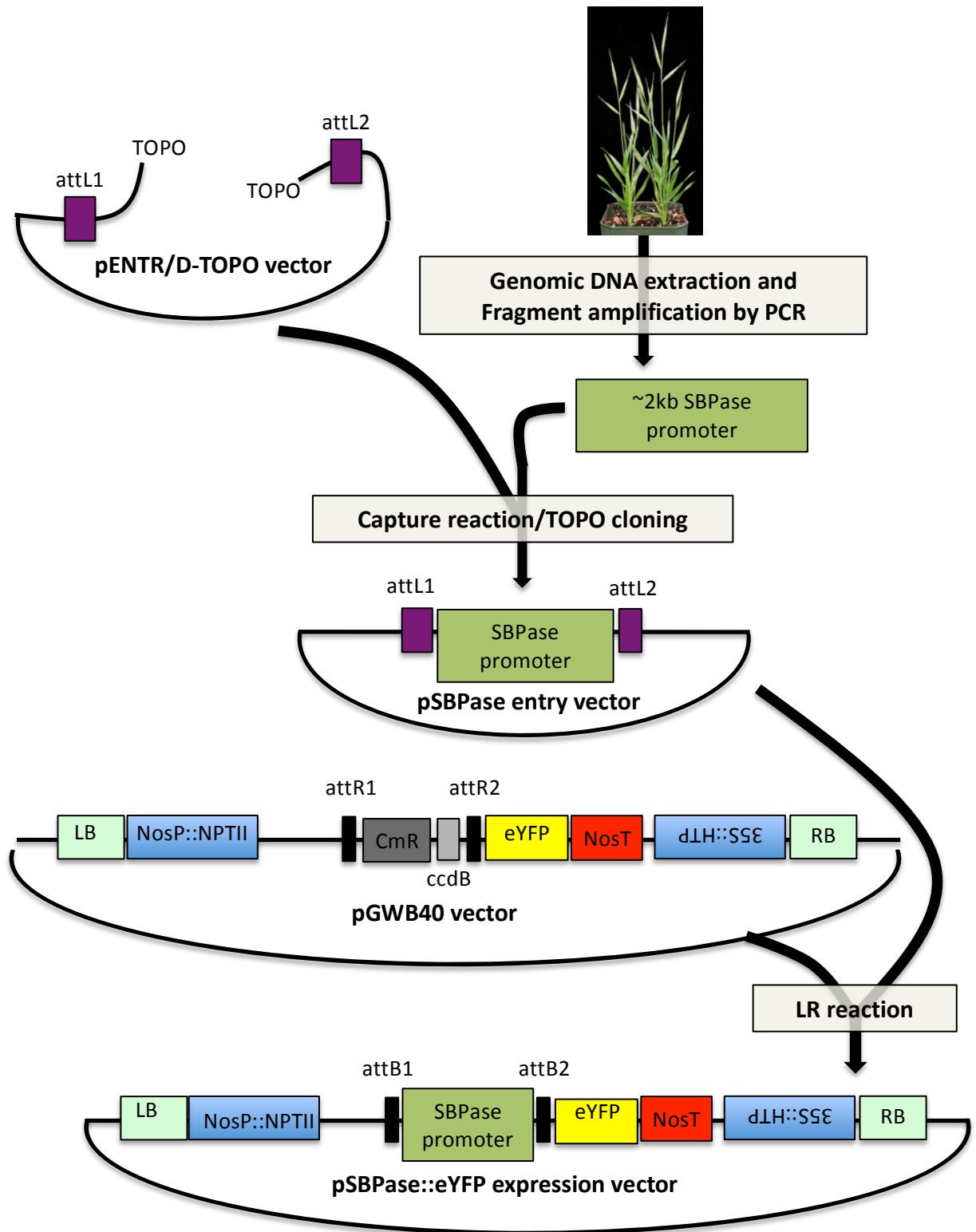


**Figure 5.5: Building transcriptional fusions of *Brachypodium* SBPase construct to the enhanced yellow fluorescence protein (eYFP) for expression analysis into *N. benthamiana* leaves.** Genomic DNA of *Brachypodium* leaves was used to amplify the native promoters of SBPase. Then the promoter fragment was cloned into pENTR/D-TOPO vector before sub-cloned into pGWB40 vector (eYFP).

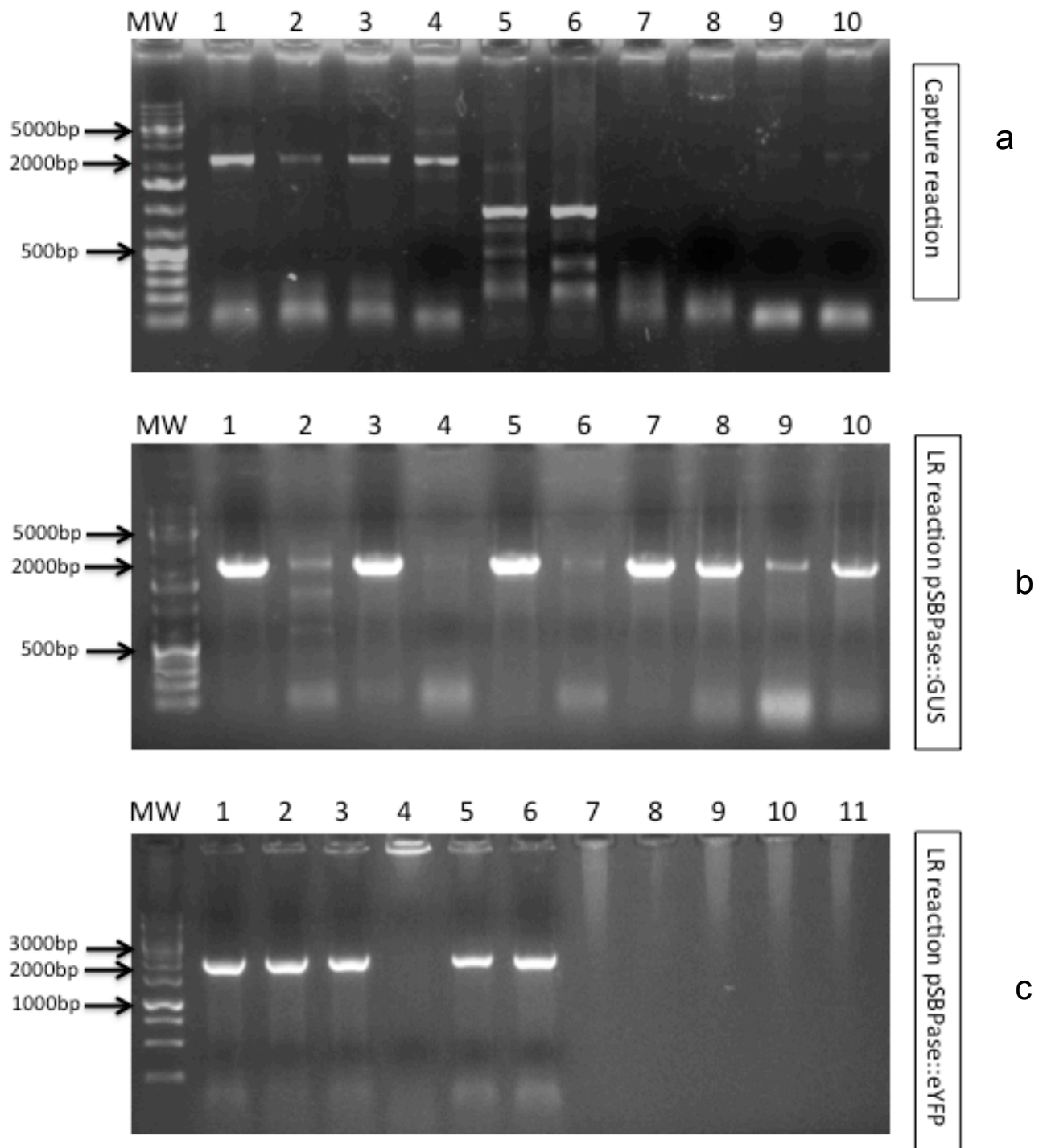


**Figure 5.6. Colony PCRs of the construction of SBPase with the chimeric expression cassettes (GUS and eYFP) into *E coli*.** **a.** Colony PCR of BP reaction (capture reaction) into pENTRY vector into *E coli*. **b.** Colony PCR of LR reaction for SBPase::GUS construct into *E coli*. **c.** Colony PCR of LR reaction for SBPase::eYFP construct into *E coli*. Each colony was subjected to PCR with suitable primers to select positive colonies at the expected size 2kb. The marker used was Generuler mix in Figure a and b and 1kb in Figure c. The PCR reaction was 20  $\mu$ l, and the PCR products were run on 0.5% agarose gel for 30 min at 110 v.

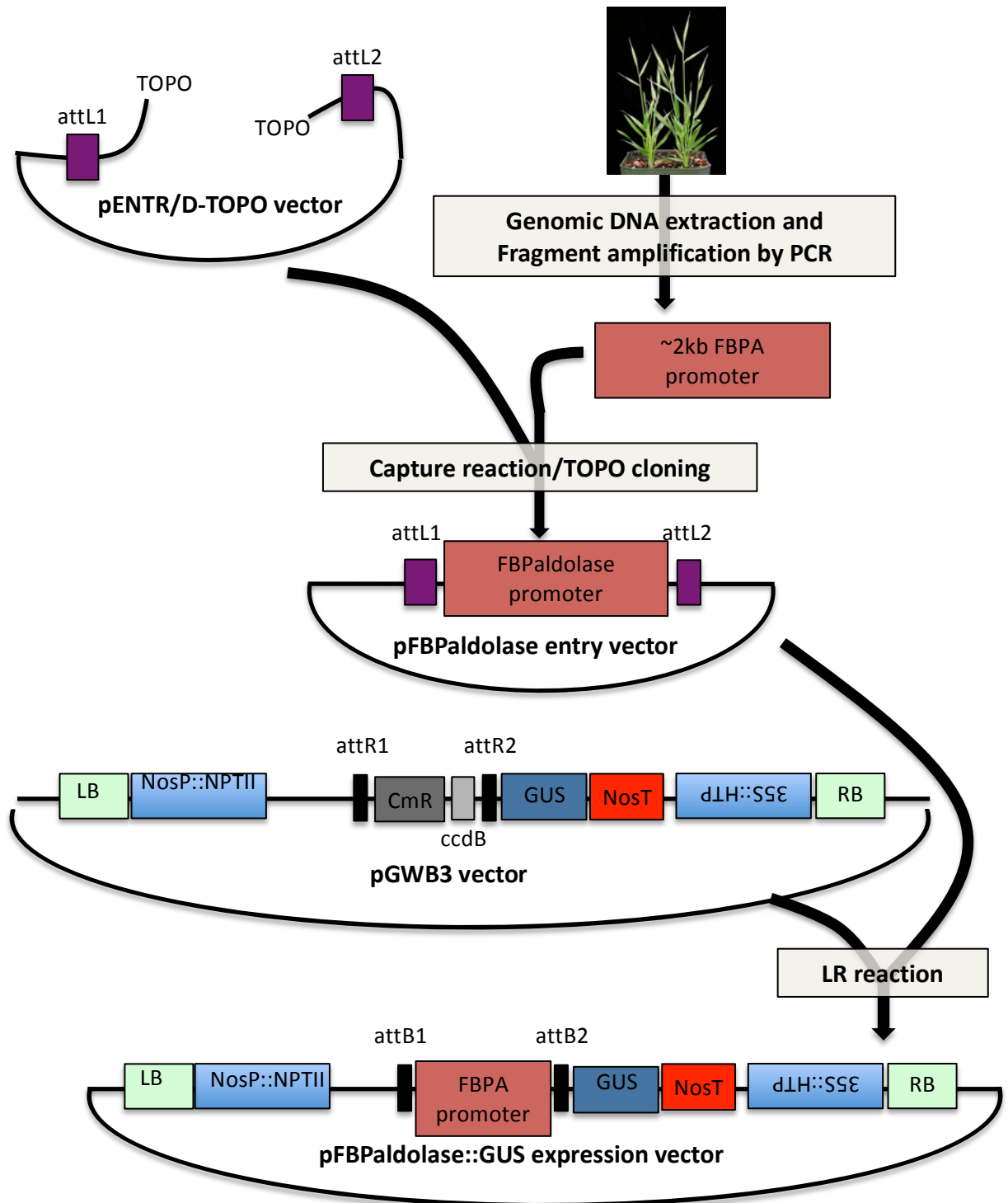


**Figure 5.7: Building transcriptional fusions of *Brachypodium* FBPA (FBPaldolase) construct to the  $\beta$ -glucuronidase (GUS) for expression analysis into *N. benthamiana* leaves.** Genomic DNA of *Brachypodium* leaves was used to amplify the native promoters of FBPA. Then the promoter fragment was cloned into pENTR/D-TOPO vector before sub-cloned into pGWB3 vector (GUS).

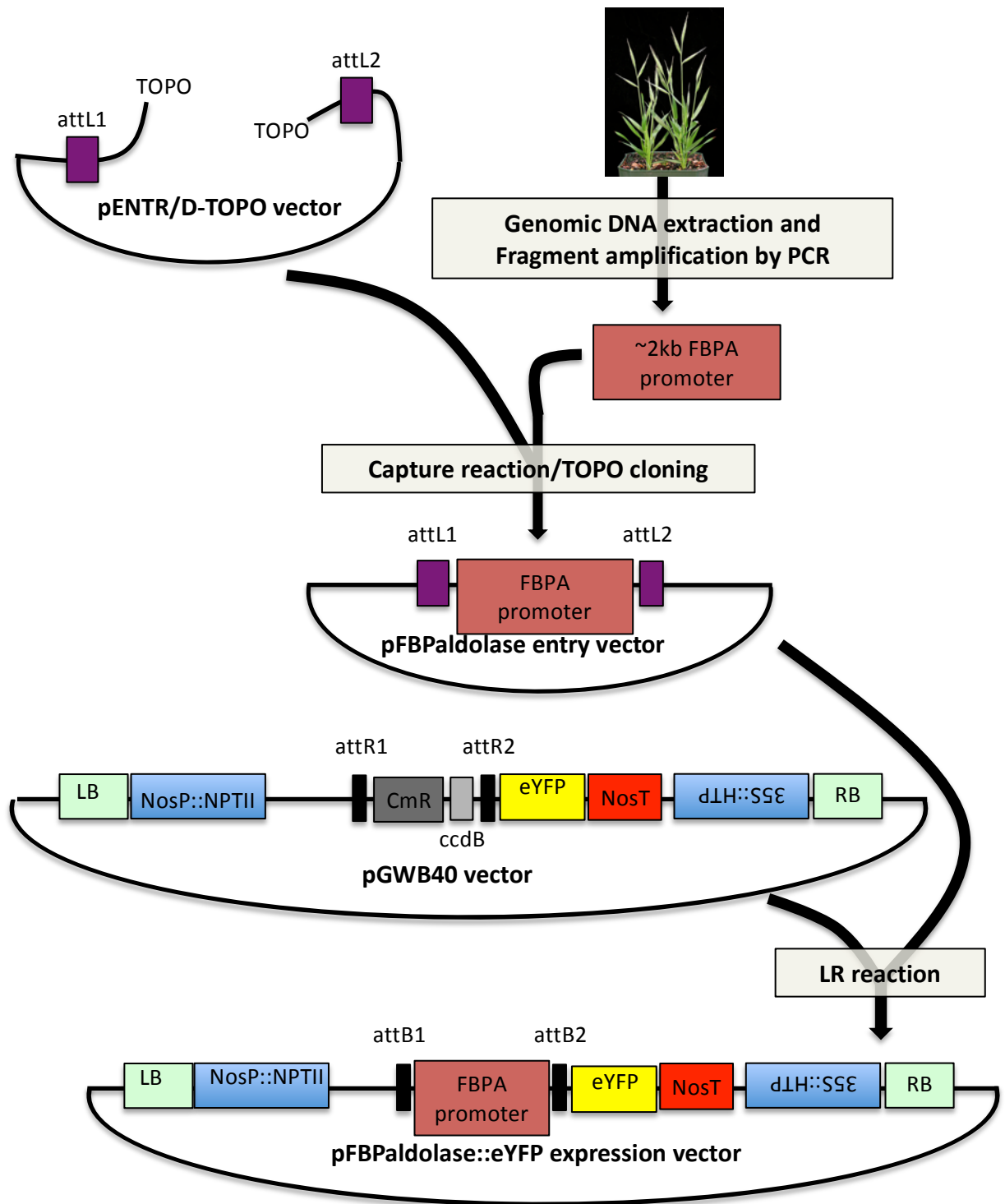


**Figure 5.8: Building transcriptional fusions of *Brachypodium* FBPA construct to the enhanced yellow fluorescence protein (eYFP) for expression analysis into *N. benthamiana* leaves.** Genomic DNA of *Brachypodium* leaves was used to amplify the native promoters of FBPA. Then the promoter fragment was cloned into pENTR/D-TOPO vector before sub-cloned into pGWB40 vector (eYFP).

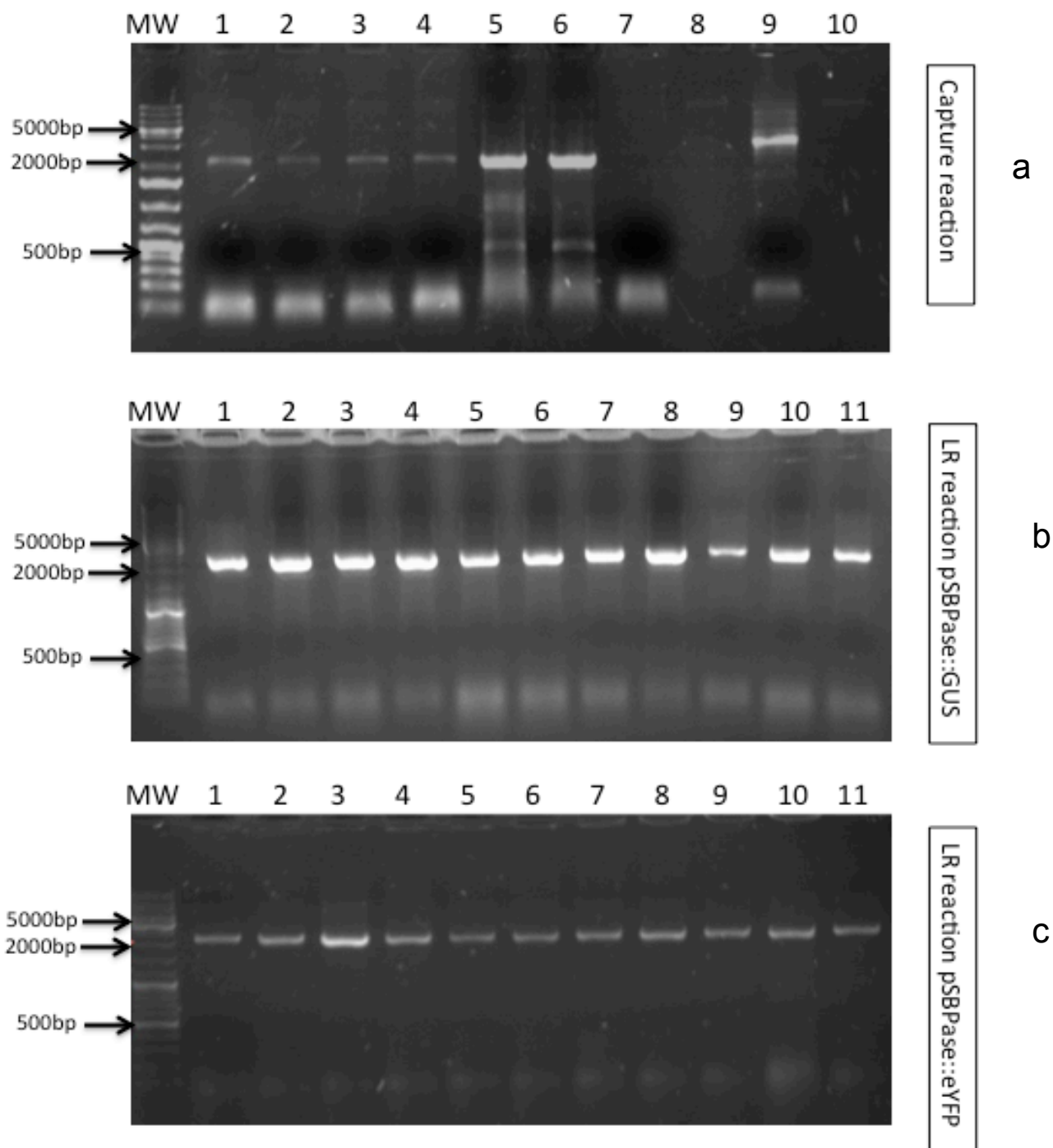


**Figure 5.9. Colony PCR of the construction of FBPA with the chimeric expression cassettes (GUS and eYFP) into *E coli*.** a. Colony PCR of BP reaction (capture reaction) into pENTRY vector into *E coli*. b. Colony PCR of LR reaction for FBPA::GUS construct into *E coli*. c. Colony PCR of LR reaction for FBPA::eYFP construct into *E coli*. Each colony was subjected to PCR with suitable primers to select positive colonies at the expected size 2kb. The marker used was Generuler mix. The PCR reaction was 20  $\mu$ l, and the PCR products were run on 0.5% agarose gel for 30 min at 110 v.

### 5.2.3 Transient expression analysis in *Nicotiana benthamiana* leaves

To test the functionalities of either GUS or eYFP fusion genes driven by the 2 kb promoters of *Brachypodium* SBPase and FBPAldolase in *N. benthamiana*, transient transformations were carried out in leaf tissue with the constructs through assay infiltrations. Following the transient assay, tissues were incubated in a controlled room for 72 h and then subjected to GUS staining and confocal imaging. As a result, the GUS staining analysis showed that a clear and strong GUS blue-staining colour was observed in the whole leaf, which indicated the expression of GUS driven by the SBPase promoter, when compared to the wild type (WT) (Figure 5.10a). Similarly, the GUS expression driven by the FBPAldolase promoter also was clearly shown, represented by strong blue spots throughout the leaf, when compared to the WT (Figure 5.10b).

To study the subcellular localisation of the eYFP fusion driven by promoters of *Brachypodium* SBPase and FBPAldolase, confocal microscopy was used on eYFP-infiltrated leaves. Consequently, as can be seen in Figure 5.11, the eYFP signals driven by the SBPase promoter were observed clearly in the cytosol of the mesophyll cells, when compared to the WT and the leaf infiltrated with only p19 plasmid with no eYFP signals. Moreover, compared to the WT leaf and the leaf infiltrated with only p19 plasmid, the subcellular localisation of the eYFP reporter gene driven by the FBPAldolase promoter was shown clearly, as the strong eYFP signals detected the mesophyll cells' cytosol around the chloroplast (Figure 5.11).

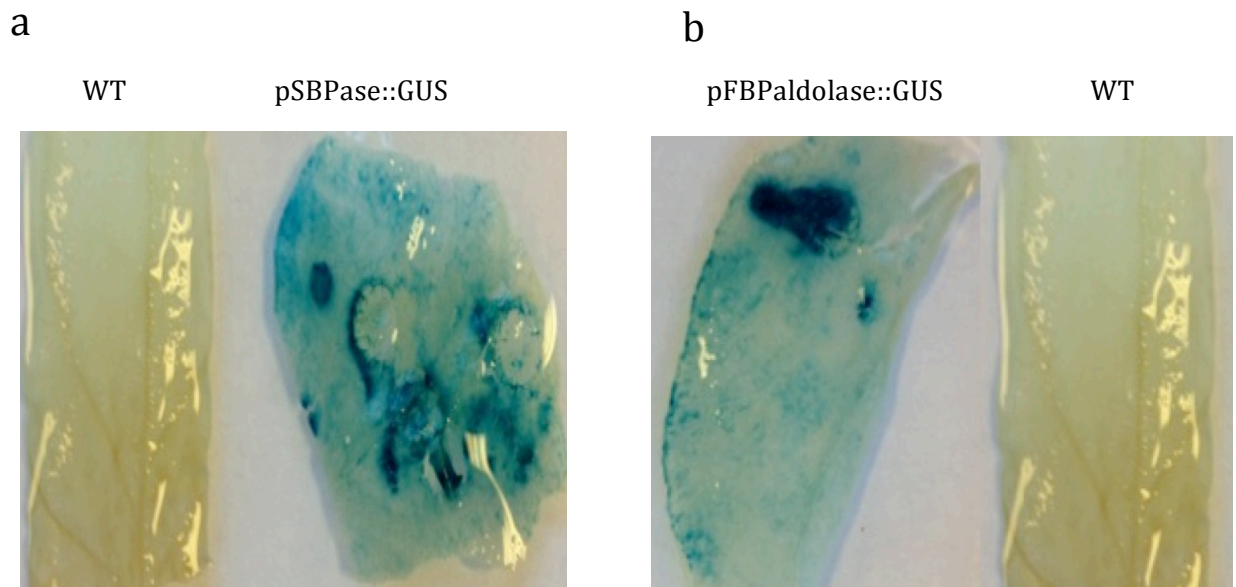


**Figure 5.10: Histochemical GUS assay of agro-infiltrated *N. benthamiana* leaves.** The transient assays were performed on 3-weeks old *N. benthamiana* leaves and incubated in a controlled room for 72 h and then subjected to GUS staining: **a.** GUS expression driven by SBPase promoter, and **b.** GUS expression driven by FBPaldolase compared with wild type leaf (non-infiltrated leaf).

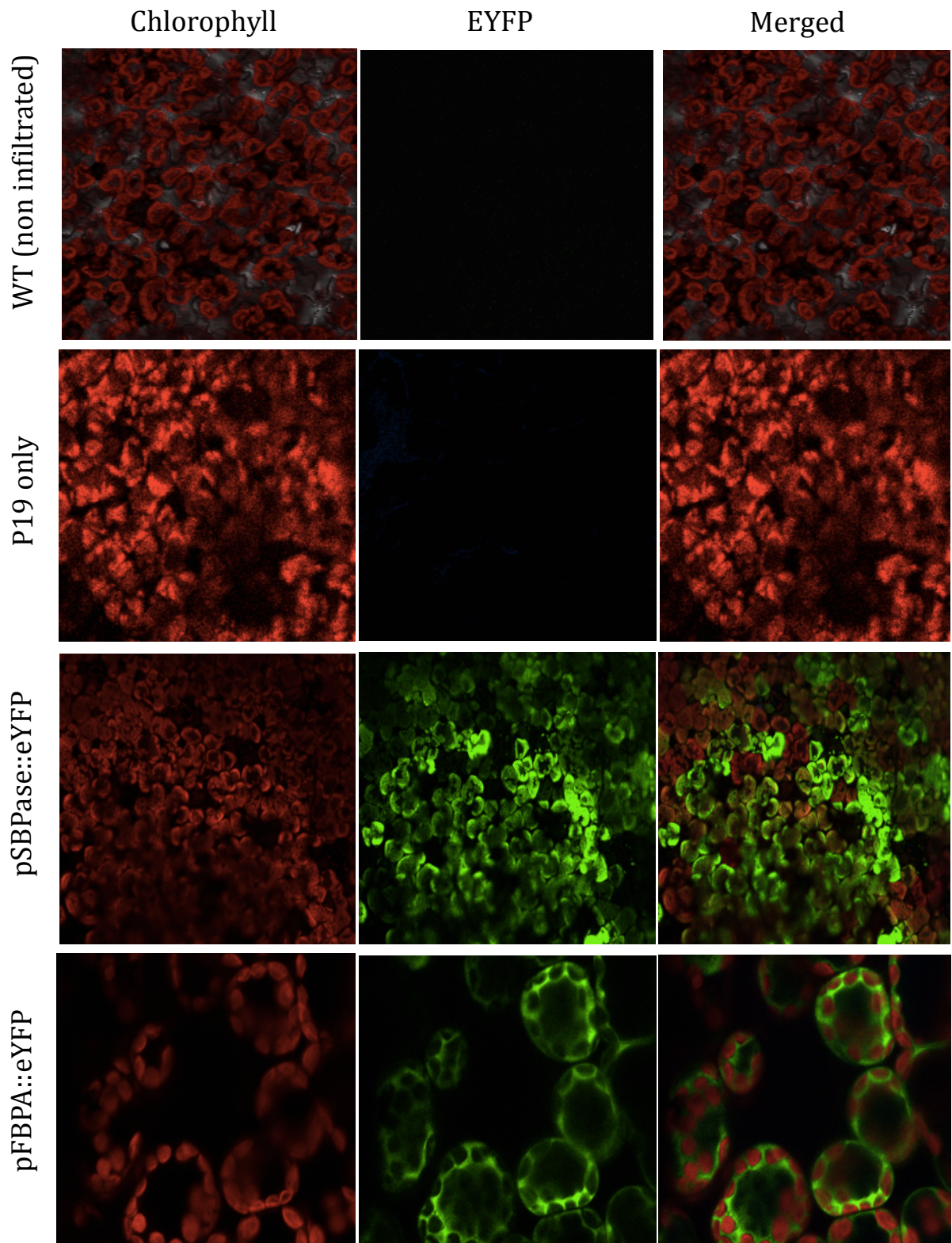


**Figure 5.11: Confocal Fluorescent images of eYFP-agro-infiltrated leaves *N. benthamiana* plants.** The transient assays were performed on 3-weeks old *N. benthamiana* leaves and incubated in a controlled room for 72 h and then subjected to confocal microscopy.

#### **5.2.4 Building transcriptional fusion constructs of *Brachypodium* SBPase and FBPaldoase promoters for transient and stable expression analysis into wheat leaves**

In order to analyse the expression of both *Brachypodium* SBPase and FBPaldoase promoters, the DNA fragments of both promoters were isolated from the *B. distachyon* genome from a region upstream of the start codon of the SBPase (Gene ID: Bradi2g55150) and FBPaldoase (Gene ID: Bradi4g24367) using specific designed primers (Table 2.1), with the addition of specific restriction enzymes sites (Ascl and Mlul sites in case of the isolation of SBPase promoter, and Xmal and EcoRI sites in case of FBPaldoase). Then, these primers were used to amplify the extracted DNA sample from the *Brachypodium* leaf. Next, 5 ul of amplified 2kb-promoters-DNA was separated on a 1% agarose gel to ensure the success of 2 kb amplification (Figure 5.14a), and the remaining reaction was cleaned up and purified. Then, they were cloned separately into the pRRes14.041 GUS vector (supplied by Rothamsted Research, Harpenden, UK) through a traditional cloning approach, one with SBPase promoter (Figure 5.12) and one with FBPaldoase promoter (Figure 6.13). They then were transformed into TOP10 cells as a preparation for transient assay, as well as stable transformation into the leaves of wheat. The colony PCRs were performed to select the positive ones that carry the promoter (Figures 5.14b and c). Both constructs were verified by sequencing using T3 and T7 primers. They also were verified by digestion enzymes, and consequently, expected bands at the desirable size were obtained that confirmed the success of cloning (Figure 5.15). They then were sent to the Rothamsted Research (Harpenden, UK) for transient assay analysis through biolistic transformation into wheat leaf.

To test the functionality of both promoters to drive GUS expression in wheat leaf, transient transformations were performed as a quick approach before the stable transformations. As a result of the transient transformation analyses, both promoters drove good GUS expression in the wheat leaves. Many excellent discrete spots in large patches were observed with reasonable intensity. However, expression driven by the SBPase promoter was stronger than that driven by the FBPaldolase (Figure 5.16).

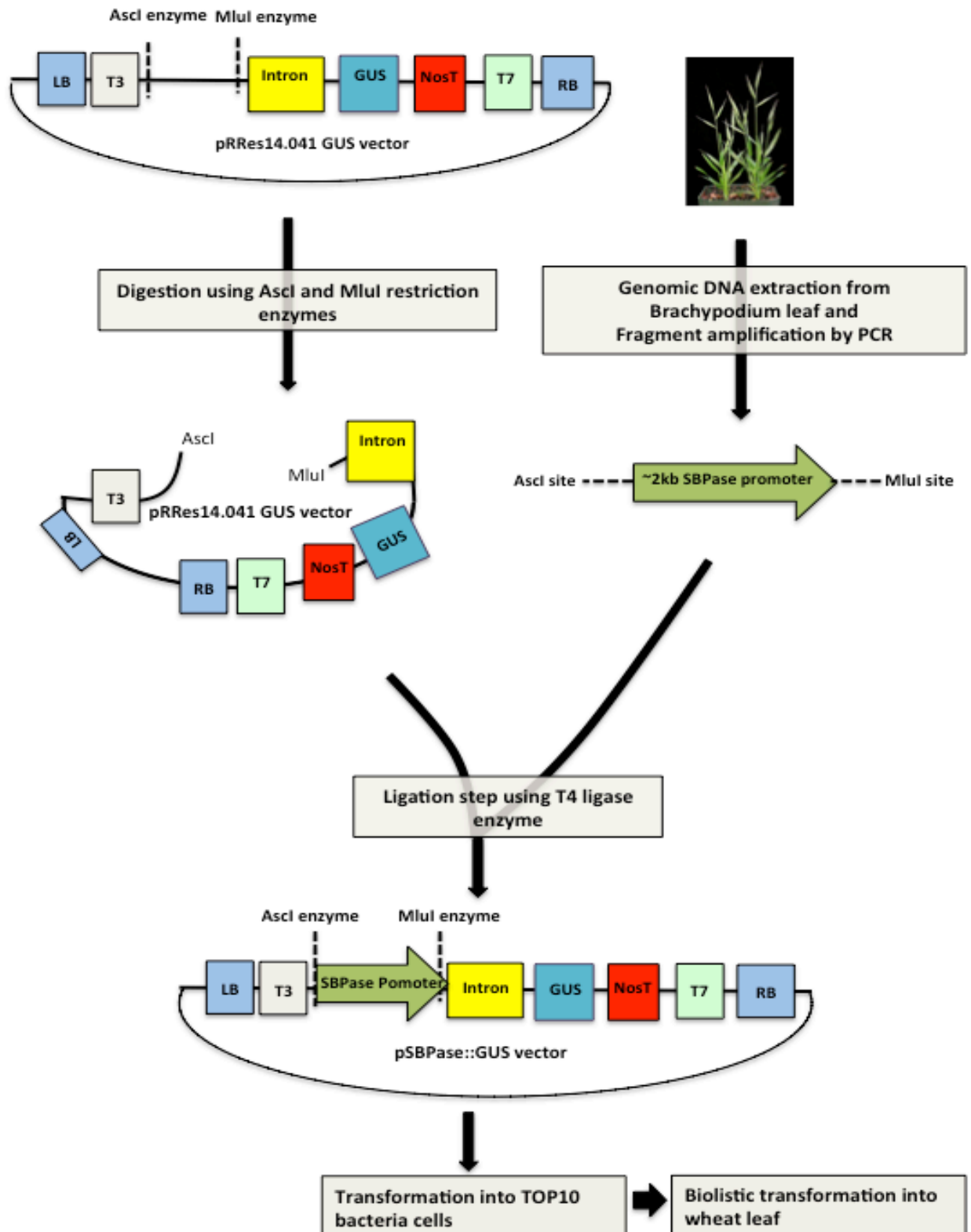


**Figure 5.12: Building transcriptional fusions of *Brachypodium* SBPase construct to the  $\beta$ -glucuronidase (GUS) for expression analysis into *wheat* leaves.** Genomic DNA of *Brachypodium* leaves was used to amplify the native promoters of SBPase. Then the promoter fragment was cloned into the Mlul and Ascl restriction sites of pRRes14.041 GUS vector.

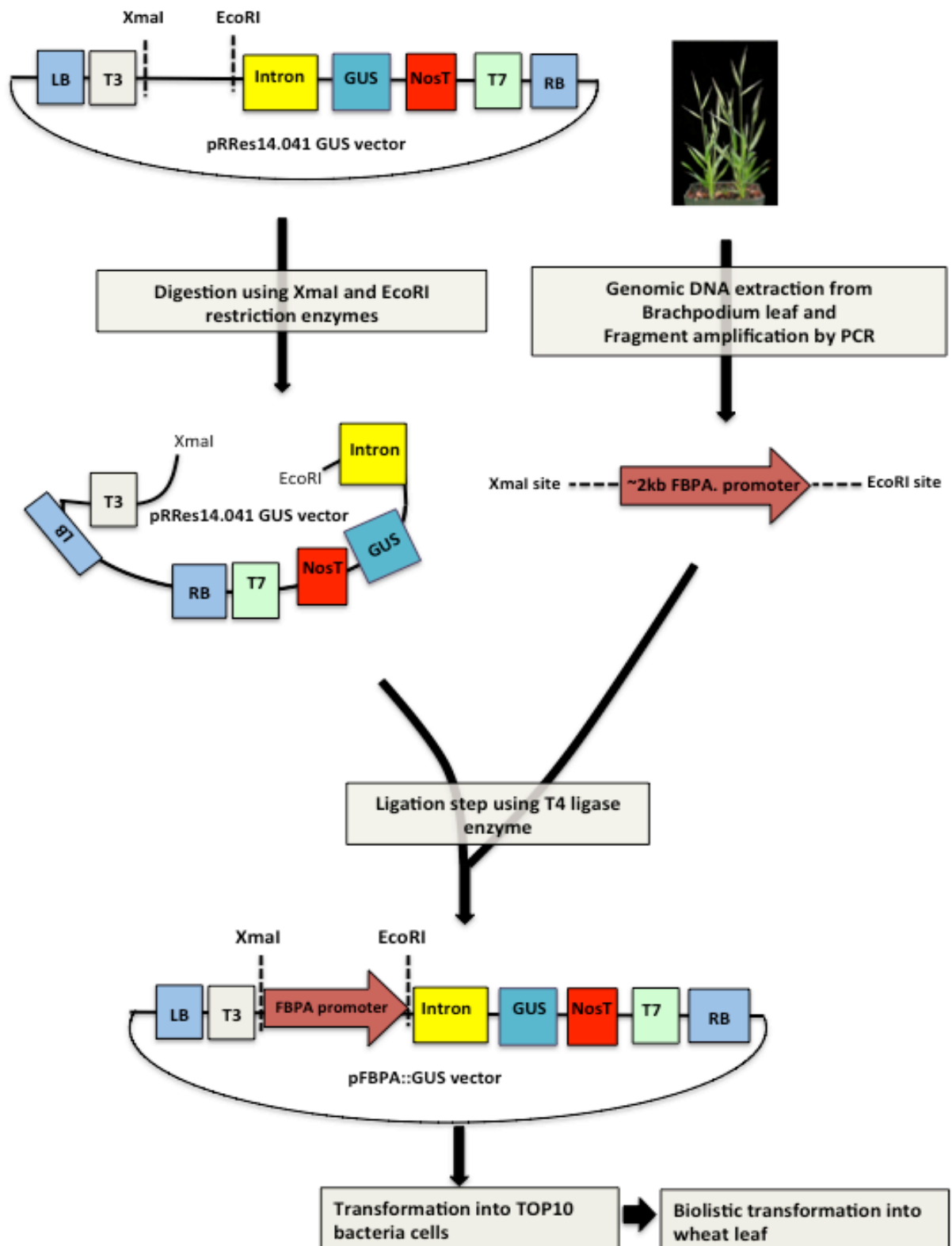


**Figure 5.13: Building transcriptional fusions of *Brachypodium* FBPA construct to the  $\beta$ -glucuronidase (GUS) for expression analysis into *wheat* leaves.** Genomic DNA of *Brachypodium* leaves was used to amplify the native promoters of FBPA. Then the promoter fragment was cloned into the EcoRI and XmaI restriction sites of pRRes14.041 GUS vector.

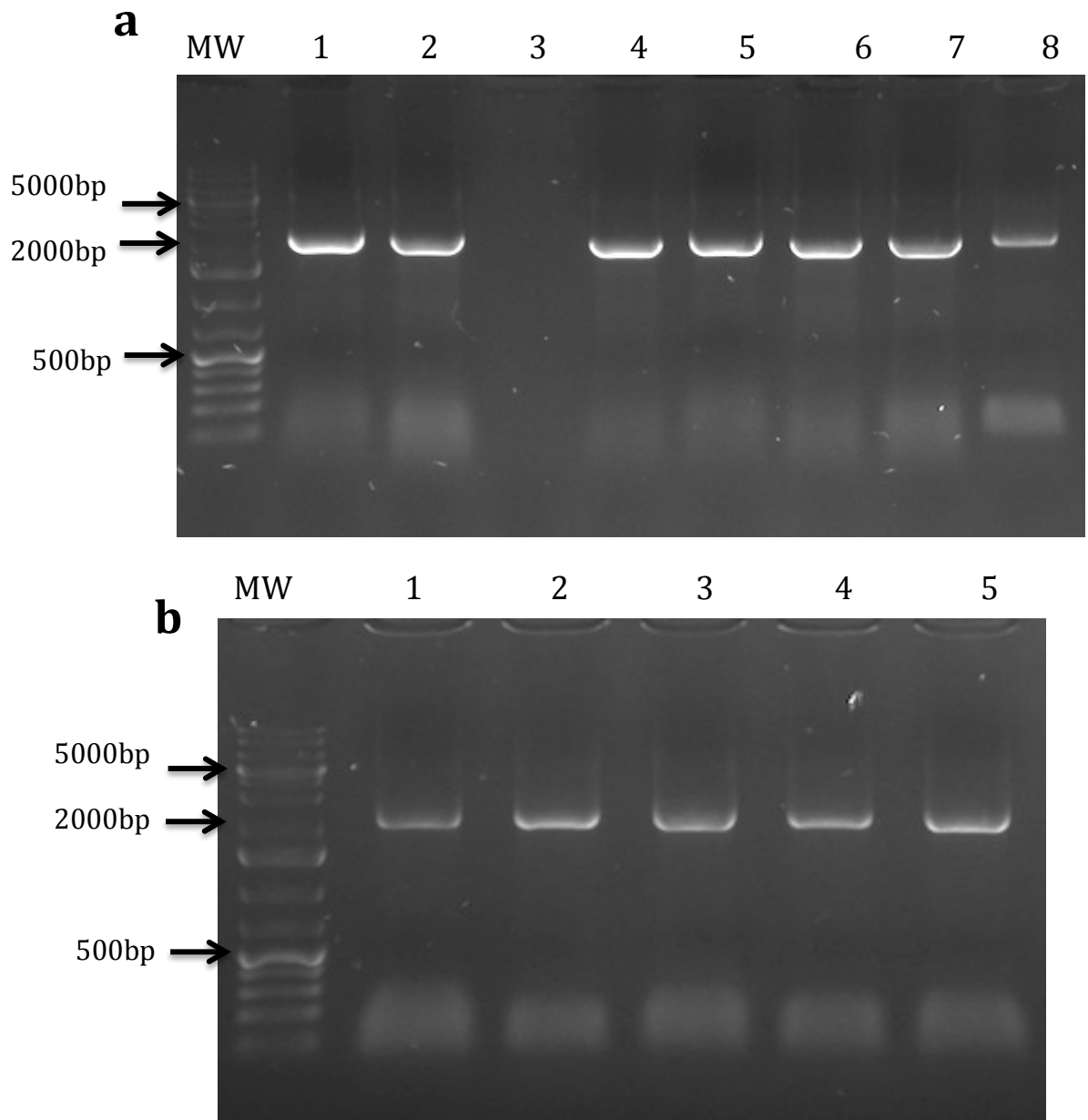


**Figure 5.14.** Colony PCR of the construction of SBPase and FBPA promoters with the chimeric expression cassettes (GUS) into *E coli*. **a.** Colony PCR of SBPase promoter into pRRes14.041 GUS vector into *E coli* cells; **b.** Colony PCR of FBPA promoter into pRRes14.041 GUS vector into *E coli*. Each colony was subjected to PCR with suitable primers to select positive colonies at the expected size 2kb. The marker used was 1kb plus. The PCR reaction was 20  $\mu$ l, and the PCR products were run on 0.5% agarose gel for 30 min at 110 v.

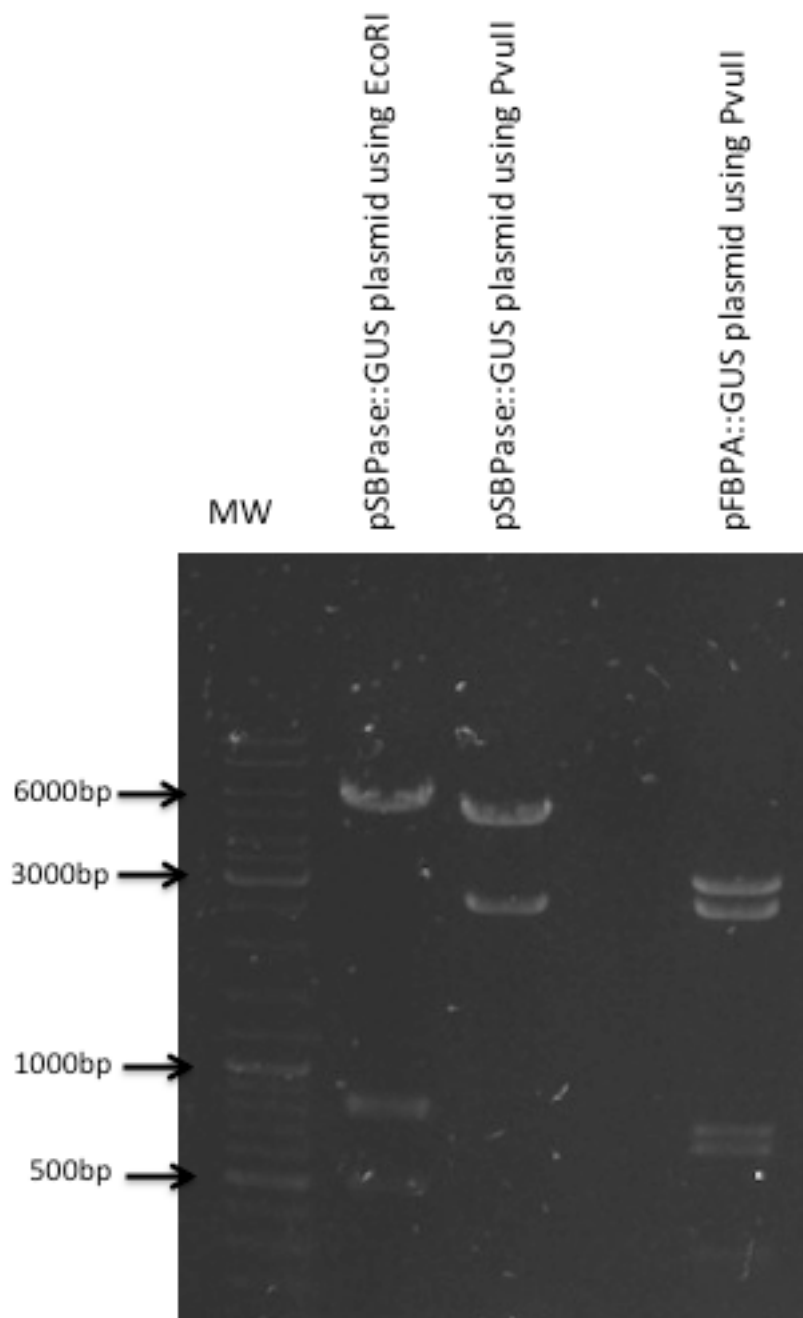


**Figure 5.15: Digestion analyses of SBPase::GUS and FBPA::GUS plasmids.**

The plasmid of SBPase::GUS was digested using two different restriction enzymes (one with EcoRI and one with PvuII enzymes); and FBPA::GUS was digested using PvuII enzyme. Both digested plasmids were run on 0.5% agarose gel for 40 min at 100v.

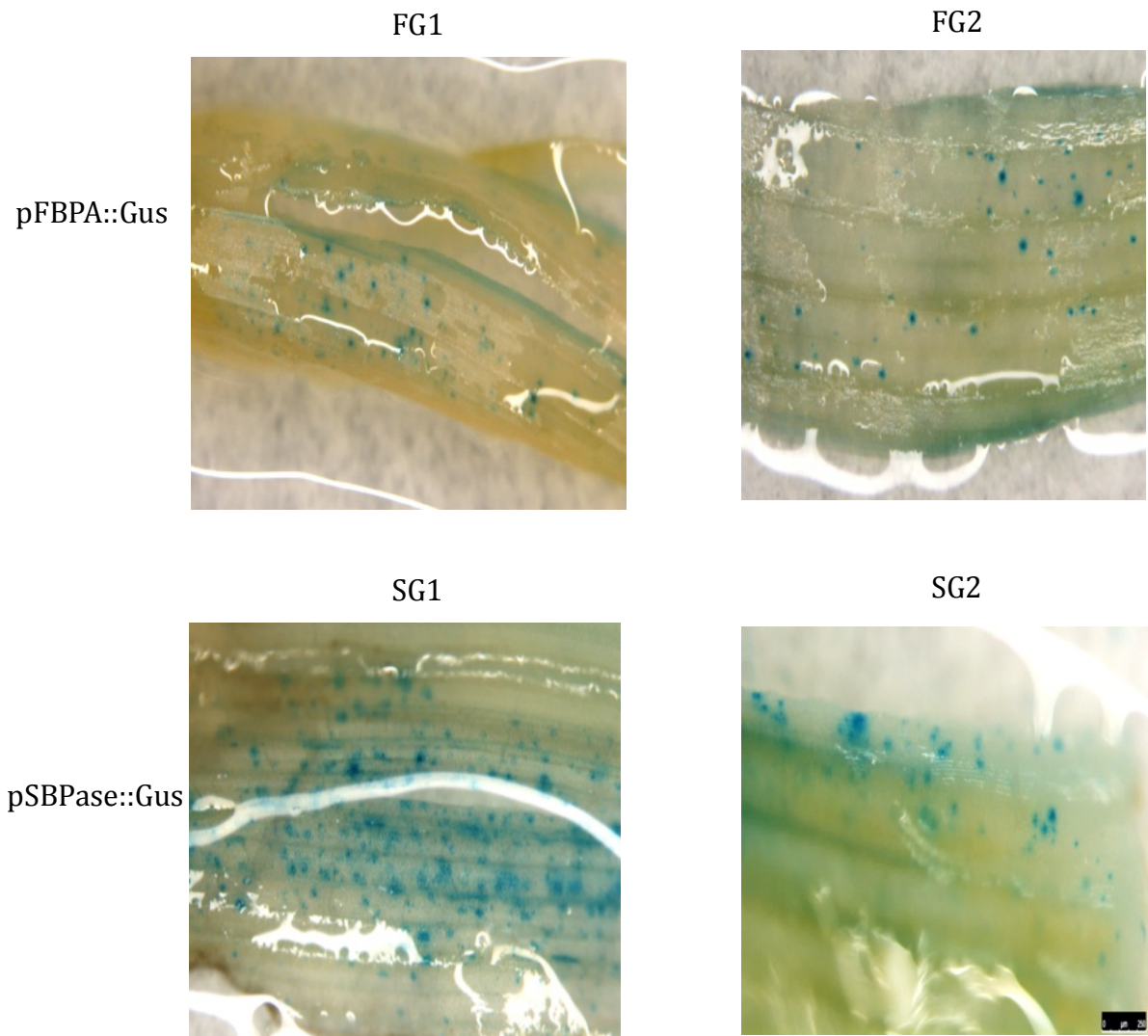


**Figure 5.16: Histochemical GUS assay for transient testing of Brachypodium SBPase and FBPA into wheat leaves.**

The transient assays were performed on young wheat leaves and incubated in a controlled room for 72 h and then subjected to GUS staining: GUS expression driven by SBPase promoter in two different samples (down), and b. GUS expression driven by FBPAldolase in two different samples (top).

Then after transient testing of both promoters to drive GUS expression in wheat leaves showed positive results, they were preceded to stable biolistic transformations for further analyses through different leaf developmental stages.

## **6.2.5 Stable expression analysis into wheat leaves**

### **6.2.5.1 GUS expression into T0 tissues**

To study the GUS expression driven by *Brachypodium* SBPase and FBPaldolase promoters at different growth stages and to confirm the usability of these promoters, stable biolistic transformations were performed at Rothamsted Research. After the production of T0 progenies, samples were taken for GUS staining from different tissues, including leaves (at two different growth stages—seedlings and flag leaves), roots and flowers.

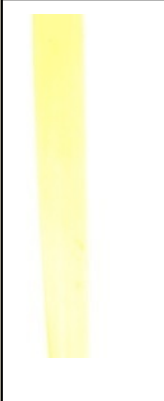
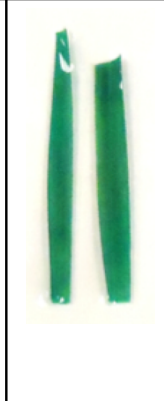
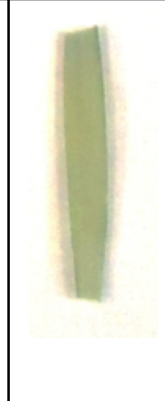
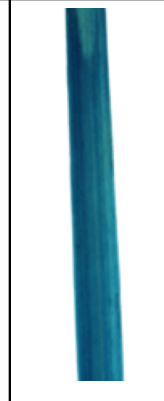
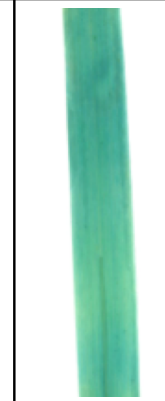
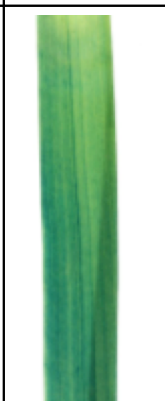
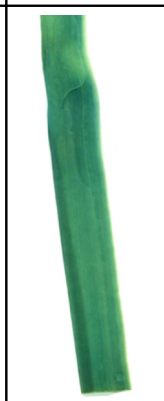
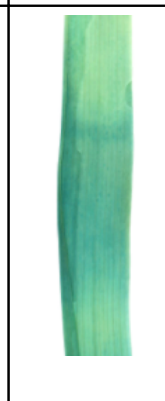
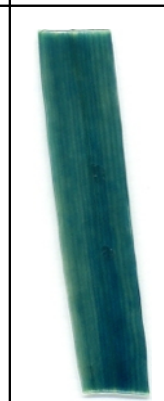
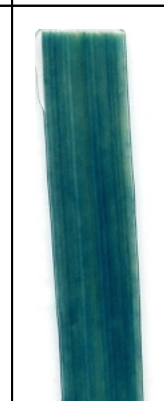
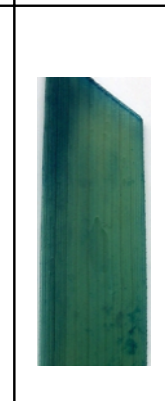
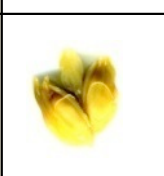
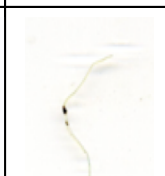
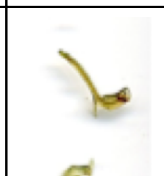
As a result of GUS staining, some strong positive blue staining in large patches was observed in the leaves and flowers of the wheat plants' T0, driven by the *Brachypodium* SBPase promoter in samples such as R4P3, R2P2, R5P3 and R9P2. However, no GUS expression appeared in the roots (Figure 5.17). Similarly, excellent and strong GUS expression driven by the *Brachypodium* FBPaldolase promoter were observed in some wheat T0 leaves and flowers such as in R3P1, R4P1, R5P1, R3P11, but, interestingly, no expression was seen in the roots (Figure 5.18).

Three positives lines from each pSBPase::GUS and pFBPaldolase::GUS were subject to the microscopy investigation in collaboration with Caroline Sparks at Rothamsted Research. Consequently, they all showed good expression in mesophyll cells and guard cells, but not in the midrib or veins, in the case of both the pSBPase::GUS (Figure 5.19) and pFBPaldolase::GUS (Figure 5.20).

	WT	R4P3	R2P2	R9P2	R5P3	R8P9	R7P3
Seedling stage							
Flag leaf							
Flowers							
Roots							

**Figure 5.17: Histochemical analysis of GUS activity in stable transformed wheat T0 plants with Brachypodium SBPase promoter.**

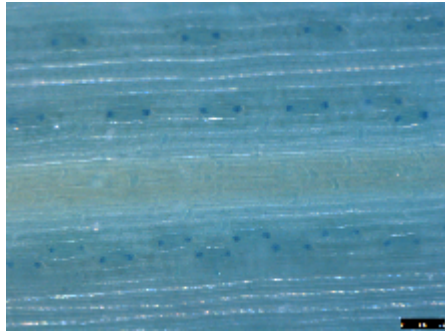
The stable transformation was done at Rothamsted Research and after the production of T0 plants, young leaves tissues were taken for GUS staining assay. GUS expression driven by SBPase promoter was tested in two different leaf developmental stages (seedlings and flag leaves), and also in different plant tissues: flowers and roots.

	WT	R4P1	R3P1	R3P7b	R5P1	R3P4	R3P11	R6P2
Seedling stage								
Flag leaf								
Flowers								
Roots								

**Figure 5.18: Histochemical analysis of GUS activity in stable transformed wheat T0 plants with Brachypodium FBPA promoter.**

The stable transformation was done at Rothamsted Research and after the production of T0 plants, young leaves tissues were taken for GUS staining assay. GUS expression driven by FBPA promoter was tested in two different leaf developmental stages (seedlings and flag leaves), and also in different plant tissues: flowers and roots.

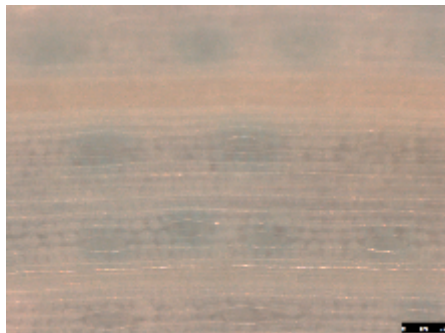
R4P3



R5P3



R9P2



R2P2



**Figure 5.19: Microscopy observation of GUS expression localisation in wheat T0 leaves driven by Brachypodium SBPase promoter.**

The stable transformations were done at Rothamsted Research and after the production of T0 plants, young leaves tissues were taken for GUS staining assay, and were subjected to microscopy observation in different T0 plants at Rothamsted Research by Caroline Sparks.

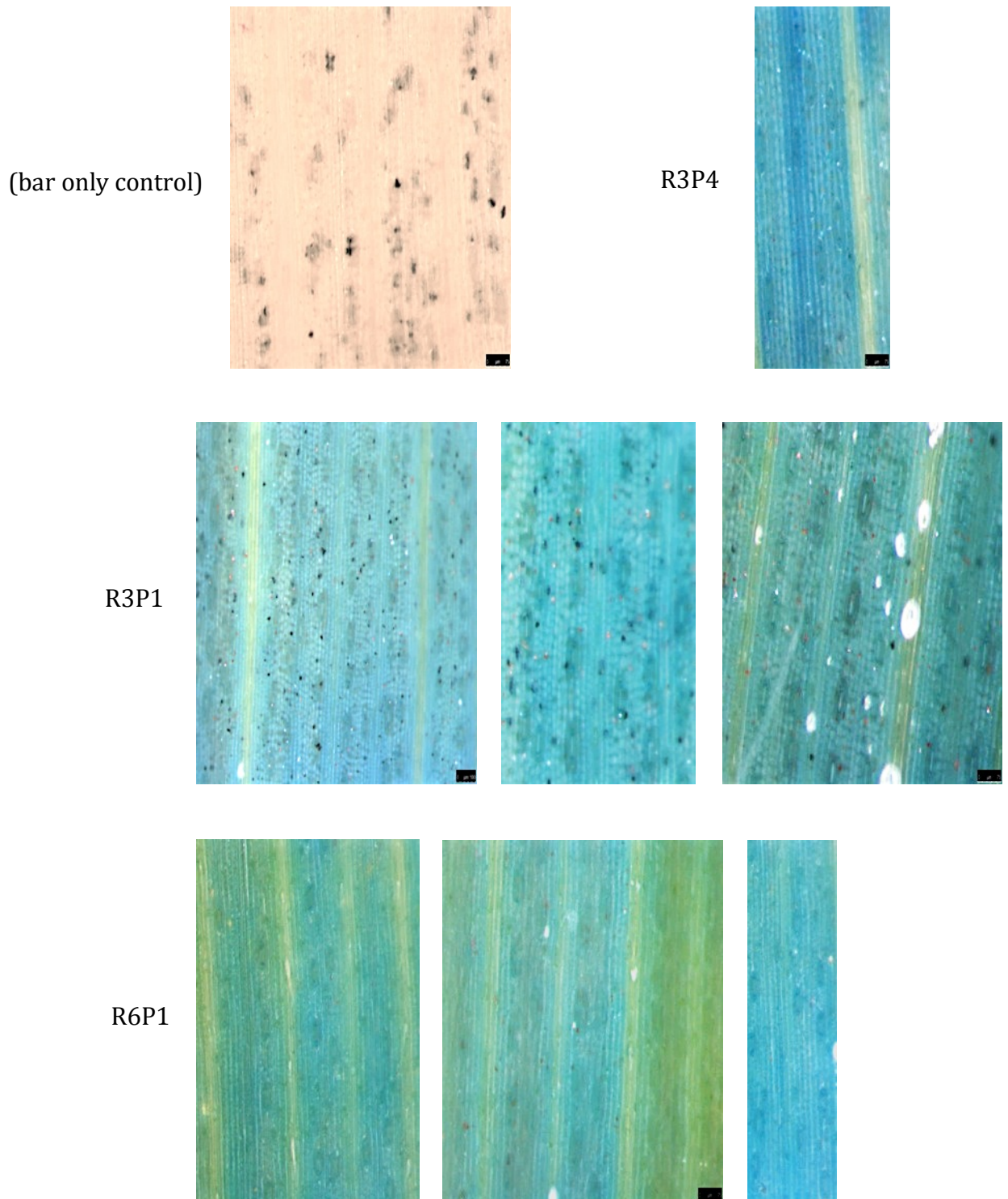


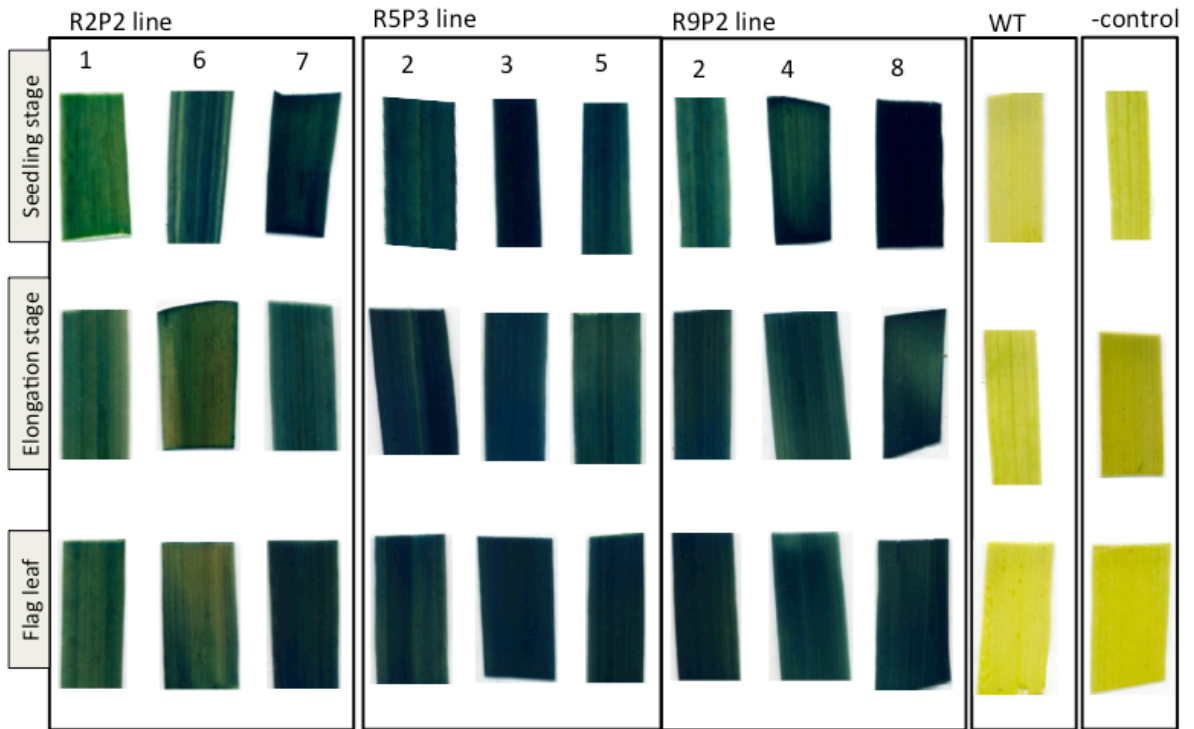
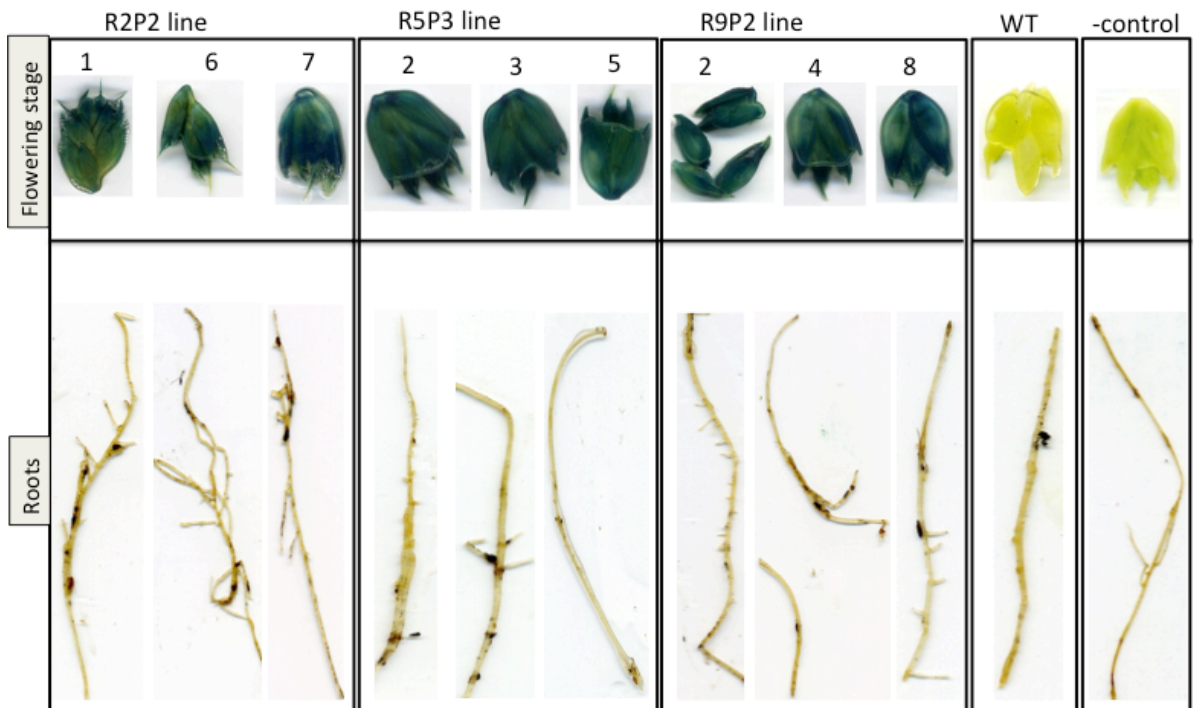
**Figure 5.20: Microscopy observation of GUS expression localisation in wheat T0 leaves driven by Brachypodium FBPA.**

The stable transformations were done at Rothamsted Research and after the production of T0 plants, young leaves tissues were taken for GUS staining assay, and were subjected to microscopy observations in different T0 plants at Rothamsted Research by Caroline Sparks.

### **5.2.5.2 GUS expression into T1 tissues at different Zadoks scale growth stages**

To confirm the stability and usability of *Brachypodium* SBPase and FBPAldolase promoters to drive good expression of GUS within the next progenies, the GUS expressions were analysed in T1 progenies from different tissues, including leaves at three different growth stages (seedling, elongation and flag leaves), flowers and roots tissues.

As a results of GUS staining, some strong positive blue staining in large patches was observed in the leaves at all three growth stages (Figure 5.21a) and flowers of wheat plants' T1, driven by the *Brachypodium* SBPase promoter (interestingly, this expression was still restricted to green tissues, as no GUS expression appeared in the roots) (Figure 5.21b). Similarly, brilliant and strong GUS expression driven by the *Brachypodium* FBPAldolase promoter was noticed in the wheat T1 leaves (Figure 5.22a) and flowers; however, fascinatingly, no expression was seen in the roots (Figure 5.22b).

**a****b**

**Figure 5.21: Histochemical analysis of GUS activity in stable transformed wheat T1 plants with Brachypodium SBPase promoter.**

Leaves were taken for GUS staining analysis at three different growth stages (seedlings, elongation and flag leaves) together with samples from different tissues: flowers and roots.

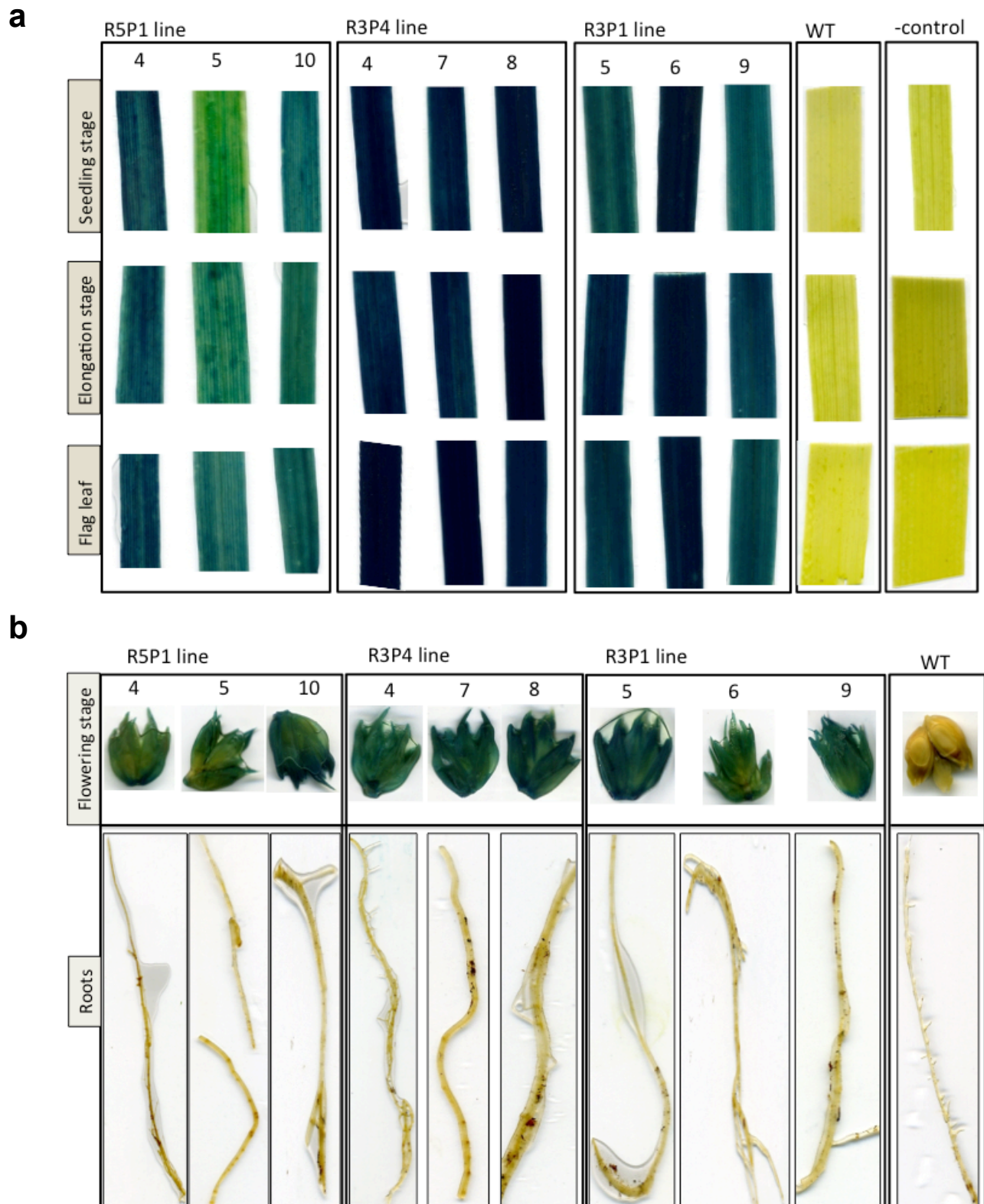


**Figure 5.22: Histochemical analysis of GUS activity in stable transformed wheat T1 plants with Brachypodium FBPA promoter.**

Leaves were taken for GUS staining analysis at three different growth stages (seedlings, elongation and flag leaves) together with samples from different tissues: flowers and roots.

### 5.3 Discussion

Although many efforts have been made to isolate and characterise efficient constitutive mesophyll-specific promoters from dicot plants and other sources, there is still a shortage of available strong and capable mesophyll promoters for driving strong expression levels in wheat (*Triticum aestivum*) under different growth and developmental stages and conditions. Therefore, it is important to continue the search and design new promoters and transcriptional regulatory elements with the desired features and characteristics to be used for driving the strong desired expression level in wheat mesophyll (Tao *et al*, 2002; Abdul *et al*, 2010; Park *et al*, 2010).

The SBPase and FBPaldolase enzymes of the Calvin-Benson cycle are both identified as significant targets displaying high flux control over leaf photosynthesis. Several studies have shown that they are both located in the plant leaf and their proteins are highly expressed into the chloroplast cells (Raines *et al*, 1999; Haake *et al*, 1999; Lefebvre *et al*, 2005). Therefore, chances are that its promoter will drive a strong expression in the mesophyll cells of wheat. Hence, this chapter identified and analysed new native promoters of these two Calvin–Benson cycle enzymes from *Brachpodium* plants, as a module grass plant, to control expression of transgenes into mesophyll tissues of the wheat leaf using molecular techniques. It has been found from bioinformatics analysis that both promoters share the similar motifs Box G and I box and TATA box (Table 5.1; 5.2). The two *cis* elements motifs (G and I) has been found to play essential function in light regulation of gene expression as well as inducing the expression of gene to which that similar to the expression that found driven by CaMV35S and *RbcS* promoters (Giuliano *et al.*, 1988; Doland and Cashmore, 1990; Song *et al.*, 2000; Mukherjee *et al* 2015).

To test the functionality of these two *Brachypodium* SBPase and FBPA promoters in dicot plants, two constructs were built for each promoter, one with GUS and the other with eYFP fusion genes, and transformed into agrobacterium cells. Then, transient assays were performed using *N. benthamiana* leaves. As a result, almost all leaf pieces had good patches of discrete, reasonably intense spots and good GUS expressions that were driven by the promoter of either the *Brachypodium* SBPase or FBPAldolase promoters, when compared to the WT leaf. Next, the subcellular localisation of the eYFP expressions driven by either the SBPase or FBPAldolase promoter were investigated in eYFP-infiltrated leaves using the confocal microscopy. Consequently, the eYFP expression signal driven by the *Brachypodium* SBPase promoter was observed clearly in the cytosol of the mesophyll cells of the *N. benthamiana* leaves, when compared with the WT leaf. Similarly, a good eYFP expression signal driven by the *Brachypodium* FBPAldolase promoter evidently was seen, yielding apparently functional promoters. Subsequently, it was demonstrated that the *Brachypodium* SBPase and FBPAldolase promoter fusions were able to drive expression of GUS and eYFP in tobacco (*N. benthamiana*, dicots). Therefore, it is worthwhile to test these promoters in wheat (monocots) in order to analyse their activities to drive expression in the wheat mesophyll cells. Consequently, the SBPase::GUS and FBPAldolase::GUS were constructed and sent to Rothamsted Research for bombardment transformations into the wheat leaf. As an introduction before stable transformations, transient transformation was performed as a quick approach to test these promoters to drive GUS expression into the wheat leaf. As a result, both promoters have driven good GUS expression in the wheat leaves, and many excellent discrete spots in large patches were observed with reasonable intensity. Then, they proceeded to stable transformation for further analyses in different growth stages.

A variety of characterised promoters have been made widely available to date. For example, the CaMV 35S constitutive promoter is commonly used to drive high expression levels of transgenic dicotyledonous plants. However, low activities also have been observed in monocotyledonous crops. It has been found that different promoters drive high levels of constitutive gene expression in transgenic monocots, such as *Ubi1* from maize (*Zea mays*) and some rice-derived promoters, including *Act1*, *OsTubA1*, *OsCc1*, *RUBQ1* and *RbcS* promoters. The most common promoters used in monocot crops are *Ubi1* and rice *Act1* promoters because they can efficiently drive strong, constitutive expression in almost all plant tissues, whereas their activity is shown only in young tissues and tends to decrease during the growth and development of organs (Jang *et al*, 2002; Park *et al*, 2010). On the other hand, in this study, GUS expressions were examined in different wheat tissues, including leaves through different growth stages, roots and flowers. Subsequently, excellent and clear GUS expressions driven by either SBPase or FBPaldolase promoters were observed in leaves at two different growth stages (seedling and flag leaves) and also in flowers in three different independent T0 lines, when compared to the WT. Interestingly, the GUS expressions were restricted mostly to the green tissues in leaves, but not in roots. The results of microscopy confirmed and showed GUS expressions driven by both promoters in mesophyll cells and guard cells, but not the midrib or veins, when compared to the WT, which is what was expected, since the SBPase and FBPaldolase are both located and highly expressed in the leaf's chloroplast; all of this is similar to the results shown in Mukherjee *et al* (2015), who isolated the rubisco small subunit gene promoter from wheat and examined and found it to drive good GUS expression in the green tissues of the tobacco plant, but not in roots. However, its activity to drive

GUS expression was not analysed throughout different plant growth stages (Mukherjee *et al*, 2015).

Therefore, this study shows the GUS expressions driven by *Brachypodium* SBPase and FBPAldolase gene promoters at different growth stages and from different tissues. To confirm the stability and usability of *Brachypodium* SBPase and FBPAldolase promoters to drive good expression of GUS within the next progenies, the GUS expressions were analysed in T1 progenies from different tissues, including leaves at different three growth stages (seedling, elongation and flag leaves), flowers and roots tissues. Consequently, the results of the GUS staining showed strong positive blue staining in large patches in leaves at all three growth stages and flowers of wheat plants' T1, driven by either *Brachypodium* SBPase or FBPAldolase promoters, and interestingly, this expression was still restricted to green tissues, as no GUS expression appeared in the roots. Therefore, these two *Brachypodium* promoters of the Calvin–Benson cycle SBPase and FBPAldolase enzymes were confirmed as robust, and new elements of choice in plant molecular biology that were found to drive and direct the expression of any targeted gene of interest, particularly, in mesophyll cells of wheat leaf (green tissues) through different developmental growth stages.

Summary:

- The promoters of *Brachypodium* SBPase and FBPA were tested in *N. benthamiana* leaves and have shown good GUS and eYFP expressions driven by these promoters.
- Both promoters were then tested in wheat leaf throughout different progenies and different growth stages.

- The results confirm that both promoters were able to drive good GUS expression in wheat leaf and at different developmental growth stages.
- Interestingly, the GUS expression was restricted to the leaf tissue but not in the roots.

## **Chapter 6: General Discussion**

This project aimed to take a molecular approach in combination with photosynthetic studies to screen and analyse transgenic wheat plants that were manipulated in an attempt to improve leaf photosynthesis, as well as NUE in wheat. Previously, several studies on tobacco and rice plants have shown that increased levels of the regeneration phase SBPase enzyme of the Calvin–Benson cycle could potentially stimulate and enhance the rate of photosynthesis and improve plant growth and total biomass (Lefebvre *et al.*, 2005; Feng *et al.*, 2007a; Feng *et al.*, 2009; Rosenthal *et al.*, 2011; Parry *et al.*, 2011). For this reason, the SBPase enzyme has been targeted for genetic manipulations in wheat, and the produced plants were subject to analysis in this study. Moreover, as the Rubisco enzyme was found to represent about 50% of the total leaf N, showing an amount exceeding that needed to maintain photosynthesis under some environmental conditions (Mae *et al.*, 1993). Alternatively, SBPase is only shown to represent less than 1% of the total leaf N (Zhu *et al.*, 2007). Therefore, this study also aimed to address the question of whether a small reduction in the amount of the Rubisco enzyme would affect wheat photosynthesis, growth and grain yield to improve NUE without any negative effects on plant yield. Furthermore, as another aspect that needs to be addressed to improve photosynthesis, there is still a shortage of promoters available to drive efficient transgene expressions in wheat mesophyll (*Triticum aestivum*) cells under different growth and developmental stages and conditions (Tao *et al.*, 2002; Abdul *et al.*, 2010; Park *et al.*, 2010). Therefore, searching for and designing new promoters with the desired features and characteristics to be used as new tools in wheat molecular studies to drive strong desirable expression levels of any transgenes in wheat mesophyll cells is a significant target to improve wheat leaf photosynthesis. Subsequently, some molecular techniques were employed

in this project to analyse new *Brachypodium* promoters to drive the GUS gene in wheat leaves in different growth stages.

### **6.1 Increased SBPase activity improves photosynthesis and grain yield in wheat grown in greenhouse conditions**

The results of this study revealed that increased SBPase activity led clearly to an improved photosynthetic rate, in particular, under higher concentrations of CO<sub>2</sub>, as well as a significant increase in total biomass, results that are similar to those previously shown in some studies on tobacco (Lefebvre *et al.*, 2005; Rosenthal *et al.*, 2011). In contrast, rice plants with increased SBPase activity did not lead to an increase in total biomass production compared to the WT plants under both ambient and controlled conditions (Feng *et al.*, 2007a; Feng *et al.*, 2009), which indicates a clear difference between the crop species (wheat and rice). However, an increased SBPase activity level has also led to enhancements in the tolerance of rice plants against salt conditions during growth (Feng *et al.*, 2007a), as well as heat stress (Feng *et al.*, 2007b); therefore, this needs to be further investigated in wheat plants.

Indeed, these results supported the hypothesis that increasing the level of SBPase activity in wheat could improve photosynthetic performance and total biomass production (Parry *et al.*, 2011). Moreover, resource use efficiency could also be improved as a result of increased SBPase activity, as shown in Rosenthal *et al.* (2011). Modelling studies suggest that an underinvestment of the enzymes SBPase and FBPAldolase is currently observed. Nevertheless, the Rubisco carboxylation reaction is increased with a continuous rise in atmospheric CO<sub>2</sub>, and this would require an increase in SBPase activity. Additionally, data obtained from transgenic and dynamic

modelling studies revealed an over-investment in the Rubisco enzyme, which led to the hypothesis that a reduction in the Rubisco enzyme activity in wheat is an essential target for molecular studies to improve NUE (Ainsworth & Long, 2005; Zhu *et al.*, 2007). Subsequently, transgenic wheat plants with a decreased level of Rubisco were produced, screened and analysed to identify to what extent Rubisco could be reduced without affecting photosynthesis, including how this reduction would affect the grain quality under natural sunlight in the UK spring/summer seasons.

## **6.2 Effect of decreased Rubisco by *RbcS* RNAi on wheat photosynthesis, growth and grain quality**

The increase in cereal production has significantly increasing in the use of N fertilization to achieve the maximum high yield together with the required quality and content of protein needed for breadmaking. Therefore, this could significantly impact on environment and threatening organisms and marine ecosystems. Additionally, there could be some toxic gaseous and ammonia emissions of oxides N causing atmospheric pollutions (Ramos, 1996). Therefore, several studies have been carried out to improve NUE in crops to make the food available for increased populations together with saving N as previous studies on antisense Rubisco plants grown in high CO<sub>2</sub> suggested that a reduction in Rubisco protein by about 15-20% would reduce the demand of nitrogen by as much as about 10%, without have an adverse effect on photosynthesis, growth or grain yield (Parry *et al*, 2013). Previous studies also showed that transgenic rice plants were produced with a reduced level of the *RbcS* subunit using RNAi technology. As a result, an improvement in photosynthetic NUE was observed in rice (Makino *et al.*, 1997) under elevated CO<sub>2</sub>; yet, this did not lead to an improvement in the NUE of the

whole plant (Makino *et al.*, 2000). However, this technology has not yet been applied to the wheat crop.

Therefore, wheat plants with decreased Rubisco were obtained. Results revealed that a wide range of Rubisco protein reductions were observed on the five T2 transgenic lines compared to the WT line. The results clearly showed the largest decrease in Rubisco activity (40% to 67%) and clear reductions in leaf CO<sub>2</sub> assimilation rates under saturated CO<sub>2</sub> measurements, as well as significant decreases in total biomass and ear number and weight, which can mainly be explained by significant reductions in total seed weight and number compared to WT plants. This reduction in seed production was not only due to the small number of ears produced per plant within the lines but also due to the small number of seeds produced per ear. However, the weight per seed was higher in plants with lower levels of Rubisco activity, where this could be seen as a consequence of a significant increase in the N content level of the seeds.

Wheat plants, as well as rice, have a greater Rubisco content than that found in tobacco plants. It was found that in wheat, approximately 30% of the N content was present in Rubisco (Makino *et al.*, 1992; Mae *et al.*, 1993) compared to in tobacco plants, where about 18% was present in Rubisco (Evans *et al.*, 1994). Therefore, a reduction in Rubisco activity could have an effect on the allocation of N to other photosynthetic components. Consequently, in this study, the N allocations in seeds and leaves were clearly observed in the *RbcS* RNAi plants with the largest reductions in Rubisco activity, as it is higher than in the WT plants. Additionally, it was clear that the growth of plants with a large reduction in Rubisco activity was also affected compared to the WT plants, as they exhibited slow growth with fewer leaves, stems and ears, and they were delayed in reaching the flowering stage. All of these characteristics are

similar to the results of a previous study on tobacco (Masle *et al.*, 1993). Therefore, this result means that a large reduction of about 40% to 67% in Rubisco activity negatively affects photosynthesis performance; growth rate and grain yield quality in UK ambient conditions that are as close to natural as possible.

Conversely, decreased Rubisco activity between 10% and 25% does not affect the photosynthetic rate, growth, and biomass production or grain quality. The N allocations in seeds and leaves were also clearly similar in the transgenic plants, with slight reductions in Rubisco activity (approximately 10% to 25%) relative to the WT. A previous study on rice by Makino *et al.* (1997 and 2000) showed that a 35% reduction in Rubisco in rice led to an improvement in the photosynthetic NUE under saturated CO<sub>2</sub> conditions. Therefore, this could be applicable to wheat, as a slight reduction in Rubisco activity (up to 25%) in wheat, as shown in this study, did not significantly affect photosynthetic capacity, growth rate or grain quality. Interestingly, this supported the hypothesis that small reductions in the Rubisco amount and activity could increase NUE without compromising photosynthetic performance (Parry *et al.*, 2013). Under elevated CO<sub>2</sub>, increases in leaf photosynthesis through an increase in the level of SBPase enzyme activity would potentially require a reallocation of several enzymes of the Calvin-Benson cycle, which could strongly include a slight reduction in the Rubisco amount and activity without any negative effect on plant photosynthesis or yield to improve NUE in the UK climate with a moderate spring temperature and light conditions. On the other hand, transgenic tobacco antisense plants with reduced level of Rubisco protein have clearly shown that Rubisco has limited the C<sub>3</sub> CO<sub>2</sub> fixation under the conditions of high light and temperature, and the nitrate pool was increased as a result of that (Stitt and Schulze, 1994). Thus, this could be applicable to wheat plants with reduced Rubisco activity. The RNAi lines that showed slightly less Rubisco

should be crossed with the transgenic wheat lines with an increased SBPase level.

### **6.3 Molecular tools to improve photosynthetic efficiency in wheat leaf**

As a different approach towards improving leaf photosynthesis in wheat, identifying new promoters to drive transgene expressions specialised to wheat leaf was also addressed in this project. The two enzymes of the Calvin-Benson cycle, SBPase and FBPAldolase, are both identified as significant targets displaying high flux control over leaf photosynthesis. Several studies have shown that they are both located in the plant leaf and their proteins are highly expressed in chloroplast cells (Raines *et al.*, 1999; Haake *et al.*, 1999; Lefebvre *et al.*, 2005). Therefore, chances are that their promoters will drive a strong expression in the mesophyll cells of wheat. Therefore, *Brachypodium* SBPase and FBPA promoters were isolated and constructed upstream of the GUS gene to be tested in both *N. benthamiana* and wheat.

To explore the functionality of *Brachypodium* SBPase and FBPA promoters in *N. benthamiana* plants, two constructs were built for each promoter, one with GUS and the other with eYFP fusion genes. Results from transient assays showed that almost all leaf pieces had good patches of discrete, reasonably intense spots, as well as good GUS and eYFP expressions that were driven by the promoter of either the *Brachypodium* SBPase or FBPAldolase promoters in *N. benthamiana* plants when compared to the WT leaf, yielding apparently functional promoters. Subsequently, it was demonstrated that the *Brachypodium* SBPase and FBPAldolase promoter fusions were able to drive the expressions of GUS and eYFP in tobacco (*N. benthamiana*, dicots). Therefore, it was worthwhile to test these promoters in wheat leaf to analyse their activities to drive expression in the wheat mesophyll cells. Consequently,

SBPase::GUS and FBPaldolase::GUS were constructed and sent to Rothamsted Research for bombardment transformations into wheat leaves. Results revealed that both promoters have driven good GUS expressions in wheat leaves at different plant growth stages, interestingly restricted to leaves and not in roots.

As the most common promoters used in monocot crops are *Ubi1* and rice *Act1* promoters, because they can efficiently drive strong, constitutive expressions in almost all plant tissues, their activity is shown only in young tissues and tends to decrease during the growth and development of organs (Jang *et al.*, 2002; Park *et al.*, 2010). On the other hand, in this study, GUS expressions were examined in different wheat tissues, including leaves, through different growth stages, roots and flowers. Subsequently, excellent and clear GUS expressions, driven by either SBPase or FBPaldolase promoters, were observed in leaves at three different growth stages (seedling, elongation and flag leaves), as well as in flowers in three different independent T1 lines when compared to the WT. Interestingly, the GUS expressions were restricted mostly to the green tissues in leaves, but not in roots. The results of microscopy confirmed and showed GUS expressions are driven by both promoters in mesophyll cells and guard cells, but not by the midrib or veins, when compared to the WT. This was expected, as SBPase and FBPaldolase are both located and highly expressed in leaf chloroplast. All of this is similar to the results shown in Mukherjee *et al.* (2015), who isolated the Rubisco small subunit gene promoter from wheat, as well as examined and found it to drive good GUS expression in the green tissues of the tobacco plant, but not in the roots. However, its activity to drive GUS expression was not analysed throughout different plant growth stages (Mukherjee *et al.*, 2015). Therefore, these two *Brachypodium* promoters of the Calvin–Benson cycle enzymes

SBPase and FBPaldolase were confirmed as robust and new elements of choice in plant molecular biology were found to drive and direct the expression of any targeted gene of interest, particularly in mesophyll cells of wheat leaves (green tissues) through different developmental growth stages.

#### **6.4 Conclusion and future works**

This project attempted to elucidate and analyse several patches of transgenic wheat plants with genetically manipulated enzymes to improve photosynthesis, as well as NUE and grain quality. Experimental works have shown that increasing the level of SBPase activity in wheat has improved photosynthetic performance and total biomass production in one aspect of this study. In the other aspect, a slight reduction in Rubisco activity (up to 25%) in wheat, shown in this study, did not significantly affect photosynthetic capacity, growth rate or grain quality. Thus, this establishes the next steps towards crossing these transgenic plants having stable and reduced Rubisco levels with wheat plants having stable and higher SBPase levels to increase yield, together with improving NUE in wheat crops. In addition, as the study on Rubisco RNAi plants was conducted in the UK climate with a moderate spring temperature, it would be of interest if the same lines could be grown in high light or high temperature conditions. Additionally, transgenic wheat plants with a reduced level of Rubisco must be further investigated under several regimes of the N application and the effect of that on photosynthesis and NUE should be studied. Moreover, the SBPase over-expression in wheat must be further investigated in other conditions, such as against salt condition and heat stress. Furthermore, both Brachypodium promoters, SBPase and FBPA, could be used as new tools in plant molecular biology to improve photosynthesis to direct the expression of any targeted gene of interest, particularly in the mesophyll cells

of wheat. Additionally, the functionality of these promoters must be explored further under different conditions.

## References

- Abdul, R., Ma, Z. and Wang, H. (2010) Genetic transformation of wheat (*Triticum aestivum* L): A Review. *Triticeae Genomics and Genetics*, **1**, 1-7.
- Abrol, Y., Uprety, D., Ahuja, V. and Naik, M. (1971) Soil fertilizer levels and protein quality of wheat grains. *Crop and Pasture Science*, **22**, 195-200.
- Adam, Z., Adamska, I., Nakabayashi, K., Ostersetzer, O., Haussuhl, K., Manuell, A., Zheng, B., Vallon, O., Rodermeil, S. R. and Shinozaki, K. (2001) Chloroplast and mitochondrial proteases in *Arabidopsis*. A proposed nomenclature. *Plant Physiology*, **125**, 1912-1918.
- Ainsworth, E. A. and Long, S. P. (2005) What have we learned from 15 years of free-air CO<sub>2</sub> enrichment (FACE)? A meta-analytic review of the responses of photosynthesis, canopy properties and plant production to rising CO<sub>2</sub>. *New Phytologist*, **165**, 351-372.
- Bassham, J. A. (2005) Mapping the carbon reduction cycle: a personal retrospective. *Discoveries in Photosynthesis*. Springer.
- Bassham, J. A., Benson, A. A. and Calvin, M. (1950) The path of carbon in photosynthesis VIII. The role of malic acid.
- Bradford, M. M. (1976) A rapid and sensitive method for the quantitation of microgram quantities of protein utilizing the principle of protein-dye binding. *Analytical biochemistry*, **72**, 248-254.
- Buchanan, B. B. (1991a) Regulation of CO<sub>2</sub> assimilation in oxygenic photosynthesis: the ferredoxin/thioredoxin system: perspective on its discovery, present status, and future development. *Archives of biochemistry and biophysics*, **288**, 1-9.
- Buchanan, B. B. (1991b) Regulation of CO<sub>2</sub> assimilation in oxygenic photosynthesis: The ferredoxin/thioredoxin system: Perspective on its discovery, present status, and future development. *Archives of biochemistry and biophysics*, **288**, 1-9.
- CARMO-SILVA, E., Scales, J. C., MADGWICK, P. J. and Parry, M. A. (2014) Optimizing Rubisco and its regulation for greater resource use efficiency. *Plant, cell & environment*.
- Chen, Q.-J., Zhou, H.-M., Chen, J. and Wang, X.-C. (2006) A Gateway-based platform for multigene plant transformation. *Plant molecular biology*, **62**, 927-936.

- Critchley, C. S. (2001) *A physiological explanation for the canopy nitrogen requirement of winter wheat*. dissertation.: University of Nottingham.
- Dale, P. J., Clarke, B. and Fontes, E. M. (2002) Potential for the environmental impact of transgenic crops. *Nature biotechnology*, **20**, 567-574.
- Donald, R. and Cashmore, A. R. (1990) Mutation of either G box or I box sequences profoundly affects expression from the Arabidopsis rbcS-1A promoter. *The EMBO journal*, **9**, 1717.
- Ellis, R. J. (1979) The most abundant protein in the world. *Trends in Biochemical Sciences*, **4**, 241-244.
- Evans, J. R. (1989) Photosynthesis and nitrogen relationships in leaves of C3 plants. *Oecologia*, **78**, 9-19.
- Evans, J. R., Caemmerer, S., Setchell, B. A. and Hudson, G. S. (1994) The relationship between CO<sub>2</sub> transfer conductance and leaf anatomy in transgenic tobacco with a reduced content of Rubisco. *Functional Plant Biology*, **21**, 475-495.
- Faske, M., Holtgreve, S., Ocheretina, O., Meister, M., Backhausen, J. E. and Scheibe, R. (1995) Redox equilibria between the regulatory thiols of light/dark-modulated chloroplast enzymes and dithiothreitol: fine-tuning by metabolites. *Biochimica et Biophysica Acta (BBA)-Protein Structure and Molecular Enzymology*, **1247**, 135-142.
- FAO. 2012. The State of Food and Agriculture. Investing in agriculture for a better future. FAO (Food and Agriculture Organization of the United Nations), Rome, Italy.
- Feng, L., Han, Y., Liu, G., An, B., Yang, J., Yang, G., Li, Y. and Zhu, Y. (2007a) Overexpression of sedoheptulose-1, 7-bisphosphatase enhances photosynthesis and growth under salt stress in transgenic rice plants. *Functional Plant Biology*, **34**, 822-834.
- Feng, L., Li, H., Jiao, J., Li, D., Zhou, L., Wan, J. and Li, Y. (2009) Reduction in SBPase activity by antisense RNA in transgenic rice plants: effect on photosynthesis, growth, and biomass allocation at different nitrogen levels. *Journal of Plant Biology*, **52**, 382-394.
- Feng, L., Wang, K., Li, Y., Tan, Y., Kong, J., Li, H., Li, Y. and Zhu, Y. (2007b) Overexpression of SBPase enhances photosynthesis against high temperature stress in transgenic rice plants. *Plant cell reports*, **26**, 1635-1646.

- Fischer, R. and Edmeades, G. O. (2010) Breeding and cereal yield progress. *Crop Science*, **50**, S-85-S-98.
- Furbank, R. T., Chitty, J. A., von Caemmerer, S. and Jenkins, C. L. (1996) Antisense RNA inhibition of RbcS gene expression reduces Rubisco level and photosynthesis in the C<sub>4</sub> plant *Flaveria bidentis*. *Plant Physiology*, **111**, 725-734.
- Gaju, O., Allard, V., Martre, P., Le Gouis, J., Moreau, D., Bogard, M., Hubbart, S. and Foulkes, M. J. (2014) Nitrogen partitioning and remobilization in relation to leaf senescence, grain yield and grain nitrogen concentration in wheat cultivars. *Field Crops Research*, **155**, 213-223.
- Geiger, D. R. and Servaites, J. C. (1994) Diurnal regulation of photosynthetic carbon metabolism in C<sub>3</sub> plants. *Annual review of plant biology*, **45**, 235-256.
- Gilmartin, P. M., Sarokin, L., Memelink, J. and Chua, N.-H. (1990) Molecular light switches for plant genes. *The Plant Cell*, **2**, 369.
- Giuliano, G., Pichersky, E., Malik, V., Timko, M., Scolnik, P. and Cashmore, A. (1988) An evolutionarily conserved protein binding sequence upstream of a plant light-regulated gene. *Proceedings of the National Academy of Sciences*, **85**, 7089-7093.
- Graciet, E., Gans, P., Wedel, N., Lebreton, S., Camadro, J.-M. and Gontero, B. (2003) The small protein CP12: a protein linker for supramolecular complex assembly. *Biochemistry*, **42**, 8163-8170.
- Ha, S.-B. and An, G. (1988) Identification of upstream regulatory elements involved in the developmental expression of the *Arabidopsis thaliana* *cab1* gene. *Proceedings of the National Academy of Sciences*, **85**, 8017-8021.
- Haake, V., Geiger, M., Walch-Liu, P., Of Engels, C., Zrenner, R. and Stitt, M. (1999) Changes in aldolase activity in wild-type potato plants are important for acclimation to growth irradiance and carbon dioxide concentration, because plastid aldolase exerts control over the ambient rate of photosynthesis across a range of growth conditions. *The Plant Journal*, **17**, 479-489.
- Harrison, E. P., Olcer, H., Lloyd, J. C., Long, S. P. and Raines, C. A. (2001) Small decreases in SBPase cause a linear decline in the apparent RuBP regeneration rate, but do not affect Rubisco carboxylation capacity. *Journal of experimental botany*, **52**, 1779-1784.
- Harrison, E. P., Willingham, N. M., Lloyd, J. C. and Raines, C. A. (1997) Reduced sedoheptulose-1, 7-bisphosphatase levels in transgenic tobacco lead to

- decreased photosynthetic capacity and altered carbohydrate accumulation. *Planta*, **204**, 27-36.
- Hawkesford, M. J. (2014) Reducing the reliance on nitrogen fertilizer for wheat production. *Journal of cereal science*, **59**, 276-283.
- Heldt, H. W., Werdan, K., Milovancev, M. and Geller, G. (1973) Alkalization of the chloroplast stroma caused by light-dependent proton flux into the thylakoid space. *Biochimica et Biophysica Acta (BBA)-Bioenergetics*, **314**, 224-241.
- Hernandez-Garcia, C., Bouchard, R., Rushton, P., Jones, M., Chen, X., Timko, M. and Finer, J. (2010) High level transgenic expression of soybean (*Glycine max*) GmERF and Gmubi gene promoters isolated by a novel promoter analysis pipeline. *BMC plant biology*, **10**, 237.
- Hernandez-Garcia, C. M. and Finer, J. J. (2014) Identification and validation of promoters and cis-acting regulatory elements. *Plant Science*, **217**, 109-119.
- Heslop-Harrison, J. and Schwarzacher, T. (2011) Organisation of the plant genome in chromosomes. *The Plant Journal*, **66**, 18-33.
- Hirel, B., Le Gouis, J., Ney, B. and Gallais, A. (2007) The challenge of improving nitrogen use efficiency in crop plants: towards a more central role for genetic variability and quantitative genetics within integrated approaches. *Journal of experimental botany*, **58**, 2369-2387.
- Horton, P. (2000) Prospects for crop improvement through the genetic manipulation of photosynthesis: morphological and biochemical aspects of light capture. *Journal of experimental botany*, **51**, 475-485.
- Hudson, G. S., Evans, J. R., von Caemmerer, S., Arvidsson, Y. B. and Andrews, T. J. (1992) Reduction of ribulose-1, 5-bisphosphate carboxylase/oxygenase content by antisense RNA reduces photosynthesis in transgenic tobacco plants. *Plant Physiology*, **98**, 294-302.
- Hughes, J. D., Estep, P. W., Tavazoie, S. and Church, G. M. (2000) Computational identification of cis-regulatory elements associated with groups of functionally related genes in *Saccharomyces cerevisiae*. *Journal of molecular biology*, **296**, 1205-1214.
- Hughes, M. A. (1996) *Plant molecular genetics*. Addison Wesley Longman Ltd.

- Jacquot, J.-P., Gelhaye, E., Rouhier, N., Corbier, C., Didierjean, C. and Aubry, A. (2002) Thioredoxins and related proteins in photosynthetic organisms: molecular basis for thiol dependent regulation. *Biochemical pharmacology*, **64**, 1065.
- Jang, I.-C., Choi, W.-B., Lee, K.-H., Song, S. I., Nahm, B. H. and Kim, J.-K. (2002) High-Level and Ubiquitous Expression of the Rice Cytochrome c Gene OsCc1 and Its Promoter Activity in Transgenic Plants Provides a Useful Promoter for Transgenesis of Monocots. *Plant Physiology*, **129**, 1473-1481.
- Jefferson, R. A., Kavanagh, T. A. and Bevan, M. W. (1987) GUS fusions: beta-glucuronidase as a sensitive and versatile gene fusion marker in higher plants. *The EMBO journal*, **6**, 3901.
- Jones, R., Ougham, H., Thomas, H. and Waaland, S. (2012) *The molecular life of plants*. John Wiley & Sons.
- Kebeish, R., Niessen, M., Thiruveedhi, K., Bari, R., Hirsch, H.-J., Rosenkranz, R., Stähler, N., Schönfeld, B., Kreuzaler, F. and Peterhänsel, C. (2007) Chloroplastic photorespiratory bypass increases photosynthesis and biomass production in *Arabidopsis thaliana*. *Nature biotechnology*, **25**, 593-599.
- Kichey, T., Hirel, B., Heumez, E., Dubois, F. and Le Gouis, J. (2007) In winter wheat (*Triticum aestivum* L.), post-anthesis nitrogen uptake and remobilisation to the grain correlates with agronomic traits and nitrogen physiological markers. *Field Crops Research*, **102**, 22-32.
- Kramer, D. M. and Evans, J. R. (2011) The importance of energy balance in improving photosynthetic productivity. *Plant Physiology*, **155**, 70-78.
- Larkin, M., Blackshields, G., Brown, N., Chenna, R., McGettigan, P. A., McWilliam, H., Valentin, F., Wallace, I. M., Wilm, A. and Lopez, R. (2007) Clustal W and Clustal X version 2.0. *Bioinformatics*, **23**, 2947-2948.
- Lawlor, D. W. (2002) Carbon and nitrogen assimilation in relation to yield: mechanisms are the key to understanding production systems. *Journal of experimental botany*, **53**, 773-787.
- Lefebvre, S., Lawson, T., Fryer, M., Zakhleniuk, O. V., Lloyd, J. C. and Raines, C. A. (2005) Increased sedoheptulose-1, 7-bisphosphatase activity in transgenic tobacco plants stimulates photosynthesis and growth from an early stage in development. *Plant Physiology*, **138**, 451-460.
- Lichtenthaler, H. K. (1999) The 1-deoxy-D-xylulose-5-phosphate pathway of isoprenoid biosynthesis in plants. *Annual review of plant biology*, **50**, 47-65.

- Mae, T., Thomas, H., Gay, A. P., Makino, A. and Hidema, J. (1993) Leaf development in *Lolium temulentum*: photosynthesis and photosynthetic proteins in leaves senescing under different irradiances. *Plant and Cell Physiology*, **34**, 391-399.
- Makino, A. and Osmond, B. (1991) Effects of nitrogen nutrition on nitrogen partitioning between chloroplasts and mitochondria in pea and wheat. *Plant Physiology*, **96**, 355-362.
- Makino, A., Shimada, T., Takumi, S., Kaneko, K., Matsuoka, M., Shimamoto, K., Nakano, H., Miyao-Tokutomi, M., Mae, T. and Yamamoto, N. (1997) Does decrease in ribulose-1, 5-bisphosphate carboxylase by antisense RbcS lead to a higher N-use efficiency of photosynthesis under conditions of saturating CO<sub>2</sub> and light in rice plants? *Plant Physiology*, **114**, 483-491.
- Masle, J., Hudson, G. S. and Badger, M. R. (1993) Effects of ambient CO<sub>2</sub> concentration on growth and nitrogen use in tobacco (*Nicotiana tabacum*) plants transformed with an antisense gene to the small subunit of ribulose-1, 5-bisphosphate carboxylase/oxygenase. *Plant Physiology*, **103**, 1075-1088.
- Maurino, V. G. and Peterhansel, C. (2010) Photorespiration: current status and approaches for metabolic engineering. *Current opinion in plant biology*, **13**, 248-255.
- Meyer, Y., Verdoucq, L. and Vignols, F. (1999) Plant thioredoxins and glutaredoxins: identity and putative roles. *Trends in plant science*, **4**, 388-394.
- Michels, A. K., Wedel, N. and Kroth, P. G. (2005) Diatom plastids possess a phosphoribulokinase with an altered regulation and no oxidative pentose phosphate pathway. *Plant Physiology*, **137**, 911-920.
- Millard, P. (1988) The accumulation and storage of nitrogen by herbaceous plants. *Plant, cell & environment*, **11**, 1-8.
- Mitchell, R., Theobald, J. C., Parry, M. and Lawlor, D. (2000) Is there scope for improving balance between RuBP-regeneration and carboxylation capacities in wheat at elevated CO<sub>2</sub>? *Journal of experimental botany*, **51**, 391-397.
- Mitchell, R. A., Joyce, P. A., Rong, H., Evans, V. J., Madgwick, P. J. and Parry, M. A. (2004) Loss of decreased-rubisco phenotype between generations of wheat transformed with antisense and sense rbcS. *Annals of applied biology*, **145**, 209-216.

- Moll, R., Kamprath, E. and Jackson, W. (1982) Analysis and interpretation of factors which contribute to efficiency of nitrogen utilization. *Agronomy Journal*, **74**, 562-564.
- Mukherjee, S., Stasolla, C., Brûlé-Babel, A. and Ayele, B. T. (2015) Isolation and characterization of rubisco small subunit gene promoter from common wheat (*Triticum aestivum* L.). *Plant signaling & behavior*, **10**, e989033.
- Murchie, E., Pinto, M. and Horton, P. (2009) Agriculture and the new challenges for photosynthesis research. *New Phytologist*, **181**, 532-552.
- Nakagawa, T., Kurose, T., Hino, T., Tanaka, K., Kawamukai, M., Niwa, Y., Toyooka, K., Matsuoka, K., Jinbo, T. and Kimura, T. (2007) Development of series of gateway binary vectors, pGWBs, for realizing efficient construction of fusion genes for plant transformation. *Journal of bioscience and bioengineering*, **104**, 34-41.
- Nishizawa, A. and Buchanan, B. (1981) Enzyme regulation in C4 photosynthesis. Purification and properties of thioredoxin-linked fructose biphosphatase and sedoheptulose biphosphatase from corn leaves. *Journal of Biological Chemistry*, **256**, 6119-6126.
- Ölçer, H., Lloyd, J. C. and Raines, C. A. (2001) Photosynthetic capacity is differentially affected by reductions in sedoheptulose-1, 7-bisphosphatase activity during leaf development in transgenic tobacco plants. *Plant Physiology*, **125**, 982-989.
- Palta, J. and Fillery, I. (1995) N application enhances remobilization and reduces losses of pre-anthesis N in wheat grown on a duplex soil. *Crop and Pasture Science*, **46**, 519-531.
- Paolacci, A. R., Tanzarella, O. A., Porceddu, E. and Ciaffi, M. (2009) Identification and validation of reference genes for quantitative RT-PCR normalization in wheat. *BMC molecular biology*, **10**, 1.
- Park, S.-H., Yi, N., Kim, Y. S., Jeong, M.-H., Bang, S.-W., Do Choi, Y. and Kim, J.-K. (2010) Analysis of five novel putative constitutive gene promoters in transgenic rice plants. *Journal of experimental botany*, **61**, 2459-2467.
- Parry, M., Andralojc, P., Mitchell, R. A., Madgwick, P. and Keys, A. (2003) Manipulation of Rubisco: the amount, activity, function and regulation. *Journal of experimental botany*, **54**, 1321-1333.
- Parry, M., Schmidt, C., Cornelius, M., Millard, B., Burton, S., Gutteridge, S., Dyer, T. and Keys, A. (1987) Variations in properties of ribulose-1, 5-bisphosphate

- carboxylase from various species related to differences in amino acid sequences. *Journal of experimental botany*, **38**, 1260-1271.
- Parry, M. A., Andralojc, P. J., Scales, J. C., Salvucci, M. E., Carmo-Silva, A. E., Alonso, H. and Whitney, S. M. (2013) Rubisco activity and regulation as targets for crop improvement. *Journal of experimental botany*, **64**, 717-730.
- Parry, M. A., Keys, A. J., Madgwick, P. J., Carmo-Silva, A. E. and Andralojc, P. J. (2008) Rubisco regulation: a role for inhibitors. *Journal of experimental botany*, **59**, 1569-1580.
- Parry, M. A., Reynolds, M., Salvucci, M. E., Raines, C., Andralojc, P. J., Zhu, X.-G., Price, G. D., Condon, A. G. and Furbank, R. T. (2011) Raising yield potential of wheat. II. Increasing photosynthetic capacity and efficiency. *Journal of experimental botany*, **62**, 453-467.
- Pengelly, J. J., Sirault, X. R., Tazoe, Y., Evans, J. R., Furbank, R. T. and von Caemmerer, S. (2010) Growth of the C4 dicot *Flaveria bidentis*: photosynthetic acclimation to low light through shifts in leaf anatomy and biochemistry. *Journal of experimental botany*, **61**, 4109-4122.
- Peremarti, A., Twyman, R. M., Gómez-Galera, S., Naqvi, S., Farré, G., Sabalza, M., Miralpeix, B., Dashevskaya, S., Yuan, D. and Ramessar, K. (2010) Promoter diversity in multigene transformation. *Plant molecular biology*, **73**, 363-378.
- Portis Jr, A. R. (1992) Regulation of ribulose 1, 5-bisphosphate carboxylase/oxygenase activity. *Annual review of plant biology*, **43**, 415-437.
- Quick, W., Schurr, U., Scheibe, R., Schulze, E.-D., Rodermeil, S., Bogorad, L. and Stitt, M. (1991) Decreased ribulose-1, 5-bisphosphate carboxylase-oxygenase in transgenic tobacco transformed with "antisense" rbcS. *Planta*, **183**, 542-554.
- Raines, C. and Paul, M. (2006) Products of leaf primary carbon metabolism modulate the developmental programme determining plant morphology. *Journal of experimental botany*, **57**, 1857-1862.
- Raines, C. A. (2003) The Calvin cycle revisited. *Photosynthesis research*, **75**, 1-10.
- Raines, C. A. (2006) Transgenic approaches to manipulate the environmental responses of the C3 carbon fixation cycle. *Plant, cell & environment*, **29**, 331-339.
- Raines, C. A. (2011) Increasing photosynthetic carbon assimilation in C3 plants to improve crop yield: current and future strategies. *Plant Physiology*, **155**, 36-42.

- Raines, C. A., Lloyd, J. C. and Dyer, T. A. (1999) New insights into the structure and function of sedoheptulose-1, 7-bisphosphatase; an important but neglected Calvin cycle enzyme. *Journal of experimental botany*, **50**, 1-8.
- Rajinikanth, M., Harding, S. A. and Tsai, C.-J. (2007) The glycine decarboxylase complex multienzyme family in *Populus*. *Journal of experimental botany*, **58**, 1761-1770.
- Ramos, C. (1996) Effect of agricultural practices on the nitrogen losses to the environment. *Fertilizers and Environment*. Springer.
- Robinson, S. P. and Portis, A. R. (1988) Release of the nocturnal inhibitor, carboxyarabinitol-1-phosphate, from ribulose bisphosphate carboxylase/oxygenase by rubisco activase. *FEBS letters*, **233**, 413-416.
- Robinson, S. P. and Portis, A. R. (1989) Ribulose-1, 5-bisphosphate carboxylase/oxygenase activase protein prevents the in vitro decline in activity of ribulose-1, 5-bisphosphate carboxylase/oxygenase. *Plant Physiology*, **90**, 968-971.
- Rodermel, S. R., Abbott, M. S. and Bogorad, L. (1988) Nuclear-organelle interactions: nuclear antisense gene inhibits ribulose bisphosphate carboxylase enzyme levels in transformed tobacco plants. *Cell*, **55**, 673-681.
- Rosenthal, D., Locke, A., Khozaei, M., Raines, C., Long, S. and Ort, D. (2011) Over-expressing the C3 photosynthesis cycle enzyme Sedoheptulose-1-7 Bisphosphatase improves photosynthetic carbon gain and yield under fully open air CO<sub>2</sub> fumigation (FACE). *BMC plant biology*, **11**, 123.
- Sage, R. F. and Pearcy, R. W. (1987) The nitrogen use efficiency of C3 and C4 plants II. Leaf nitrogen effects on the gas exchange characteristics of *Chenopodium album* (L.) and *Amaranthus retroflexus* (L.). *Plant Physiology*, **84**, 959-963.
- Salvucci, M. E., Portis Jr, A. R. and Ogren, W. L. (1985) A soluble chloroplast protein catalyzes ribulosebisphosphate carboxylase/oxygenase activation in vivo. *Photosynthesis research*, **7**, 193-201.
- Scheibe, R. (1990) Light/dark modulation: regulation of chloroplast metabolism in a new light. *Botanica acta*, **103**, 327-334.
- Schnarrenberger, C., Flechner, A. and Martin, W. (1995) Enzymatic evidence for a complete oxidative pentose phosphate pathway in chloroplasts and an incomplete pathway in the cytosol of spinach leaves. *Plant Physiology*, **108**, 609-614.

- Schürmann, P. and Jacquot, J.-P. (2000) Plant thioredoxin systems revisited. *Annual review of plant biology*, **51**, 371-400.
- Sharma-Natu, P. and Ghildiyal, M. (2005) Potential targets for improving photosynthesis and crop yield. *Current Science*, **88**, 1918-1928.
- Shewry, P. (2009) Wheat. *Journal of experimental botany*, **60**, 1537-1553.
- Shewry, P. R., Tatham, A. S., Barro, F., Barcelo, P. and Lazzeri, P. (1995) Biotechnology of breadmaking: unraveling and manipulating the multi-protein gluten complex. *Bio/technology*, **13**, 1185-1190.
- Simpson, R. J., Lambers, H. and Dalling, M. J. (1983) Nitrogen redistribution during grain growth in wheat (*Triticum aestivum* L.) IV. Development of a quantitative model of the translocation of nitrogen to the grain. *Plant Physiology*, **71**, 7-14.
- Somerville, C., Portis, A. R. and Ogren, W. L. (1982) A mutant of *Arabidopsis thaliana* which lacks activation of RuBP carboxylase in vivo. *Plant Physiology*, **70**, 381-387.
- Song, P., Heinen, J. L., Burns, T. H. and Allen, R. D. (2000) Expression of two tissue-specific promoters in transgenic cotton plants. *J Cotton Sci*, **4**, 217-223.
- Sparkes, I. A., Runions, J., Kearns, A. and Hawes, C. (2006) Rapid, transient expression of fluorescent fusion proteins in tobacco plants and generation of stably transformed plants. *Nature protocols*, **1**, 2019-2025.
- Sparks, C. A. and Jones\*, H. D. (2009) Biolistics transformation of wheat. *Transgenic Wheat, Barley and Oats: Production and Characterization Protocols*, 71-92.
- Spreitzer, R. J. (1993) Genetic dissection of Rubisco structure and function. *Annual review of plant biology*, **44**, 411-434.
- Spreitzer, R. J. and Salvucci, M. E. (2002) Rubisco: structure, regulatory interactions, and possibilities for a better enzyme. *Annual review of plant biology*, **53**, 449-475.
- Stitt, M., Lunn, J. and Usadel, B. (2010) *Arabidopsis* and primary photosynthetic metabolism—more than the icing on the cake. *The Plant Journal*, **61**, 1067-1091.
- Stitt, M., Quick, W., Schurr, U., Schulze, E.-D., Rodermeil, S. and Bogorad, L. (1991) Decreased ribulose-1, 5-bisphosphate carboxylase-oxygenase in transgenic tobacco transformed with 'antisense' rbcS. *Planta*, **183**, 555-566.
- Stitt, M. and Schulze, D. (1994) Does Rubisco control the rate of photosynthesis and plant growth? An exercise in molecular ecophysiology. *Plant, cell & environment*, **17**, 465-487.

- Tamoi, M., Nagaoka, M., Yabuta, Y. and Shigeoka, S. (2005b) Carbon metabolism in the Calvin cycle. *Plant biotechnology*, **22**, 355-360.
- Tao, L.-z., Cheung, A. Y. and Wu, H.-m. (2002) Plant Rac-like GTPases are activated by auxin and mediate auxin-responsive gene expression. *The Plant Cell Online*, **14**, 2745-2760.
- Taulemesse, F., Le Gouis, J., Gouache, D., Gibon, Y. and Allard, V. (2016) Bread Wheat (*Triticum aestivum* L.) Grain Protein Concentration Is Related to Early Post-Flowering Nitrate Uptake under Putative Control of Plant Satiety Level. *PloS one*, **11**, e0149668.
- Travella, S., Klimm, T. E. and Keller, B. (2006) RNA interference-based gene silencing as an efficient tool for functional genomics in hexaploid bread wheat. *Plant Physiology*, **142**, 6-20.
- Tzafrir, I., Torbert, K. A., Lockhart, B. E., Somers, D. A. and Olszewski, N. E. (1998) The sugarcane bacilliform badnavirus promoter is active in both monocots and dicots. *Plant molecular biology*, **38**, 347-356.
- Uematsu, K., Suzuki, N., Iwamae, T., Inui, M. and Yukawa, H. (2012) Increased fructose 1, 6-bisphosphate aldolase in plastids enhances growth and photosynthesis of tobacco plants. *Journal of experimental botany*, **63**, 3001-3009.
- Untergasser, A., Cutcutache, I., Koressaar, T., Ye, J., Faircloth, B. C., Remm, M. and Rozen, S. G. (2012) Primer3—new capabilities and interfaces. *Nucleic acids research*, **40**, e115-e115.
- Voinnet, O., Rivas, S., Mestre, P. and Baulcombe, D. (2003) An enhanced transient expression system in plants based on suppression of gene silencing by the p19 protein of tomato bushy stunt virus. *The Plant Journal*, **33**, 949-956.
- Von Caemmerer, S. v. and Farquhar, G. (1981) Some relationships between the biochemistry of photosynthesis and the gas exchange of leaves. *Planta*, **153**, 376-387.
- Wang, Z. Y. and Portis, A. R. (1992) Dissociation of ribulose-1, 5-bisphosphate bound to ribulose-1, 5-bisphosphate carboxylase/oxygenase and its enhancement by ribulose-1, 5-bisphosphate carboxylase/oxygenase activase-mediated hydrolysis of ATP. *Plant Physiology*, **99**, 1348-1353.
- Wedel, N. and Soll, J. (1998) Evolutionary conserved light regulation of Calvin cycle activity by NADPH-mediated reversible

- phosphoribulokinase/CP12/glyceraldehyde-3-phosphate dehydrogenase complex dissociation. *Proceedings of the National Academy of Sciences*, **95**, 9699-9704.
- Wedel, N., Soll, J. and Paap, B. K. (1997) CP12 provides a new mode of light regulation of Calvin cycle activity in higher plants. *Proceedings of the National Academy of Sciences*, **94**, 10479-10484.
- Wei, T. and Wang, A. (2008) Biogenesis of cytoplasmic membranous vesicles for plant potyvirus replication occurs at endoplasmic reticulum exit sites in a COPI-and COPII-dependent manner. *Journal of virology*, **82**, 12252-12264.
- Wenderoth, I., Scheibe, R. and von Schaewen, A. (1997) Identification of the cysteine residues involved in redox modification of plant plastidic glucose-6-phosphate dehydrogenase. *Journal of Biological Chemistry*, **272**, 26985-26990.
- Werdan, K., Heldt, H. W. and Milovancev, M. (1975) The role of pH in the regulation of carbon fixation in the chloroplast stroma. Studies on CO<sub>2</sub> fixation in the light and dark. *Biochimica et Biophysica Acta (BBA)-Bioenergetics*, **396**, 276-292.
- Willingham, N. M., Lloyd, J. C. and Raines, C. A. (1994) Molecular cloning of the *Arabidopsis thaliana* sedoheptulose-1, 7-biphosphatase gene and expression studies in wheat and *Arabidopsis thaliana*. *Plant molecular biology*, **26**, 1191-1200.
- Woodrow, I. E. and Berry, J. (1988) Enzymatic regulation of photosynthetic CO<sub>2</sub> fixation in C<sub>3</sub> plants. *Annual Review of Plant Physiology and Plant Molecular Biology*, **39**, 533-594.
- Wydro, M., Kozubek, E. and Lehmann, P. (2006) Optimization of transient *Agrobacterium*-mediated gene expression system in leaves of *Nicotiana benthamiana*. *ACTA BIOCHIMICA POLONICA-ENGLISH EDITION*-, **53**, 289.
- ZADOKS, J. C., CHANG, T. T., & KONZAK, C. F. (1974). A decimal code for the growth stages of cereals. *Weed research*, *14*(6), 415-421.
- Zhu, X.-G., de Sturler, E. and Long, S. P. (2007) Optimizing the distribution of resources between enzymes of carbon metabolism can dramatically increase photosynthetic rate: a numerical simulation using an evolutionary algorithm. *Plant Physiology*, **145**, 513-526.